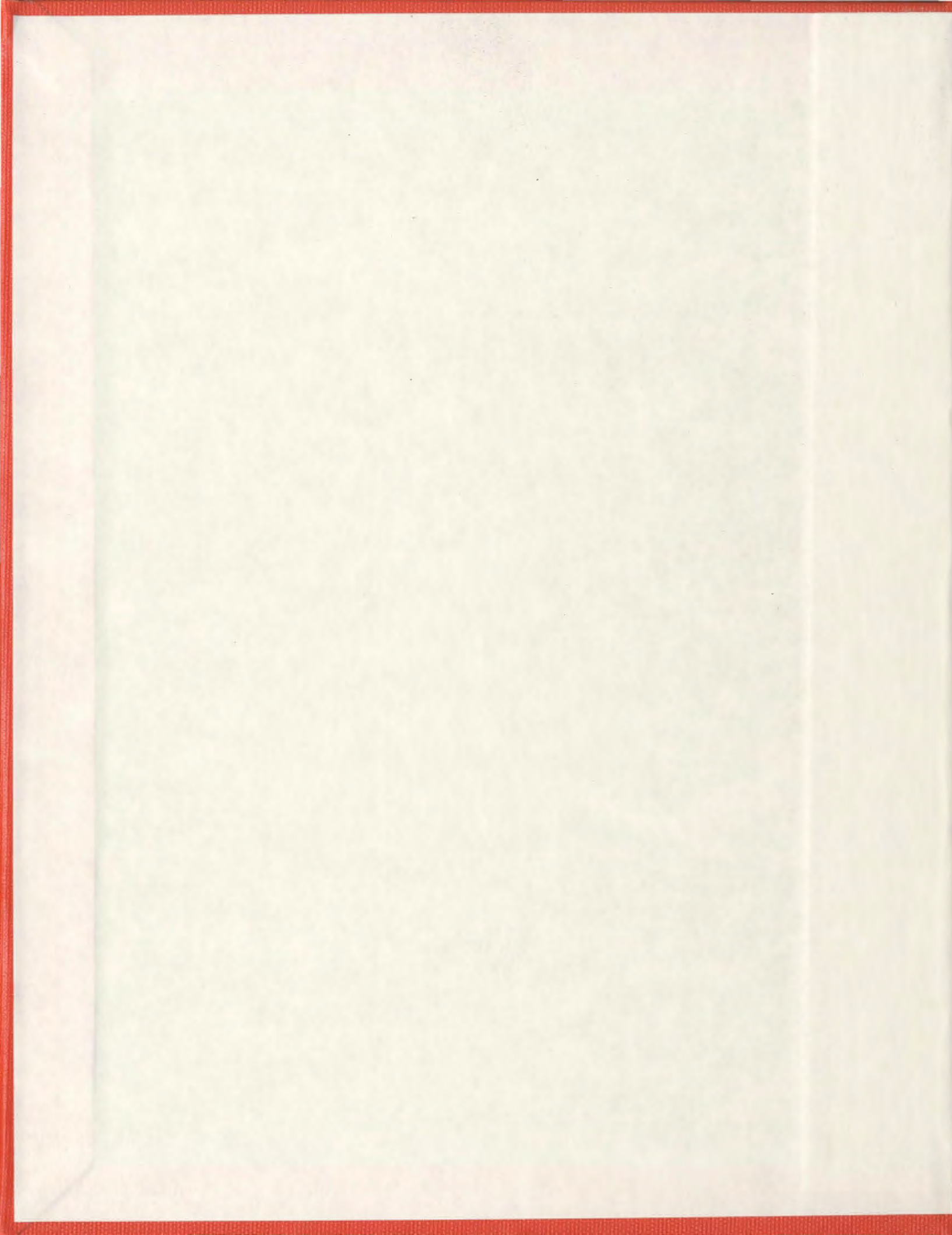


BLIND MODULATION CLASSIFICATION OF
LINEARLY DIGITALLY MODULATED SIGNALS

FAHED HAMEED



9/10/2006

**BLIND MODULATION CLASSIFICATION OF
LINEARLY DIGITALLY MODULATED SIGNALS**



Submitted By

Fahed Hameed
(ID#: 200388734)

In partial fulfillment of the requirements for the

Degree of Master of Engineering

Faculty of Engineering and Applied Science

**Memorial University of Newfoundland
St. John's, Newfoundland**

Copyright 2006, Fahed Hameed

ABSTRACT

Blind modulation classification (MC) is an intermediate step between signal detection and demodulation, with both military and civilian applications. MC is a challenging task, especially in a non-cooperative environment, as no prior information on the incoming signal is available at the receiver.

In this thesis, we investigate classification of linear digital modulations in slowly varying flat fading channels. With unknown channel amplitude, phase and noise power at the receive-side, we investigate hybrid likelihood ratio test (HLRT) and quasi-HLRT (QHLRT) -based classifiers, and discuss their performance versus computational complexity. Both classifiers rely on the likelihood function (LF) of the received signal, and the decision is made based on the likelihood ratio test. To compute the LF, the former employs maximum likelihood (ML) estimates of the unknown parameters, whereas the latter uses method-of-moment (MoM) estimates of these parameters. It is shown that the QHLRT algorithm provides a low computational complexity solution, yet yielding performance close to the HLRT algorithm.

We further study the performance of MoM estimators employed in the QHLRT algorithm, in terms of their variance. We derive Cramer-Rao Lower Bounds (CRLBs) of estimators of the channel amplitude, phase and noise power, for Binary Phase Shift Keying (BPSK) and Quadrature Phase Shift Keying (QPSK) modulated signals. CRLB provides a lower bound on the variance of an unbiased estimator. The CRLB expressions are evaluated for different signal-to-noise ratios (SNRs) and number of processed symbols. Variance of MoM estimators is compared with corresponding CRLB and

numerical results reveal reasonable accuracy of MoM method of parameter estimation, for the SNR range in which these estimators remain unbiased¹.

An application of the CRLB to MC is presented, by developing an idealized reference for QHLRT-based classifiers². This is referred to as the QHLRT-IR (QHLRT-IR) classifier. The QHLRT-IR classifier employs unbiased and normally-distributed estimators of the unknown parameters, with mean as the true value of the parameter and variance given by the CRLB of the parameter estimator. Performance of the QHLRT and QHLRT-IR classifiers² are compared. QHLRT-IR provides an upper bound on the classification performance in the SNR range where the MoM estimators of the unknown parameters remain unbiased and normally-distributed¹. In this SNR range, it is observed that the performance of the two classifiers is close to each other, which indicates the reasonable accuracy of MoM method for such SNRs. It is shown that the classification performance improves with an increase in the number of processed symbols, due to the increase in estimation accuracy.

¹ These estimators are asymptotically unbiased and normally-distributed, i.e., they are unbiased and normally distributed in a certain SNR range when the number of processed symbols is large enough.

² With such classifiers, no prior information of the signal is available at the receiver. As we already mentioned, we assume here the channel amplitude, phase and noise power as unknown, and we blindly (non-data aided (NDA)) estimate these parameters.

ACKNOWLEDGEMENTS

I would like to thank Allah (God) Almighty for his special blessings upon me and for giving me opportunity to complete my degree.

I would like to thank my family, especially my parents and my wife who supported me and prayed for my success throughout.

I would like to thank Dr. Gosine, Dr. Venkatesan and Dr. Heys for their enormous support in the completion of my degree. At one time, I came across a difficult situation that I wanted to quit my program. But they encouraged me and helped me to overcome that situation. I greatly appreciate their moral and administrative backing.

I would like to thank Reza Shahidi for his help during the course of my degree. His help was of great value, especially with running simulations on CLUSTER and very useful discussions on some mathematical concepts.

Finally, I would like to give special thanks to my supervisor, Dr. Octavia Dobre, for her tremendous support in my research. I suppose it was not an easy decision at that time when she decided to supervise me but she showed trust in me and took this bold decision. She always encouraged me and guided me with kindness. She is really a great person to work with.

TABLE OF CONTENTS

ABSTRACT.....	iii
ACKNOWLEDGEMENTS	v
TABLE OF CONTENTS	vi
LIST OF FIGURES	viii
LIST OF ABBREVIATIONS	ix
LIST OF SYMBOLS	x
1. INTRODUCTION.....	1
1.1. Modulation Classification: Problem Formulation.....	1
1.2. Thesis Objectives.....	3
1.3. Thesis Organization.....	5
2. LIKELIHOOD-BASED MODULATION CLASSIFIERS FOR LINEARLY DIGITALLY MODULATED SIGNALS.....	6
2.1. Signal Model.....	6
2.2. Hybrid Likelihood Ratio Test (HLRT)- and Quasi HLRT-based Classifiers .	9
2.2.1. HLRT-based Classifier.....	9
2.2.1.1. Maximum Likelihood (ML) Parameter Estimators	10
2.2.1.2. The HLRT Classification Algorithm.....	13
2.2.2. QHLRT-based Classifier.....	14
2.2.2.1. Method of Moment (MoM) Parameter Estimators	15
2.2.2.2. The QHLRT Classification Algorithm.....	17
2.3. Complexity Analysis of Proposed Classifiers	17
2.4. Performance Measure	18
2.5. Simulation Results	18

2.6.	Chapter Summary	25
3.	CRAMER-RAO LOWER BOUNDS (CRLB) OF CHANNEL PARAMETER ESTIMATORS	26
3.1.	Introduction to CRLB	26
3.2.	CRLBs of Channel Amplitude, Phase and Noise Power Estimators for BPSK	29
3.3.	CRLBs of Channel Amplitude, Phase and Noise Power Estimators for QPSK	31
3.4.	Numerical Results	32
3.5.	Chapter Summary	44
4.	APPLICATION OF CRAMER-RAO LOWER BOUND (CRLB) TO MODULATION CLASSIFICATION.....	45
4.1.	Proposed QHLRT-idealized reference (QHLRT-IR) Classifier.....	45
4.2.	Simulation Results	47
4.3.	Chapter Summary	51
5.	SUMMARY AND FUTURE WORK.....	52
	REFERENCES.....	55
	APPENDIX A	58
	APPENDIX B	59
	APPENDIX C	62
	APPENDIX D	64
	APPENDIX E	65
	APPENDIX F	66

LIST OF FIGURES

Fig. 1. System block diagram.....	2
Fig. 2. Performance comparison of likelihood-based algorithms in Rayleigh fading, when discriminating BPSK and QPSK, with $K = 10$ symbols.....	22
Fig. 3. Performance of QHLRT when discriminating BPSK, QPSK, 8-PSK and 16-PSK in Rayleigh fading, with $K = 100$ and $K = 1000$ symbols.....	23
Fig. 4. Performance of QHLRT when discriminating BPSK, QPSK, 8-PSK, 16-PSK in Ricean fading, with $K = 1000$ symbols.	24
Fig. 5. Cramer-Rao lower bounds of channel amplitude estimators for BPSK and QPSK signals, with different observation interval lengths K	35
Fig. 6. Cramer-Rao lower bounds of channel phase estimators for BPSK and QPSK signals, with different observation interval lengths K	36
Fig. 7. Cramer-Rao lower bounds of noise power estimators for BPSK and QPSK signals, with different observation interval lengths K	37
Fig. 8. Comparison of the variance of channel amplitude MoM estimators and corresponding CRLB for BPSK signals.....	38
Fig. 9. Comparison of the variance of channel amplitude MoM estimators and corresponding CRLB for QPSK signals.....	39
Fig. 10. Comparison of the variance of channel phase MoM estimators and corresponding CRLB for BPSK signals.....	40
Fig. 11. Comparison of the variance of channel phase MoM estimators and corresponding CRLB for QPSK signals.	41
Fig. 12. Comparison of the variance of noise power MoM estimators and corresponding CRLB for BPSK signals.....	42
Fig. 13. Comparison of the variance of noise power MoM estimators and corresponding CRLB for QPSK signals.	43
Fig. 14. Performance comparison of ALRT, QHLRT-IR and QHLRT classifiers in AWGN, when discriminating BPSK and QPSK, with $K = 100$ symbols.....	49
Fig. 15. Performance comparison of ALRT, QHLRT-IR and QHLRT classifiers in AWGN, when discriminating BPSK and QPSK, with $K = 1000$ symbols.....	50

LIST OF ABBREVIATIONS

ALRT	Average Likelihood Ratio Test
AWGN	Additive White Gaussian Noise
BPSK	Binary Phase Shift Keying
CRLB	Cramer-Rao Lower Bound
FIM	Fisher Information Matrix
GLRT	Generalized Likelihood Ratio Test
HF	High Frequency
HLRT	Hybrid Likelihood Ratio Test
LF	Likelihood Function
MC	Modulation Classification
ML	Maximum Likelihood
MoM	Method-of-Moment
<i>M</i> -PSK	<i>M</i> -ary Phase Shift Keying
<i>M</i> -QAM	<i>M</i> -ary Quadrature Amplitude Modulation
NDA	Non-data aided
pdf	Probability density function
QHLRT	Quasi-HLRT
QPSK	Quadrature Phase Shift Keying
SDR	Software Defined Radio
SNR	Signal to Noise Ratio
w.r.t.	with respect to

LIST OF SYMBOLS

α	Channel amplitude
$b^{(i)}$	Parameter specific to i th modulation format
$\frac{\partial}{\partial \theta}$	Partial derivative with respect to θ
$E[\cdot]$	Statistical expectation operator
E_p	Pulse energy
E_{s_i}	Energy of the transmitted signal
f_c	Carrier frequency
$f(\mathbf{r}; H_i)$	Likelihood function of \mathbf{r} under hypothesis H_i
$f(\mathbf{r} \boldsymbol{\theta})$	Likelihood function of \mathbf{r} conditioned on $\boldsymbol{\theta}$
γ	Instantaneous SNR
H_i	Hypothesis that i th modulation was transmitted
i	Transmitted modulation format
$\mathbf{I}(\cdot)$	Fisher Information Matrix
$I(\cdot)$	In-phase component of observed signal sample, r_k
$I_{n,k}$	In-phase component of n_k
K	Number of symbols in the observation interval
K_R	Rice factor
$\text{LF}^{(i)}(\mathbf{r})$	Likelihood function of \mathbf{r} under hypothesis H_i
M_{21}	Second-order moment of the received signal
M_{42}	Fourth-order moment of the received signal
M_i	Number of points in the signal constellation corresponding to the i th modulation format
N	Noise power
N_{mod}	Number of modulations considered for classification

\mathbf{n}	Noise vector with components normally distributed
n_k	Noise sample at moment k
$\ \cdot\ $	Norm of a vector
$n(t)$	Additive white Gaussian noise (AWGN)
φ	Channel phase
P_{cc}	Average probability of correct classification
$P_c^{(di)}$	Conditional probability of the event that the i th modulation is received, when indeed the i th modulation was originally transmitted
$Q(\cdot)$	Quadrature-phase component of observed signal sample, r_k
$Q_{n,k}$	Quadrature-phase component of n_k
\mathbf{r}	Vector of received samples
r_k	Sample at the output of receive matched filter at moment k
$r(t)$	Received signal
$\rho^{(i)}$	Correlation coefficient between \mathbf{r} and $\mathbf{s}^{(i)}$
σ^2	Variance of a Gaussian random variable
$\sigma_{s_i}^2$	Variance of the zero-mean i th signal constellation
$S^{(i)}$	Transmitted signal power for the i th modulation format
$\mathbf{s}^{(i)}$	Transmitted symbol sequence specific to the i th modulation format
$s^{(i)}(t)$	Signal corresponding to the i th modulation format, at the receive-side
T	Symbol period
$\boldsymbol{\theta}$	Vector of unknown parameters
$u_T(t)$	Rectangular pulse shape of duration T seconds and of unit amplitude
w_k	Gaussian noise sample rotated by a random phase
w_k^I	In-phase component of w_k
w_k^Q	Quadrature-phase component of w_k
\hat{x}	Estimate of a parameter x

CHAPTER 1

1. INTRODUCTION

1.1. Modulation Classification: Problem Formulation

Modulation Classification (MC) is a branch of communication theory that combines several aspects of communication areas, such as signal detection, channel monitoring, and parameter estimation. MC is an intermediate step between signal detection and demodulation, and plays an important role in various civilian and military applications. Implementation of advanced information services and systems for military applications, in a crowded electromagnetic spectrum, is a challenging task for communication engineers. Friendly signals should be securely transmitted and received, whereas hostile signals must be located, identified and jammed. The spectrum of these signals may range from high frequency (HF) to millimeter frequency band, and their format can vary from simple narrowband modulations to wideband schemes. Under such conditions, advanced techniques are required for real-time signal interception and processing, which are vital for decisions involving electronic warfare operations and other tactical actions. Furthermore, blind recognition of the modulation format of the received signal is an important problem in commercial systems, especially in software defined radio (SDR), which copes with the variety of communication systems. Usually, supplementary information is transmitted to reconfigure the SDR system. Blind techniques can be used with an intelligent receiver, yielding an increase in the throughput by reducing the overhead. This is achieved by transmitting useful data instead

of sending the modulation information of the transmitted signal. Such applications have emerged the need for flexible intelligent communication systems, where the automatic recognition of the modulation of a detected signal is a major task. A simplified block diagram of the system model is shown in Fig. 1. The design of a modulation classifier essentially involves two steps: signal preprocessing and proper selection of the classification algorithm. Preprocessing tasks may include, but not limited to perform some or all of, noise reduction, estimation of carrier frequency, symbol period, and signal power, equalization, etc. Depending on the classification algorithm chosen in the second step, preprocessing tasks with different levels of accuracy are required; some classification methods require precise estimates, whereas others are less sensitive to the unknown parameters.

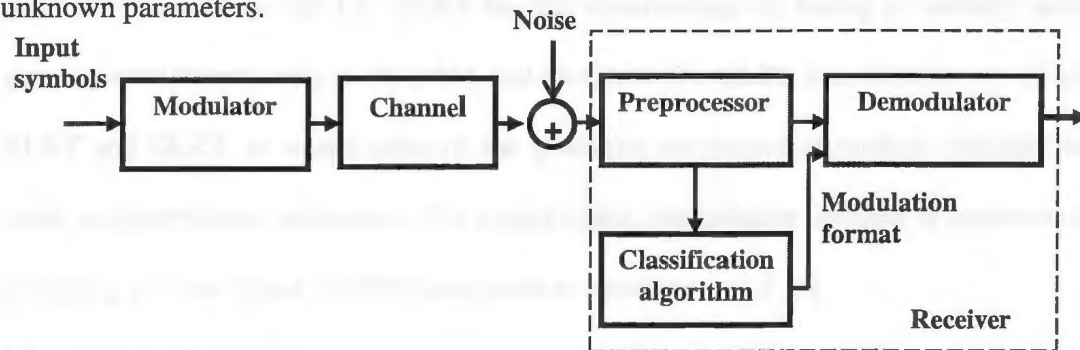


Fig. 1. System block diagram.

With no prior knowledge of the incoming signal, blind MC is a difficult task. Generally, two approaches are followed to tackle this problem: a likelihood-based approach, in which the likelihood function (LF) of the received signal is computed and a likelihood ratio test is used for decision-making [1]-[7], and a statistical pattern recognition

approach, in which features are extracted from the received signal and a decision is made based on their differences [7]-[11].

The likelihood-based methods can be divided into three categories: Average Likelihood Ratio Test (ALRT) [1]-[3], [5], Generalized Likelihood Ratio Test (GLRT) [3], and Hybrid Likelihood Ratio Test (HLRT) [3]-[4]. With the ALRT, the unknown quantities are treated as random variables, and the LF is computed by averaging over them. Although ALRT provides an optimal solution in the sense that it minimizes the probability of misclassification, it suffers from high computational complexity in many cases of practical interest [1], [5]. On the other hand, the GLRT treats the unknown quantities as deterministic unknowns, and employs maximum likelihood (ML) estimates of these quantities to compute the LF. GLRT has the disadvantage of failing to identify nested signal constellations, such as 16-QAM and 64-QAM [3]. HLRT is a combination of both ALRT and GLRT, in which some of the quantities are treated as random variables and some as deterministic unknowns. The nested signal constellation problem is overcome by averaging over the signal constellation points to calculate the LF [3].

1.2. Thesis Objectives

The main objective of this research is to find a likelihood-based blind modulation classification algorithm for linear digital modulations, which is simple to implement, and yet provides reasonable classification performance. To achieve this objective, we investigate the Hybrid Likelihood Ratio Test (HLRT) -based classifier, as well as a Quasi HLRT (QHLRT)-based classifier. These classifiers employ ML and MoM estimates of the unknown parameters, respectively. We study the case of unknown channel amplitude, phase and noise

power². Both classification performance and complexity of these classifiers are investigated. An ALRT-based classifier is used as an idealized reference for performance evaluation; this assumes perfect knowledge of the unknown parameters.

The performance of the QHLRT algorithm depends on the estimators employed for the unknown parameters²; therefore, we further investigate the accuracy of the MoM estimators of these parameters. These estimators are asymptotically unbiased¹ [9], [12]. Their bias is investigated through simulations. The Cramer-Rao Lower Bounds (CRLBs) of the unknown parameter estimators are derived and used for comparison with the variance of corresponding MoM estimators. Note that the CRLB provides a lower bound only on the variance of an unbiased estimator [13].

The ALRT-based classifier, which assumes perfect knowledge of all the unknown parameters, is first used as an idealized reference to evaluate the performance of HLRT- and QHLRT-based classifiers. Then, a QHLRT-idealized reference (QHLRT-IR) classifier is developed by using unbiased and normally-distributed estimators of the unknown parameters, with mean as the true value of the parameter and variance given by the CRLB of the parameter estimator. This is a more suitable idealized reference for performance evaluation of QHLRT-based classifiers that employ unbiased and normally-distributed estimators of unknown parameters. Moreover, this classifier provides an upper bound on classification performance for the QHLRT-based classifiers which employ asymptotically unbiased and normally-distributed estimators of unknown parameters, but only in a certain SNR range¹. For a certain estimation technique and modulation format, the SNR

range in which the asymptotic results apply depends on the length of the observation interval.

1.3. Thesis Organization

The thesis is organized as follows. In Chapter 2, the signal model of linearly digitally modulated signals is presented, followed by the proposed Hybrid Likelihood Ratio Test (HLRT) and Quasi HLRT (QHLRT)-based classifiers. In Chapter 3, the Cramer-Rao Lower Bounds of the channel parameter estimators are derived, and the performance of MoM estimators of these parameters assessed. Application of Cramer-Rao Lower Bounds to Modulation Classification is given in Chapter 4. The summary and suggested future work is presented in Chapter 5.

CHAPTER 2

2. LIKELIHOOD-BASED MODULATION CLASSIFIERS FOR LINEARLY DIGITALLY MODULATED SIGNALS

In this Chapter, HLRT- and quasi-HLRT (QHLRT)-based classifiers are investigated for modulation classification of linearly digitally modulated signals in slowly varying flat fading channels. In [5], a QHLRT-based classifier is investigated, for the discrimination of linear digital modulations, which employs method-of-moment (MoM) estimators of unknown channel amplitude and phase. Similarly, in [8], MoM estimators of channel amplitude and noise power are derived. Here, we investigate the HLRT- and QHLRT-based classifier by employing the estimators of three unknown parameters for linear digital modulations. To compute the likelihood function of the received signal, the former employs ML estimators of the unknown parameters, i.e., channel amplitude, phase and noise power, whereas the latter uses MoM estimators of these parameters. The comparison of computational complexity is performed here for the two classifiers. The performance of the two classifiers is evaluated through simulations, when discriminating M -ary Phase Shift Keying (M -PSK) signals in block fading channels³. The average probability of correct classification, P_{cc} , is used as a performance measure for the evaluation of performance⁴.

2.1. Signal Model

The received signal is expressed as

³ In this work, we assume block fading channel, in which the channel amplitude and phase are constant over the observation interval.

⁴ For the definition of P_{cc} , see Section 2.4

$$r(t) = s^{(i)}(t) + n(t), \quad 0 \leq t \leq KT, \quad (2.1)$$

where T is the symbol period, K is the number of observed (processed) symbols, $n(t)$ is the additive white Gaussian noise (AWGN) with zero-mean and 2-sided power spectral density $N_0/2$ (Watts/Hz), and $s^{(i)}(t)$ is given as

$$s^{(i)}(t) = \text{Re} \left\{ a e^{j\varphi} \sum_{k=1}^K s_k^{(i)} u_T(t - (k-1)T) e^{j2\pi f_c t} \right\}, \quad 0 \leq t \leq KT, \quad i = 1, \dots, N_{\text{mod}}, \quad (2.2)$$

with $a = \alpha \sqrt{2E_s / \sigma_{s_i}^2 E_p}$ as the signal amplitude, α as the channel amplitude, φ as the channel phase (which also includes the carrier phase offset), E_s as the normalized energy of the transmitted signal, $\sigma_{s_i}^2$ as the variance of the zero-mean i th signal constellation, $u_T(t)$ as the rectangular pulse shape of duration T seconds and of unit amplitude, E_p as the pulse energy, f_c as the carrier frequency, and N_{mod} as the number of constellations considered for classification. The sequence $\{s_k^{(i)}\}$ is independent and identically distributed, with values drawn from a finite set specific to the i th modulation format, $i = 1, \dots, N_{\text{mod}}$.

In this work, linearly digitally modulated signals are considered. For the constellations of such signals, see [14], Ch. 4.

The pulse shape energy is given by

$$E_p = \int_{-\infty}^{\infty} u_T^2(t) dt = T. \quad (2.3)$$

Without loss of generality, we consider here unit variance constellations, i.e., $E\{|s^{(i)}|^2\} = \sigma_{s_i}^2 = 1$, and set the transmitted signal power to one, i.e., $E_{s_i}/T = 1$, $i = 1, \dots, N_{\text{mod}}$. Thus, (2.2) becomes

$$s^{(i)}(t) = \text{Re} \left\{ \sqrt{2} \alpha e^{j\varphi} \sum_{k=1}^K s_k^{(i)} u_T(t - (k-1)T) e^{j2\pi f_c t} \right\}, \quad 0 \leq t \leq KT, \quad i = 1, \dots, N_{\text{mod}}. \quad (2.4)$$

The output of the receive matched filter, sampled at T seconds is given by

$$r_k = \sqrt{2} \int_{(k-1)T}^{kT} r(t) u_T(t - (k-1)T) e^{-j2\pi f_c t} dt, \quad k = 1, \dots, K. \quad (2.5)$$

According to derivations in Appendix A, (2.5) can be written in a vector form as [5]

$$\mathbf{r} = T \alpha e^{j\varphi} \mathbf{s}^{(i)} + \mathbf{n}, \quad i = 1, \dots, N_{\text{mod}}, \quad (2.6)$$

where $\mathbf{r} = [r_1, \dots, r_K]^\dagger$ is the vector of the samples taken at the output of the receive matched filter, $\mathbf{s}^{(i)} = [s_1^{(i)}, \dots, s_K^{(i)}]^\dagger$ is the transmitted symbol sequence, and $\mathbf{n} = [n_1, \dots, n_K]^\dagger$ is the noise vector. The noise components $\{n_k\}_{k=1}^K$ are independent zero-mean Gaussian random variables whose in-phase and quadrature components have variance σ^2 . These are defined as

$$n_k = \sqrt{2} \int_{(k-1)T}^{kT} n(t) e^{-j2\pi f_c t} dt, \quad (2.7)$$

and \dagger denotes the transpose.

Without loss of generality, T is set to one, i.e., $T = 1$, and (2.6) becomes

$$\mathbf{r} = \alpha e^{j\varphi} \mathbf{s}^{(i)} + \mathbf{n}. \quad (2.8)$$

With the noise power as $N = 2\sigma^2$, we define the (average) signal-to-noise ratio (SNR) as the ratio of the (average) signal power to the noise power, i.e.,

$$\text{SNR} = E[\alpha^2]/N = E[\alpha^2]/2\sigma^2. \quad (2.9)$$

with $E[\cdot]$ as the statistical expectation operator.

2.2. Hybrid Likelihood Ratio Test (HLRT) - and Quasi HLRT-based Classifiers

With the HLRT and Quasi HLRT, the likelihood function (LF) is computed by using ML and MoM estimators of the signal amplitude, α , phase, φ , and noise power, N , respectively. Assuming that the received symbols are statistically independent, the conditional likelihood function conditioned on the unknown quantities, i.e., unknown points in the signal constellation $\{s_k^{(i)}\}$, and unknown parameters α , φ , and N , is given by [3]

$$f(\mathbf{r} | \{s_k^{(i)}\}, \alpha, \varphi, N) = \prod_{k=1}^K \frac{1}{\pi N} \exp\left\{-\frac{1}{N} |r_k - \alpha e^{j\varphi} s_k^{(i)}|^2\right\}, \quad (2.10)$$

or, equivalently,

$$f(\mathbf{r} | \{s_k^{(i)}\}, \alpha, \varphi, N) = \frac{1}{(\pi N)^K} \exp\left\{-\frac{1}{N} \|\mathbf{r}_k - \alpha e^{j\varphi} \mathbf{s}^{(i)}\|^2\right\}, \quad (2.11)$$

where $\|\cdot\|$ represents the norm of a vector.

2.2.1. HLRT-based Classifier

The likelihood function under the i th hypothesis, i.e., H_i : the i th modulation was transmitted, is computed by using ML estimates of the unknown parameters, and averaging over all possible combinations of K symbols. With the parameters estimated under each hypothesis, $H_i, i=1, \dots, N_{\text{mod}}$, the likelihood function under the i th hypothesis, $\text{LF}_{\text{HLRT}}^{(i)}(\mathbf{r})$, becomes

$$\text{LF}_{\text{HLRT}}^{(i)}(\mathbf{r}) = f(\mathbf{r}; H_i) = \frac{1}{M_i^K} \sum_{m=1}^{M_i^K} \frac{1}{(\pi \hat{N}_m^{(i)})^K} \exp\left\{-\frac{1}{\hat{N}_m^{(i)}} \|\mathbf{r} - \hat{\alpha}_m^{(i)} e^{j\hat{\varphi}_m^{(i)}} \mathbf{s}_m^{(i)}\|^2\right\}, \quad i=1, \dots, N_{\text{mod}}, \quad (2.12)$$

where M_i is the number of points in the i th signal constellation, $\hat{\alpha}_m^{(i)}$, $\hat{\phi}_m^{(i)}$ and $\hat{N}_m^{(i)}$ are the signal amplitude, phase and noise power ML estimates, respectively, under hypothesis H_i , based on the m th combination of K symbols, $m=1, \dots, M_i^K$.

For a binary-hypothesis-testing problem, the likelihood ratio test employed for decision on the modulation format, is given by

$$\frac{\text{LF}_{HLRT}^{(i)}(\mathbf{r})}{\text{LF}_{HLRT}^{(j)}(\mathbf{r})} = \frac{\frac{1}{M_i^K} \sum_{m=1}^{M_i^K} \frac{1}{(\pi \hat{N}_m^{(i)})^K} \exp\left\{-\frac{1}{\hat{N}_m^{(i)}} \|\mathbf{r} - \hat{\alpha}_m^{(i)} e^{j\hat{\phi}_m^{(i)}} \mathbf{s}_m^{(i)}\|^2\right\}}{\frac{1}{M_j^K} \sum_{m=1}^{M_j^K} \frac{1}{(\pi \hat{N}_m^{(j)})^K} \exp\left\{-\frac{1}{\hat{N}_m^{(j)}} \|\mathbf{r} - \hat{\alpha}_m^{(j)} e^{j\hat{\phi}_m^{(j)}} \mathbf{s}_m^{(j)}\|^2\right\}} \underset{H_j}{\overset{H_i}{\geq}} \eta_{ij}, \quad (2.13)$$

$i \neq j, i, j = 1, \dots, N_{\text{mod}},$

where η_{ij} is a threshold.

Equally likely hypotheses are assumed and the threshold η_{ij} is set to one. Hence, for an N_{mod} -ary hypothesis-testing problem, the decision rule becomes

$$\hat{i} = \arg \max_{i=1, \dots, N_{\text{mod}}} \text{LF}_{HLRT}^{(i)}(\mathbf{r}), \quad (2.14)$$

where \hat{i} is the estimate of the transmitted modulation format.

2.2.1.1. Maximum Likelihood (ML) Parameter Estimators

For the HLRT-based classifier, the ML estimators of channel amplitude, phase and noise power are used. Details of the derivations of these estimators are given in Appendix B. Here, we only present the main results of these derivations.

Phase ML Estimator

By differentiating the likelihood function given in (2.11) with respect to (w.r.t.) the phase ϕ , one has

$$\frac{\partial f(\mathbf{r} | \{s_k^{(i)}\}, \alpha, \varphi, N)}{\partial \varphi} = 0. \quad (2.15)$$

After taking the derivative, applying (2.15) and performing simplifications, one obtains⁵

$$e^{-j\varphi} \mathbf{s}^{(i)H} \mathbf{r} = e^{j\varphi} \mathbf{r}^H \mathbf{s}^{(i)}, \quad (2.16)$$

or, equivalently,

$$e^{j2\varphi} = \frac{\mathbf{s}^{(i)H} \mathbf{r}}{\mathbf{r}^H \mathbf{s}^{(i)}}, \quad (2.17)$$

where ' H ' stands for Hermitian. It is now straightforward that the phase ML estimator under hypothesis H_i is given by

$$\hat{\varphi}^{(i)} = -\frac{j}{2} \ln \left(\frac{\mathbf{s}^{(i)H} \mathbf{r}}{\mathbf{r}^H \mathbf{s}^{(i)}} \right), \quad i = 1, \dots, N_{\text{mod}}. \quad (2.18)$$

One can notice that the estimator depends on the sequence of K symbols, $\mathbf{s}^{(i)}$. Thus, in order to compute $\text{LF}_{HLRT}^{(i)}(\mathbf{r})$, an estimate of the phase is needed for each of the M_i^K terms in (2.12), i.e., $m = 1, \dots, M_i^K$. To emphasize this dependency, we used the notation

$$\hat{\varphi}_m^{(i)} = -\frac{j}{2} \ln \left(\frac{\mathbf{s}_m^{(i)H} \mathbf{r}}{\mathbf{r}^H \mathbf{s}_m^{(i)}} \right), \quad m = 1, \dots, M_i^K, \quad i = 1, \dots, N_{\text{mod}}. \quad (2.19)$$

Signal Amplitude ML Estimator

By differentiating the likelihood function given in (2.11) w.r.t. the amplitude α , one has

$$\frac{\partial f(\mathbf{r} | \{s_k^{(i)}\}, \alpha, \varphi, N)}{\partial \alpha} = 0. \quad (2.20)$$

It can be shown that⁵

⁵ Derivation of this equation is given in Appendix B.

$$2\alpha \|\mathbf{s}^{(i)}\|^2 = e^{-j\varphi} \mathbf{s}^{(i)H} \mathbf{r} + e^{j\varphi} \mathbf{r}^H \mathbf{s}^{(i)}. \quad (2.21)$$

Hence, the signal amplitude ML estimator under hypothesis H_i is given by,

$$\hat{\alpha}^{(i)} = [e^{-j\varphi} \mathbf{s}^{(i)H} \mathbf{r} + e^{j\varphi} \mathbf{r}^H \mathbf{s}^{(i)}] / 2 \|\mathbf{s}^{(i)}\|^2, \quad i = 1, \dots, N_{\text{mod}}. \quad (2.22)$$

By using (2.17), (2.22) becomes

$$\hat{\alpha}^{(i)} = \text{Re}\{\sqrt{(\mathbf{s}^{(i)H} \mathbf{r})(\mathbf{r}^H \mathbf{s}^{(i)})}\} / \|\mathbf{s}^{(i)}\|^2, \quad i = 1, \dots, N_{\text{mod}}. \quad (2.23)$$

For each of the M_i^K combinations of K symbols for the i th modulation, $m = 1, \dots, M_i^K$,

this can be written as

$$\hat{\alpha}_m^{(i)} = \text{Re}\{\sqrt{(\mathbf{s}_m^{(i)H} \mathbf{r})(\mathbf{r}^H \mathbf{s}_m^{(i)})}\} / \|\mathbf{s}_m^{(i)}\|^2, \quad m = 1, \dots, M_i^K, \quad i = 1, \dots, N_{\text{mod}}. \quad (2.24)$$

For M -PSK signals $\|\mathbf{s}_m^{(i)}\|^2 = K$, and, thus, (2.24) reduces to,

$$\hat{\alpha}_m^{(i)} = \text{Re}\{\sqrt{(\mathbf{s}_m^{(i)H} \mathbf{r})(\mathbf{r}^H \mathbf{s}_m^{(i)})}\} / K, \quad m = 1, \dots, M_i^K, \quad i = 1, \dots, N_{\text{mod}}. \quad (2.25)$$

Note that in (2.24) and (2.25), we emphasize the dependency on the combination of K symbols taken from the constellation of the i th modulation.

Noise Power ML Estimator

By differentiating the likelihood function given in (2.11) w.r.t. the noise power N , one has

$$\frac{\partial f(\mathbf{r} | \{\mathbf{s}_k^{(i)}\}, \alpha, \varphi, N)}{\partial N} = 0. \quad (2.26)$$

This leads to the following expression for the noise power ML estimator under the hypothesis H_i ⁵,

$$\hat{N}^{(i)} = \frac{1}{K} \|\mathbf{r} - \alpha e^{j\varphi} \mathbf{s}^{(i)}\|^2, \quad i = 1, \dots, N_{\text{mod}}. \quad (2.27)$$

When joint estimation of channel amplitude, phase and noise power is performed, by substituting (2.16) and (2.22) into (2.27), the expression for the noise power ML estimator under the i th hypothesis, H_i , becomes,

$$\hat{N}^{(i)} = \frac{1}{K} \left(\|\mathbf{r}\|^2 - |\mathbf{r}^H \mathbf{s}^{(i)}|^2 / \|\mathbf{s}^{(i)}\|^2 \right), \quad i = 1, \dots, N_{\text{mod}}. \quad (2.28)$$

For each of the M_i^K combinations of K symbols for the i th modulation, $m = 1, \dots, M_i^K$, this can be written as

$$\hat{N}_m^{(i)} = \frac{1}{K} \left(\|\mathbf{r}\|^2 - |\mathbf{r}^H \mathbf{s}_m^{(i)}|^2 / \|\mathbf{s}_m^{(i)}\|^2 \right), \quad m = 1, \dots, M_i^K, \quad i = 1, \dots, N_{\text{mod}}. \quad (2.29)$$

From (2.19), (2.24) and (2.29), one can conclude that for a certain modulation, the ML estimators depend on the combination of K symbols, and in order to compute the LF in (2.12), these have to be calculated for all M_i^K symbol combinations.

2.2.1.2. The HLRT Classification Algorithm

After we get the expressions of the estimators of the unknown parameters, the LF is computed in the sequel by using these estimators. Using (2.22) and (2.16), one gets,

$$\hat{\alpha}^{(i)} e^{j\hat{\phi}^{(i)}} = \mathbf{s}^{(i)H} \mathbf{r} / \|\mathbf{s}^{(i)}\|^2, \quad (2.30)$$

and, further,

$$\hat{\alpha}^{(i)} e^{-j\hat{\phi}^{(i)}} = \mathbf{r}^H \mathbf{s}^{(i)} / \|\mathbf{s}^{(i)}\|^2. \quad (2.31)$$

Then, it can be easily shown that⁵

$$\|\mathbf{r} - \hat{\alpha}^{(i)} e^{j\hat{\phi}^{(i)}} \mathbf{s}^{(i)}\|^2 = \|\mathbf{r}\|^2 - |\mathbf{r}^H \mathbf{s}^{(i)}|^2 / \|\mathbf{s}^{(i)}\|^2, \quad i = 1, \dots, N_{\text{mod}}. \quad (2.32)$$

For each of the M_i^K combinations of K symbols, $m = 1, \dots, M_i^K$, this becomes

$$\|\mathbf{r} - \hat{\alpha}_m^{(i)} e^{j\hat{\theta}_m^{(i)}} \mathbf{s}_m^{(i)}\|^2 = \|\mathbf{r}\|^2 - |\mathbf{r}^H \mathbf{s}_m^{(i)}|^2 / \|\mathbf{s}_m^{(i)}\|^2, \quad m=1, \dots, M_i^K, \quad i=1, \dots, N_{\text{mod}}, \quad (2.33)$$

By substituting (2.29) and (2.33) in (2.12), one can easily prove that,

$$\text{LF}_{\text{HLRT}}^{(i)}(\mathbf{r}) = \frac{1}{M_i^K} \sum_{m=1}^{M_i^K} \frac{K^K}{(\pi e)^K \left(\|\mathbf{r}\|^2 - |\mathbf{r}^H \mathbf{s}_m^{(i)}|^2 / \|\mathbf{s}_m^{(i)}\|^2 \right)^K}, \quad i=1, \dots, N_{\text{mod}}, \quad (2.34)$$

which can be further written as,

$$\text{LF}_{\text{HLRT}}^{(i)}(\mathbf{r}) = \left(\frac{K}{\pi e M_i \|\mathbf{r}\|^2} \right)^K \sum_{m=1}^{M_i^K} \frac{1}{\left(1 - \left(|\mathbf{r}^H \mathbf{s}_m^{(i)}| / \|\mathbf{r}\| \|\mathbf{s}_m^{(i)}\| \right)^2 \right)^K}, \quad i=1, \dots, N_{\text{mod}}, \quad (2.35)$$

or, equivalently,

$$\text{LF}_{\text{HLRT}}^{(i)}(\mathbf{r}) = \left(\frac{K}{\pi e M_i \|\mathbf{r}\|^2} \right)^K \sum_{m=1}^{M_i^K} \frac{1}{(1 - \rho_m^{(i)2})^K}, \quad i=1, \dots, N_{\text{mod}}, \quad (2.36)$$

with $\rho_m^{(i)} = |\mathbf{r}^H \mathbf{s}_m^{(i)}| / (\|\mathbf{r}\| \|\mathbf{s}_m^{(i)}\|)$ as the correlation coefficient between \mathbf{r} and $\mathbf{s}_m^{(i)}$.

One can easily conclude from (2.36) that the LF for the HLRT classifier depends on the number of symbols K , the modulation format (through M_i and $\mathbf{s}_m^{(i)}$) and the received vector, \mathbf{r} .

2.2.2. QHLRT-based Classifier

With the QHLRT-based classifier, the likelihood function under the i th hypothesis, i.e., H_i : the i th modulation was transmitted, is computed by using MoM estimates of the unknown parameters and averaging over unknown constellation points.

With these parameters estimated under each hypothesis H_i , the likelihood function,

$\text{LF}_{\text{QHLRT}}^{(i)}(\mathbf{r})$, becomes

$$\text{LF}_{\text{QHLRT}}^{(i)}(\mathbf{r}) = \prod_{k=1}^K \frac{1}{M_i} \sum_{m=1}^{M_i} \frac{1}{\pi \hat{N}^{(i)}} \exp\left\{-\frac{1}{\hat{N}^{(i)}} |r_k - \hat{\alpha}^{(i)} e^{j\hat{\phi}^{(i)}} s_{k,m}^{(i)}|^2\right\}, \quad i=1, \dots, N_{\text{mod}}, \quad (2.37)$$

where $\hat{\alpha}^{(i)}$, $\hat{\phi}^{(i)}$ and $\hat{N}^{(i)}$ are the signal amplitude, phase and noise power MoM estimates, respectively, under hypothesis H_i .

A likelihood ratio test can be developed for the QHLRT-based classifier, similar to that given in (2.13) for the HLRT-based classifier. The decision rule for the HLRT-based classifier is given in (2.14), and is the same as for the QHLRT-based classifier.

2.2.2.1. Method of Moment (MoM) Parameter Estimators

Signal Amplitude and Noise Power MoM Estimators

By using (2.8) with $\mathbf{x}^{(i)} = \alpha e^{j\phi} \mathbf{s}^{(i)}$, we define the received signal power and noise power respectively as,

$$S^{(i)} = \text{E}[|x_k^{(i)}|^2] = \alpha^2 \text{E}[|s_k^{(i)}|^2], \quad i=1, \dots, N_{\text{mod}}, \quad (2.38)$$

and

$$N = \text{E}[|n_k|^2]. \quad (2.39)$$

Note that here we treat α as deterministic unknown. By using the results obtained in Appendix C for the first-, second-, third- and fourth-order moments of n_k , the following results are derived in Appendix D.

By using (2.38), (2.39), (C.3) and (C.4), it is straightforward that,

$$M_{21} = S^{(i)} + N, \quad (2.40)$$

where $M_{21} = E[|r_k|^2]$ is the second-order (one conjugate) moment of the received signal.

Similarly, by using (2.38), (2.39), (C.3), (C.4), (C.5), (C.6) and (C.7), it is straightforward that,

$$M_{42} = E[|x_k^{(i)}|^4] + 2N^2 + 4S^{(i)}N, \quad (2.44)$$

or

$$M_{42} = b^{(i)}S^{(i)2} + 4S^{(i)}N + 2N^2, \quad (2.41)$$

where $M_{42} = E[|r_k|^4]$ is the fourth-order (two conjugate) moment of the received signal

and $b^{(i)} = E[|x_k^{(i)}|^4] / (E[|x_k^{(i)}|^2])^2 = E[|s_k^{(i)}|^4] / (E[|s_k^{(i)}|^2])^2$, $i = 1, \dots, N_{\text{mod}}$.

Note that the parameter $b^{(i)}$ depends on the modulation format, i . For example, this is equal to 1 for M -PSK, 1.64 for 8-QAM, and 1.32 for 16-QAM [8].

The second- and fourth-order moments of the received signal, i.e., M_{21} and M_{42} , can be estimated respectively as [5],

$$\hat{M}_{21} = \frac{1}{K} \sum_{k=1}^K |r_k|^2 \quad \text{and} \quad \hat{M}_{42} = \frac{1}{K} \sum_{k=1}^K |r_k|^4. \quad (2.46)$$

From (2.40), the noise power estimator under hypothesis H_i is thus given by

$$\hat{N} = \hat{M}_{21} - \hat{S}^{(i)}. \quad (2.42)$$

By substituting (2.42) in (2.41), one gets the MoM estimator for received signal power under hypothesis H_i , as

$$\hat{S}^{(i)} = \sqrt{\frac{\hat{M}_{42} - 2\hat{M}_{21}^2}{b^{(i)} - 2}}, \quad i = 1, \dots, N_{\text{mod}}. \quad (2.43)$$

By using (2.38) and (2.43), the MoM estimator for the channel amplitude under hypothesis H_i becomes

$$\hat{\alpha}^{(i)} = \sqrt{\frac{\hat{S}^{(i)}}{\mathbb{E}[|s_k^{(i)}|^2]}} = \left(\frac{\hat{M}_{42} - 2\hat{M}_{21}^2}{b^{(i)} - 2} \right)^{1/4} (\mathbb{E}[|s_k^{(i)}|^2])^{-1/2}, \quad i = 1, \dots, N_{\text{mod}}. \quad (2.44)$$

Phase MoM Estimator

The MoM phase estimators for M -PSK and M -ary Quadrature Amplitude Modulations (M -QAM) signals under the i th hypothesis (i th modulation format) are calculated based on the output of matched filter, and are respectively given by [15].

$$\hat{\Phi}_{M\text{-PSK}}^{(i)} = \frac{1}{M_i} \arg \left(\sum_{k=1}^K r_k^{M_i} \right), \quad (2.45)$$

and

$$\hat{\Phi}_{M\text{-QAM}}^{(i)} = \frac{1}{4} \arg \left(-\sum_{k=1}^K r_k^4 \right). \quad (2.46)$$

2.2.2.2. The QHLRT Classification Algorithm

The LF under each hypothesis H_i , $i = 1, \dots, N_{\text{mod}}$ is calculated as given in (2.37), with MoM-based estimates of the channel amplitude, phase and noise power computed as shown in Section 2.2.2.1. Then, with the LFs calculated under all N_{mod} hypotheses, the criterion in (2.14) is applied for decision-making.

2.3. Complexity Analysis of Proposed Classifiers

With the HLRT-based classifier, the LF under each hypothesis H_i , $i = 1, \dots, N_{\text{mod}}$, is computed by averaging over M_i^K possible K symbol combinations (corresponding to

the modulation format i , with M_i points in signal constellation). Hence, the complexity for the i th modulation format is of the order of $\mathcal{O}(KM_i^K)$. For an N_{mod} -ary classification problem, the computational complexity becomes $\mathcal{O}(K\sum_{i=1}^{N_{\text{mod}}} M_i^K)$. This increases at a rate faster than exponential with an increase in the number of symbols K . Also, it increases for higher modulation schemes involved in classification.

On the other hand, for the QHLRT-based classifier, the overall complexity reduces to $\mathcal{O}(K\sum_{i=1}^{N_{\text{mod}}} M_i)$, as in this case averaging over combinations of symbols is not required.

It is apparent that the computation complexity is significantly reduced with the QHLRT-based classifier.

2.4. Performance Measure

We evaluate the performance of the HLRT- and QHLRT-based classifiers through simulations. The average probability of correct classification is used as the performance measure. This is defined as

$$P_{cc} = N_{\text{mod}}^{-1} \sum_{i=1}^{N_{\text{mod}}} P_c^{(ii)}, \quad (2.47)$$

where $P_c^{(ii)}$ is the conditional probability of the event that the i th modulation is received, when indeed the i th modulation was originally transmitted.

2.5. Simulation Results

We chose MATLAB as the simulation tool as it provides access to a large number of powerful tools and built-in functions, when compared to other simulation packages. Also, it gives flexibility and easy options to modify and format figures. Classification

results achieved with investigated HLRT- and QHLRT-based algorithms to discriminate M -PSK signals in block fading channel³ are subsequently presented. In addition, performance of an ALRT-based algorithm is shown for comparison. This is developed under the assumption of perfect estimates of the unknown parameters, with the likelihood function computed by averaging over unknown constellation points only [2]. Note that this serves as an idealized reference against which performance of the HLRT- and QHLRT-based classifiers is evaluated. In the sequel, we consider BPSK, QPSK, 8-PSK and 16-PSK as candidate modulations, unless otherwise mentioned. Without any loss of generality, normalized constellations are generated in simulations, i.e., $E[|s_k^{(i)}|^2] = 1$. The averaging fading power is also set to one, i.e., $E[\alpha^2] = 1$. Thus, the (average) SNR is changed by varying the noise power only. The number of Monte Carlo trials used to calculate $P_c^{(lit)}$ is 1000.

In Fig. 2, we show classification performance of the ALRT-, HLRT- and QHLRT-based algorithms in Rayleigh fading channel³. Due to the high complexity of the HLRT-based algorithm, simulations are run only for smaller size constellations, i.e., BPSK and QPSK, with $K = 10$ symbols. As expected, ALRT shows the best performance; 3.25 dB and 3.75 dB increase in SNR is required with the HLRT- and QHLRT-based algorithms, respectively, to achieve an average probability of correct classification, P_{cc} , of 0.9, when compared with ALRT. On the other hand, one can easily notice that HLRT does not provide significant performance improvement over QHLRT.

In Fig. 3, classification results achieved with the ALRT- and QHLRT-based algorithms in Rayleigh fading channel³ are presented, with $K=100$ and $K=1000$ symbols, respectively. Apparently, there is a significant improvement in the performance of both algorithms with the increase in the number of symbols. The HLRT-based algorithm was dropped because of its high complexity. The simulations for HLRT, when discriminating BPSK and QPSK with $K=10$ symbols took about couple of days to complete but with $K=100$ and $K=1000$, we suspect that the simulations would easily over months even with high-performance machines.

In Fig. 4, classification performance of the ALRT- and QHLRT-based algorithms in Ricean fading channel is given, with $K=1000$ symbols. The average probability of correct classification, P_{cc} , is plotted against the Rice factor, K_R ⁶. The values $K_R=0$ and $K_R=\infty$ correspond to the cases of Rayleigh fading and no fading, respectively [5]. Simulation results reveal the reasonable performance of the QHLRT-based classifier for the whole range of K_R values.

Note that simulation results show that the QHLRT-based algorithm can collapse in identifying M -PSK modulations as the SNR decreases, as the MoM method can fail to estimate the channel amplitude⁷ and consequently, the noise power. For example, at 0dB SNR, and with $K=100$ processed symbols, the MoM method failed 162 times out of 1000 to estimate the channel amplitude and noise power, when BPSK signals are

⁶ For the definition of the Rice factor, see [16] Ch. 2.

⁷ As noticed from simulations, the channel amplitude MoM estimate can become a complex number. This is because in (2.43), the quantity inside the square root becomes negative when the estimates \hat{M}_{21} and \hat{M}_{42} are not accurate enough.

received (see Fig. 3). Apparently, more failures occur as the SNR decreases. However, when recognizing BPSK, QPSK, 8-PSK and 16-PSK signals with $K = 1000$ processed symbols, there were only few failures at an SNR of 10 dB and above.

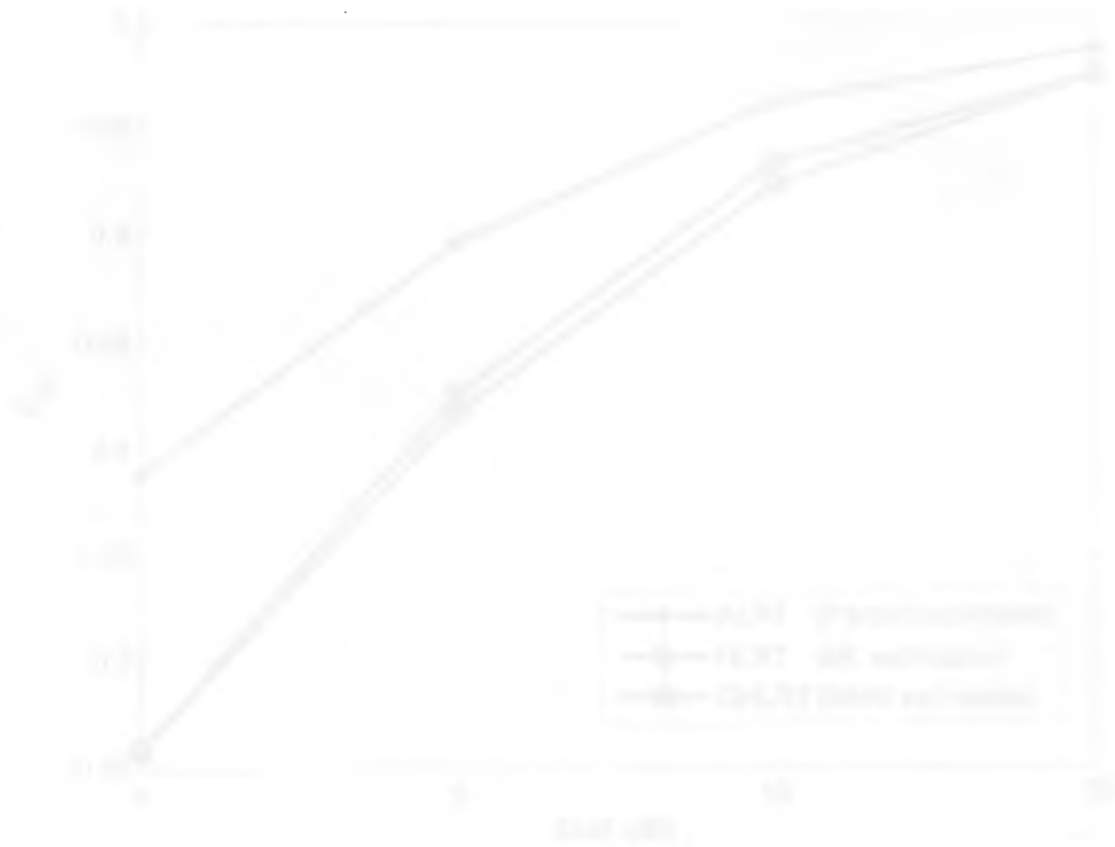


Fig. 3 Performance comparison of Maximum Likelihood (MLSE) algorithm to Karim's MLSE, MLSE with channel estimation and MLSE with channel estimation.

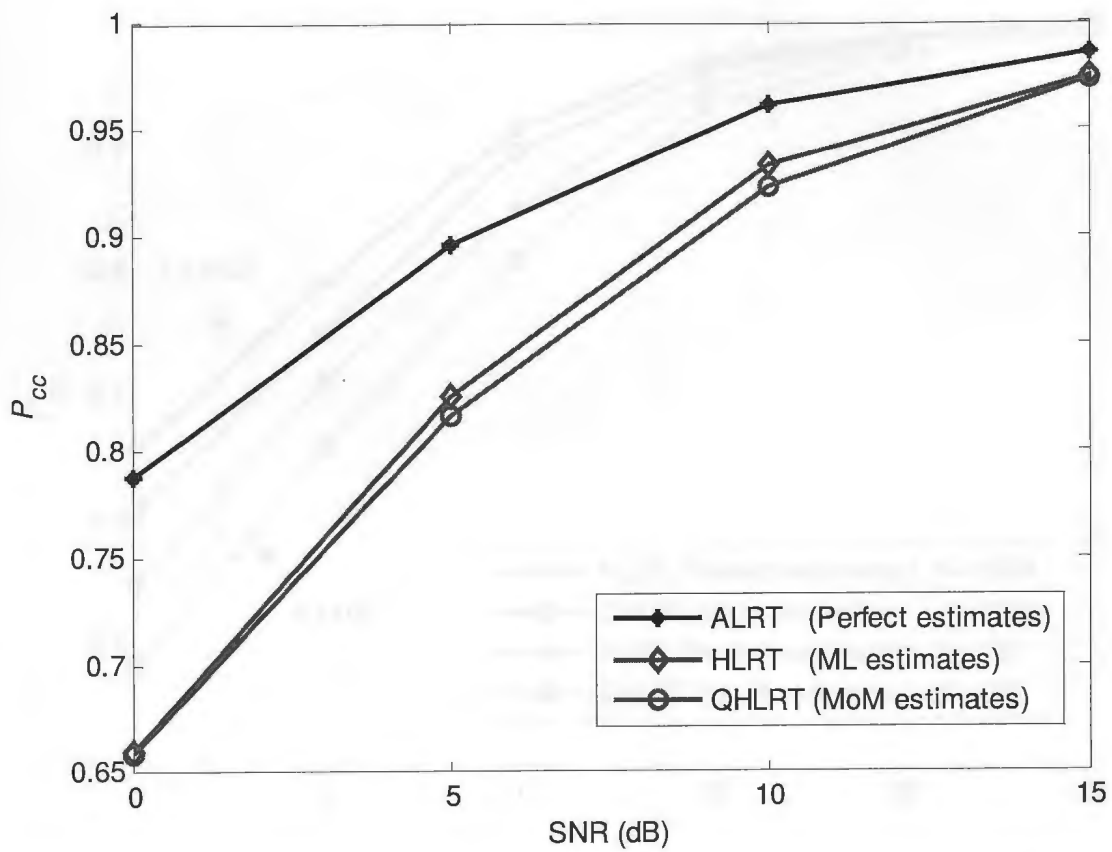


Fig. 2. Performance comparison of likelihood-based algorithms in Rayleigh fading, when discriminating BPSK and QPSK, with $K = 10$ symbols.

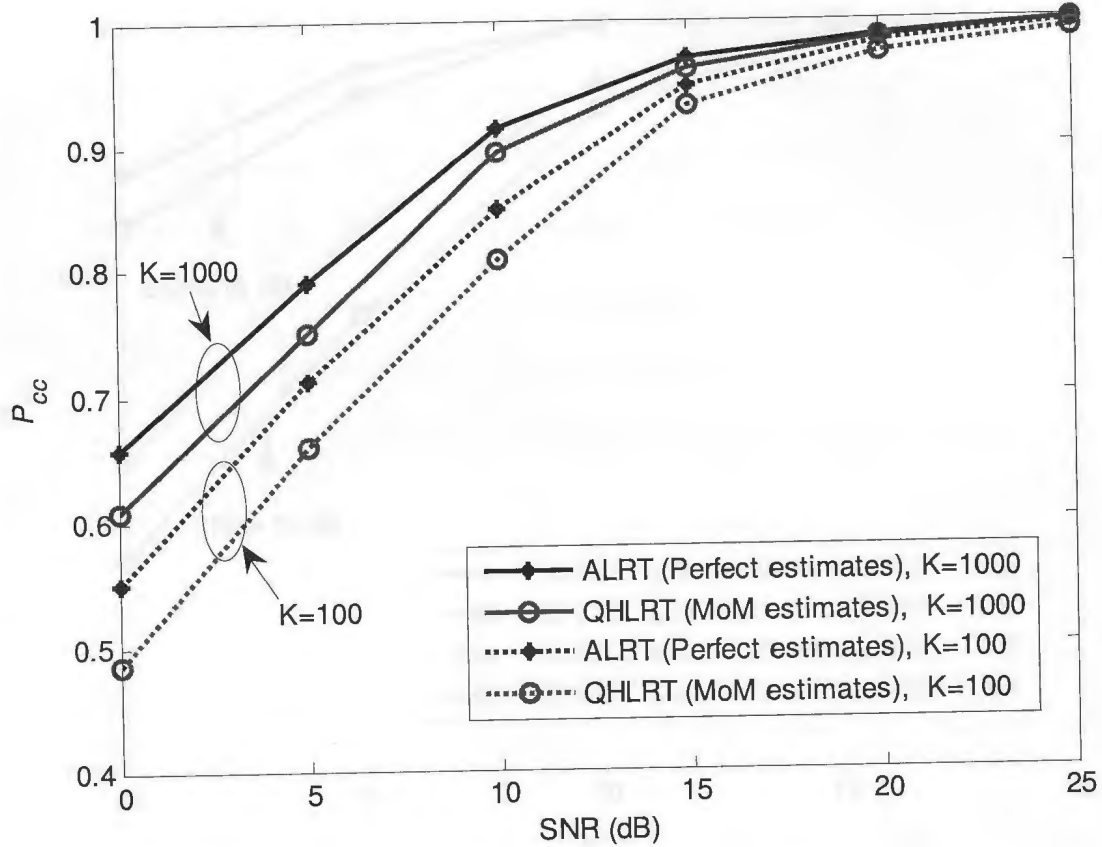


Fig. 3. Performance of QHLRT when discriminating BPSK, QPSK, 8-PSK and 16-PSK in Rayleigh fading, with $K = 100$ and $K = 1000$ symbols.

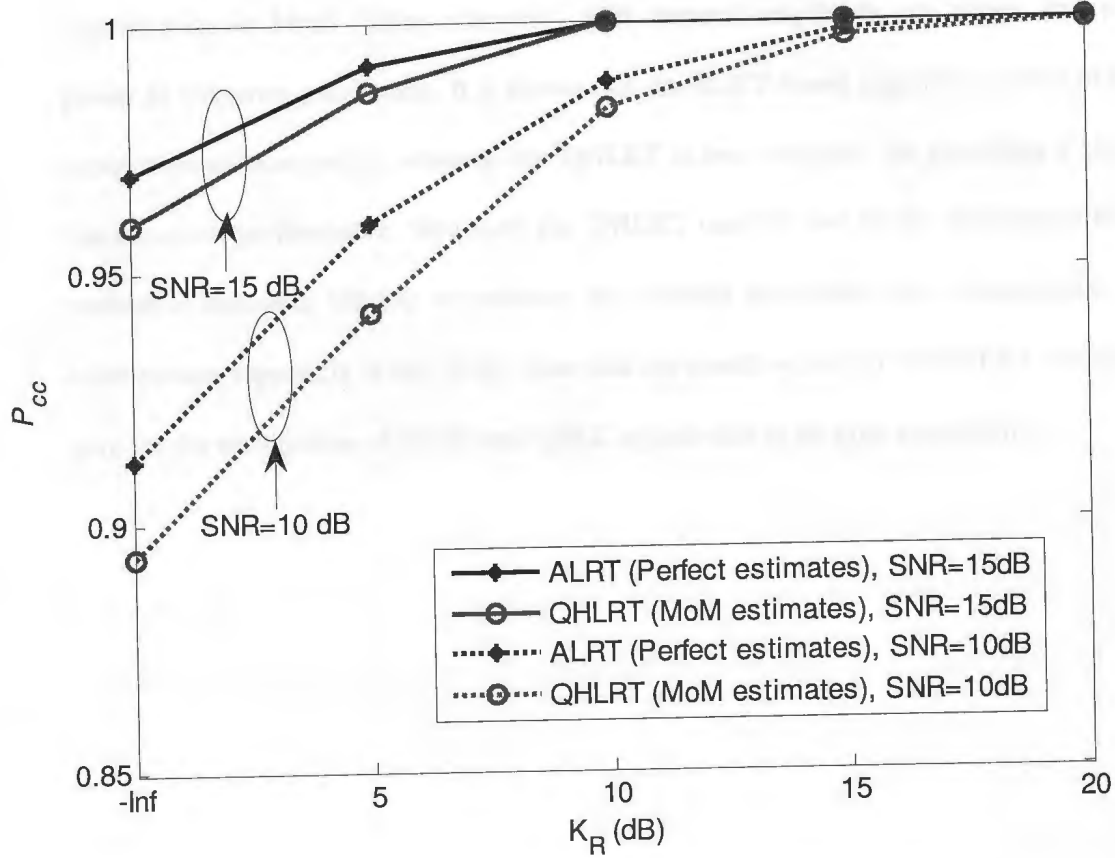


Fig. 4. Performance of QHLRT when discriminating BPSK, QPSK, 8-PSK, 16-PSK in Ricean fading, with $K = 1000$ symbols.

2.6. Chapter Summary

The performance and complexity of the hybrid likelihood ratio test (HLRT)- and quasi-HLRT (QHLRT)-based algorithms are investigated for linear digital modulation classification in block fading channels³, with channel amplitude and phase, and noise power as unknown parameters. It is shown that the HLRT-based algorithm suffers of high computational complexity, whereas the QHLRT is less complex, yet providing a similar classification performance. However, the QHLRT can fail due to the inadequacy of the method-of-moments (MoM) to estimate the channel amplitude and, consequently, the noise power, especially at low SNR. Note that the results achieved with HLRT are shown only for the recognition of BPSK and QPSK signals due to its high complexity.

CHAPTER 3

3. CRAMER-RAO LOWER BOUNDS (CRLB) OF CHANNEL PARAMETER ESTIMATORS

3.1. Introduction to CRLB

In many communication systems, it is essential to estimate the incoming signal parameters. Typical unknown parameters include the time-delay, frequency offset, channel amplitude, phase, noise power, etc. For example, timing recovery is a critical aspect of digital receivers. The incoming signal needs to be synchronized with the receiver clock in order to achieve accurate demodulation. Similarly, carrier recovery is important for coherent demodulation. In many applications, the parameters are estimated with no prior knowledge of the transmitted signal, as in case of blind modulation classification. Apart from computational complexity, it is important to assess the performance of these estimators in terms of their bias and variance. The bias of a parameter estimator, $\hat{\theta}$, is defined as

$$\text{bias}(\hat{\theta}) = E[\hat{\theta}] - \theta, \quad (3.1)$$

where $E[\hat{\theta}]$ is the expected value of the parameter estimate and θ is the true value of that parameter.

The Cramer-Rao lower bound (CRLB) is a well-known lower bound on the variance of any unbiased estimator [13]. This provides an idealized reference against which we can compare the performance of an unbiased estimator; it indicates the

impossibility of finding an unbiased estimator whose variance is less than the CRLB. The CRLB theorem for a scalar parameter θ is stated as follows [17].

Theorem: It is assumed that the probability density function (pdf) $f(\mathbf{r};\theta)$ satisfies the regularity condition

$$E\left[\frac{\partial \ln f(\mathbf{r};\theta)}{\partial \theta}\right] = 0, \text{ for all } \theta, \quad (3.2)$$

where \mathbf{r} is the vector of the samples taken at the output of receive matched filter and the expectation is taken with respect to $f(\mathbf{r};\theta)$, then the variance of any unbiased estimator $\hat{\theta}$ must satisfy

$$\text{var}(\hat{\theta}) \geq \frac{1}{-E\left[\frac{\partial^2 \ln f(\mathbf{r};\theta)}{\partial \theta^2}\right]}, \quad (3.3)$$

where the derivative is evaluated at the true value of θ and the expectation is taken with respect to $f(\mathbf{r};\theta)$. The expectation is explicitly given by [17]

$$E\left[\frac{\partial^2 \ln f(\mathbf{r};\theta)}{\partial \theta^2}\right] = \int \frac{\partial^2 \ln f(\mathbf{r};\theta)}{\partial \theta^2} f(\mathbf{r};\theta) d\mathbf{r}, \quad (3.4)$$

since the second derivative is a random variable dependent on \mathbf{r} .

CRLB can be extended to the case of vector parameter $\boldsymbol{\theta} = [\theta_1 \ \theta_2 \ \dots \ \theta_p]^\dagger$, with the assumption that the estimator of the vector parameter, $\hat{\boldsymbol{\theta}}$, is unbiased [17]. The CRLB for the vector parameter estimator allows us to place a bound on the variance of each element. The CRLB is the $[i, i]$ element of the inverse of a matrix or,

$$\text{var}(\hat{\theta}_i) \geq [\mathbf{I}^{-1}(\boldsymbol{\theta})]_{ii}, \quad (3.5)$$

where $\mathbf{I}(\boldsymbol{\theta})$ is the $p \times p$ Fisher Information Matrix (FIM) [17]. The $[i, j]$ element of the FIM is defined as

$$[\mathbf{I}(\boldsymbol{\theta})]_{ij} = -\mathbb{E} \left[\frac{\partial^2 \ln f(\mathbf{r}; \boldsymbol{\theta})}{\partial \theta_i \partial \theta_j} \right], \quad (3.6)$$

with $i=1,2,\dots,p$, and $j=1,2,\dots,p$. In evaluating the above expression, the true value of $\boldsymbol{\theta}$ is used. Note that in the scalar case ($p=1$), $\mathbf{I}(\boldsymbol{\theta})=I(\theta)$ and we have the scalar CRLB [17]. With three unknown parameters (our case here), the FIM can be written as,

$$\mathbf{I}(\boldsymbol{\theta}) = \begin{bmatrix} [\mathbf{I}(\boldsymbol{\theta})]_{11} & [\mathbf{I}(\boldsymbol{\theta})]_{12} & [\mathbf{I}(\boldsymbol{\theta})]_{13} \\ [\mathbf{I}(\boldsymbol{\theta})]_{21} & [\mathbf{I}(\boldsymbol{\theta})]_{22} & [\mathbf{I}(\boldsymbol{\theta})]_{23} \\ [\mathbf{I}(\boldsymbol{\theta})]_{31} & [\mathbf{I}(\boldsymbol{\theta})]_{32} & [\mathbf{I}(\boldsymbol{\theta})]_{33} \end{bmatrix}. \quad (3.7)$$

In this work, we considered the vector of unknown parameters as $\boldsymbol{\theta} = [\alpha \ N \ \varphi]^T$, with $N = 2\sigma^2$ as the noise power. Thus, (3.7) can be further written as

$$\mathbf{I}(\boldsymbol{\theta}) = \begin{bmatrix} -\mathbb{E} \left(\frac{\partial^2 \ln f(\mathbf{r} | \boldsymbol{\theta})}{\partial \alpha^2} \right) & -\mathbb{E} \left(\frac{\partial^2 \ln f(\mathbf{r} | \boldsymbol{\theta})}{\partial \alpha \partial N} \right) & -\mathbb{E} \left(\frac{\partial^2 \ln f(\mathbf{r} | \boldsymbol{\theta})}{\partial \alpha \partial \varphi} \right) \\ -\mathbb{E} \left(\frac{\partial^2 \ln f(\mathbf{r} | \boldsymbol{\theta})}{\partial N \partial \alpha} \right) & -\mathbb{E} \left(\frac{\partial^2 \ln f(\mathbf{r} | \boldsymbol{\theta})}{\partial N^2} \right) & -\mathbb{E} \left(\frac{\partial^2 \ln f(\mathbf{r} | \boldsymbol{\theta})}{\partial N \partial \varphi} \right) \\ -\mathbb{E} \left(\frac{\partial^2 \ln f(\mathbf{r} | \boldsymbol{\theta})}{\partial \varphi \partial \alpha} \right) & -\mathbb{E} \left(\frac{\partial^2 \ln f(\mathbf{r} | \boldsymbol{\theta})}{\partial \varphi \partial N} \right) & -\mathbb{E} \left(\frac{\partial^2 \ln f(\mathbf{r} | \boldsymbol{\theta})}{\partial \varphi^2} \right) \end{bmatrix}. \quad (3.8)$$

In [18], CRLB of the estimators of SNR for BPSK and QPSK are derived, while in [19], this is derived for the phase estimators. In this Chapter, we derive CRLB expressions of the unknown channel amplitude, phase and noise power NDA estimators for BPSK and QPSK signals. After that, we compare the variance of MoM (NDA) estimators of these unknown parameters, against their respective CRLBs. This gives us

an indication about the degree of accuracy of the MoM estimators (for the SNR range in which these estimators are unbiased¹). The bias of these estimators was investigated through simulations.

3.2. CRLBs of Channel Amplitude, Phase and Noise Power Estimators for BPSK

We present here the results obtained for CRLBs of channel amplitude, phase and noise power estimators for the BPSK signals⁸.

By averaging (2.10) over $s_k^{(BPSK)}$, ($s_k^{(BPSK)} \in \{-1, 1\}$), one can easily show that

$$f_B(\mathbf{r} | \boldsymbol{\theta}) = \prod_{k=1}^K \frac{1}{\pi N} \exp\left\{-\frac{1}{N}(|r_k|^2 + \alpha^2)\right\} \cosh\left(\frac{2\alpha}{N} \operatorname{Re}\{r_k e^{-j\varphi}\}\right), \quad (3.9)$$

with the subscript 'B' standing for the BPSK signals. This result is derived in Appendix E. Taking the natural logarithm of (3.9), one obtains

$$\begin{aligned} \ln f_B(\mathbf{r} | \boldsymbol{\theta}) = & -K \ln(\pi N) - \frac{1}{N} \sum_{k=1}^K (I^2(k) + Q^2(k) + \alpha^2) \\ & + \sum_{k=1}^K \ln\left(\cosh\left(\frac{2\alpha}{N} (I(k) \cos \varphi + Q(k) \sin \varphi)\right)\right), \end{aligned} \quad (3.10)$$

where $I(k)$ and $Q(k)$ are the real and imaginary parts of observed signal samples r_k , respectively, known at the receive-side. With $\boldsymbol{\theta} = [\alpha \ N \ \varphi]^T$ as unknown parameters and for BPSK constellation, the FIM becomes⁸

$$\mathbf{I}_B(\boldsymbol{\theta}) = \frac{2K}{N^2} \begin{bmatrix} N - Nf_1(\gamma) & \alpha f_1(\gamma) & 0 \\ \alpha f_1(\gamma) & \frac{1}{2} - \frac{\alpha^2}{N} f_1(\gamma) & 0 \\ 0 & 0 & \alpha^2 N - \alpha^2 N f_2(\gamma) \end{bmatrix}, \quad (3.11)$$

where $\gamma = \alpha^2 / N = \alpha^2 / 2\sigma^2$ is the (instantaneous) SNR,

⁸ The derivations are given in Appendix F.

$$f_1(\gamma) = \frac{\exp(-\gamma)}{\sqrt{2\pi}} \int_{-\infty}^{\infty} \frac{u^2 \exp(-u^2/2)}{\cosh(u\sqrt{2\gamma})} du, \quad (3.12)$$

and

$$f_2(\gamma) = \frac{\exp(-\gamma)}{\sqrt{2\pi}} \int_{-\infty}^{\infty} \frac{\exp(-u^2/2)}{\cosh(u\sqrt{2\gamma})} du. \quad (3.13)$$

One can notice that the functions $f_1(\gamma)$ and $f_2(\gamma)$ depend only on the instantaneous SNR, γ , and not on the actual values of the parameters α , N or φ .

By taking the inverse of the FIM in (3.11) and using (3.12) and (3.13), one gets the following expressions of the CRLBs

$$\text{CRLB}_B(\hat{\alpha}) = [\mathbf{I}_B^{-1}(\boldsymbol{\theta})]_{11} = \frac{\alpha^2 \frac{1}{2\gamma} - f_1(\gamma)}{K (1 - f_1(\gamma) - 2\gamma f_1(\gamma))}, \quad (3.14)$$

$$\text{CRLB}_B(\hat{N}) = [\mathbf{I}_B^{-1}(\boldsymbol{\theta})]_{22} = \frac{N^2 (1 - f_1(\gamma))}{K (1 - f_1(\gamma) - 2\gamma f_1(\gamma))}, \quad (3.15)$$

and

$$\text{CRLB}_B(\hat{\varphi}) = [\mathbf{I}_B^{-1}(\boldsymbol{\theta})]_{33} = \frac{1}{2\gamma K (1 - f_2(\gamma))}. \quad (3.16)$$

One can easily notice the dependency of the CRLBs of the parameter estimators on γ and K . CRLBs of the estimators of α , N and φ are inversely proportional to K , i.e., the bound values decrease as K increases. This is in agreement with the behavior of the estimators, that their variance decreases as the size of the observation interval K increases, due to the improvement in the estimation accuracy. Furthermore, CRLBs of the estimators of α and N also depend on the actual value of the parameter, whereas the

CRLB of the estimator of φ does not. Therefore, for the same SNR value, CRLB of the estimators of the former parameters will be different for different values of the parameter, whereas, this is not the case with the latter parameter.

3.3. CRLBs of Channel Amplitude, Phase and Noise Power Estimators for QPSK

Next, we present the results of the derivation of CRLBs of the estimators of the parameters, α , N and φ , for the QPSK signals. These results can be similarly derived, as presented for BPSK signals in Appendix F. The log-likelihood function, obtained by averaging (2.10) over $s_k^{(QPSK)}$, with

$$s_k^{(QPSK)} \in \left\{ \frac{1}{\sqrt{2}}(1+j), \frac{1}{\sqrt{2}}(-1+j), \frac{1}{\sqrt{2}}(1-j), \frac{1}{\sqrt{2}}(-1-j) \right\},$$

and taking the natural logarithm, is given by

$$\begin{aligned} \ln f_Q(\mathbf{r} | \boldsymbol{\theta}) = & -K \ln(\pi N) - \frac{1}{N} \sum_{k=1}^K (I^2(k) + Q^2(k) + \alpha^2) \\ & + \sum_{k=1}^K \ln \left(\cosh \left(\frac{\alpha \sqrt{2}}{N} (I(k) \cos \varphi + Q(k) \sin \varphi) \right) \right) \\ & + \sum_{k=1}^K \ln \left(\cosh \left(\frac{\alpha \sqrt{2}}{N} (-I(k) \sin \varphi + Q(k) \cos \varphi) \right) \right). \end{aligned} \quad (3.17)$$

With $\boldsymbol{\theta} = [\alpha \ N \ \varphi]^T$ as unknown parameters, the FIM for the QPSK signals becomes

$$\mathbf{I}_Q(\boldsymbol{\theta}) = \frac{2K}{N^2} \begin{bmatrix} N - N f_1\left(\frac{\gamma}{2}\right) & \alpha f_1\left(\frac{\gamma}{2}\right) & 0 \\ \alpha f_1\left(\frac{\gamma}{2}\right) & \frac{1}{2} - \frac{\alpha^2}{N} f_1\left(\frac{\gamma}{2}\right) & 0 \\ 0 & 0 & \alpha^2 N - \alpha^2 N(1+\gamma) f_2\left(\frac{\gamma}{2}\right) \end{bmatrix}, \quad (3.18)$$

where $f_1(\cdot)$ and $f_2(\cdot)$ are defined in (3.12) and (3.13), respectively and the subscript 'Q' stands for QPSK signals. The CRLB expressions of the estimators of α , N and φ are obtained by taking the inverse of FIM in (3.18) and using the functions given in (3.12) and (3.13). They thus become

$$\text{CRLB}_Q(\hat{\alpha}) = [\mathbf{I}_Q^{-1}(\boldsymbol{\theta})]_{11} = \frac{\alpha^2}{K} \frac{\frac{1}{2\gamma} - f_1\left(\frac{\gamma}{2}\right)}{1 - f_1\left(\frac{\gamma}{2}\right) - 2\gamma f_1\left(\frac{\gamma}{2}\right)}, \quad (3.19)$$

$$\text{CRLB}_Q(\hat{N}) = [\mathbf{I}_Q^{-1}(\boldsymbol{\theta})]_{22} = \frac{N^2}{K} \frac{1 - f_1\left(\frac{\gamma}{2}\right)}{1 - f_1\left(\frac{\gamma}{2}\right) - 2\gamma f_1\left(\frac{\gamma}{2}\right)}, \quad (3.20)$$

and

$$\text{CRLB}_Q(\hat{\varphi}) = [\mathbf{I}_Q^{-1}(\boldsymbol{\theta})]_{33} = \frac{1}{2\gamma K} \frac{1}{1 - (1 + \gamma)f_2\left(\frac{\gamma}{2}\right)}. \quad (3.21)$$

Again, it can be noticed that the CRLB expressions in (3.19), (3.20) and (3.21) depend on γ and K . The bound values decrease with an increase in the size of the observation interval K . Also, the CRLBs of the α and N parameter estimators vary with the actual parameter values, whereas the CRLB of the φ parameter estimator does not.

3.4. Numerical Results

With the functions in (3.12) and (3.13), calculated through numerical integration, the CRLB expressions derived for the estimators of the channel amplitude, α , channel phase, φ , and noise power, N , are evaluated for both BPSK and QPSK signals.

CRLBs of the estimators of the channel amplitude and noise power depend on the actual value of the parameter, whereas CRLB of the φ parameter estimator does not. Results are shown here for AWGN channel, i.e., α constant ($\alpha=1$) and with $K=100$ and $K=1000$ symbols, respectively. Note that the CRLB expressions are also valid for fading channels.

Fig. 5, Fig. 6 and Fig. 7 show the CRLBs of the estimators of channel amplitude α , phase, φ , and noise power, N , respectively for BPSK and QPSK signals. For a given SNR and for a certain parameter estimator, the CRLB for BPSK is lower compared with that obtained for QPSK. This is because estimation for BPSK can be more accurate than for QPSK. Furthermore, at low SNR, the difference between the CRLBs of the parameter estimators for BPSK and QPSK is more significant. Apparently, for both BPSK and QPSK, the CRLB becomes lower as K increases.

In Fig. 8 - Fig. 13, variance of MoM estimators of α , φ and N for BPSK and QPSK are shown along with corresponding CRLB. This variance is calculated based on the Monte-Carlo trials out of 1000, in which the MoM estimators do not fail. It can be noticed that the variance of MoM estimators becomes lower than the CRLB below a certain SNR value. This can easily be explained by the fact that MoM estimators are asymptotically unbiased [9], [12], i.e., unbiased as K reaches infinity. However, with a finite K , as the SNR decreases below a certain limit, these estimators become biased. With both $K=100$ and $K=1000$ symbols, and at low SNR, the MoM estimators become biased and thus, the CRLBs no longer remain applicable. With $K=100$ symbols, the MoM estimators of α , φ and N for QPSK become biased at SNR value of

around -1.5 dB (see Fig. 9, Fig. 11 and Fig. 13), whereas for BPSK, the MoM estimators of α and φ become biased around -20 dB and -10 dB, respectively (see Fig. 8 and Fig. 10). Interestingly, the MoM estimator of N for BPSK remains unbiased in the investigated SNR range, i.e., between -30dB and 0dB (see Fig. 12). To be noted that the SNR value at which MoM estimators become biased is shifted to lower SNR as K increases, due to increased estimation accuracy. In the SNR range where CRLBs hold for the estimators, the variance of MoM estimators of α , φ and N for BPSK and QPSK is reasonably close to their corresponding CRLBs. Furthermore, this difference reduces with an increase in SNR and number of symbols, K .

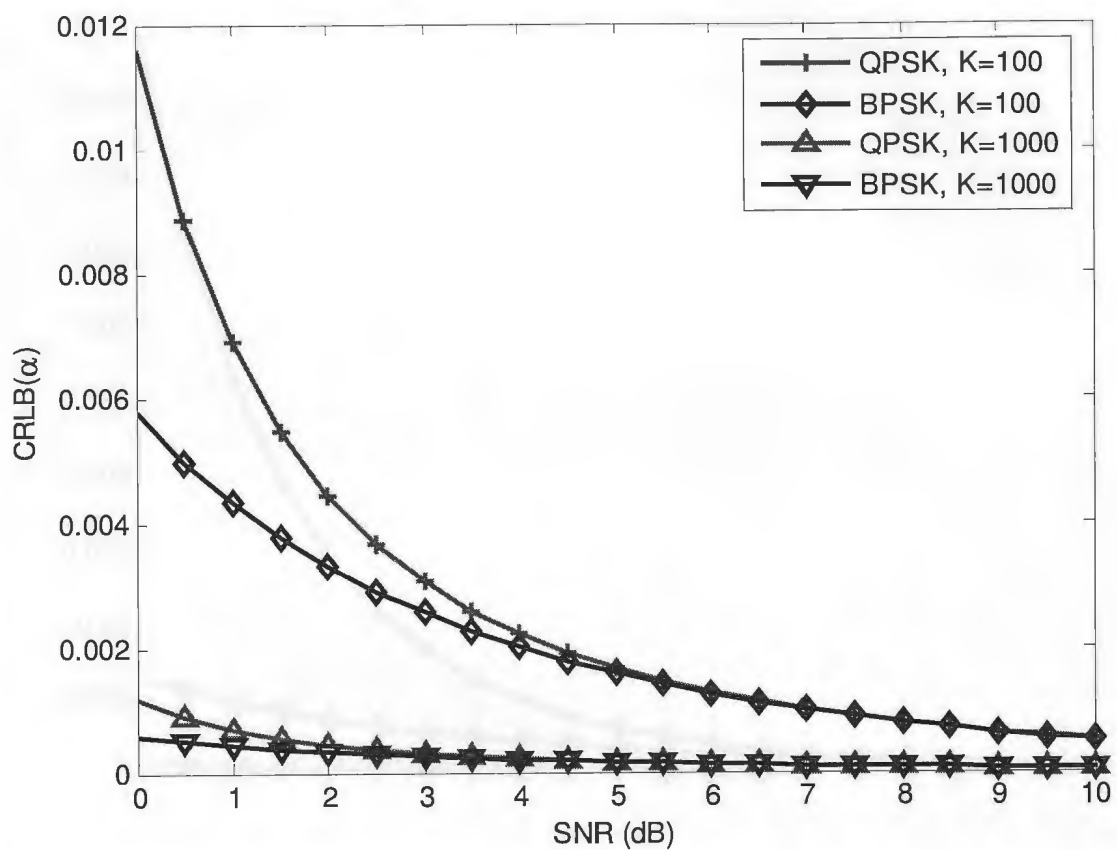


Fig. 5. Cramer-Rao lower bounds of channel amplitude estimators for BPSK and QPSK signals, with different observation interval lengths K .

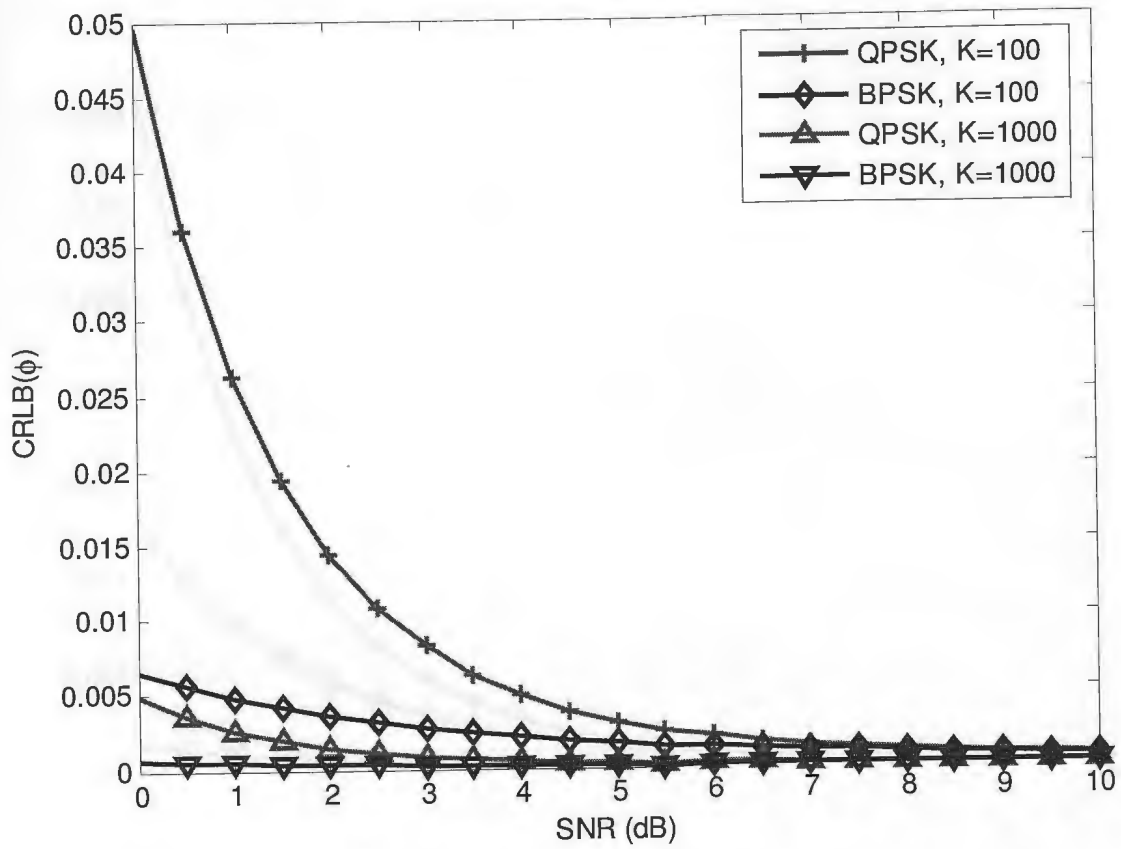


Fig. 6. Cramer-Rao lower bounds of channel phase estimators for BPSK and QPSK signals, with different observation interval lengths K .

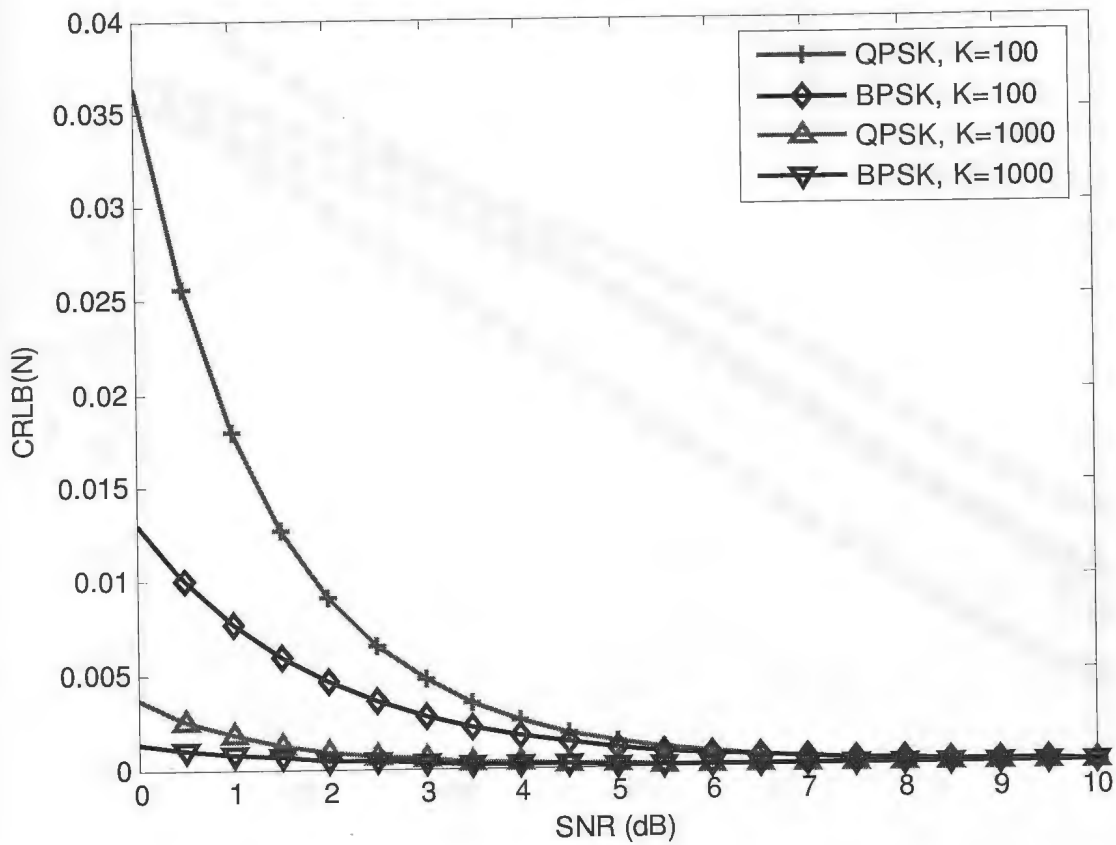


Fig. 7. Cramer-Rao lower bounds of noise power estimators for BPSK and QPSK signals, with different observation interval lengths K .

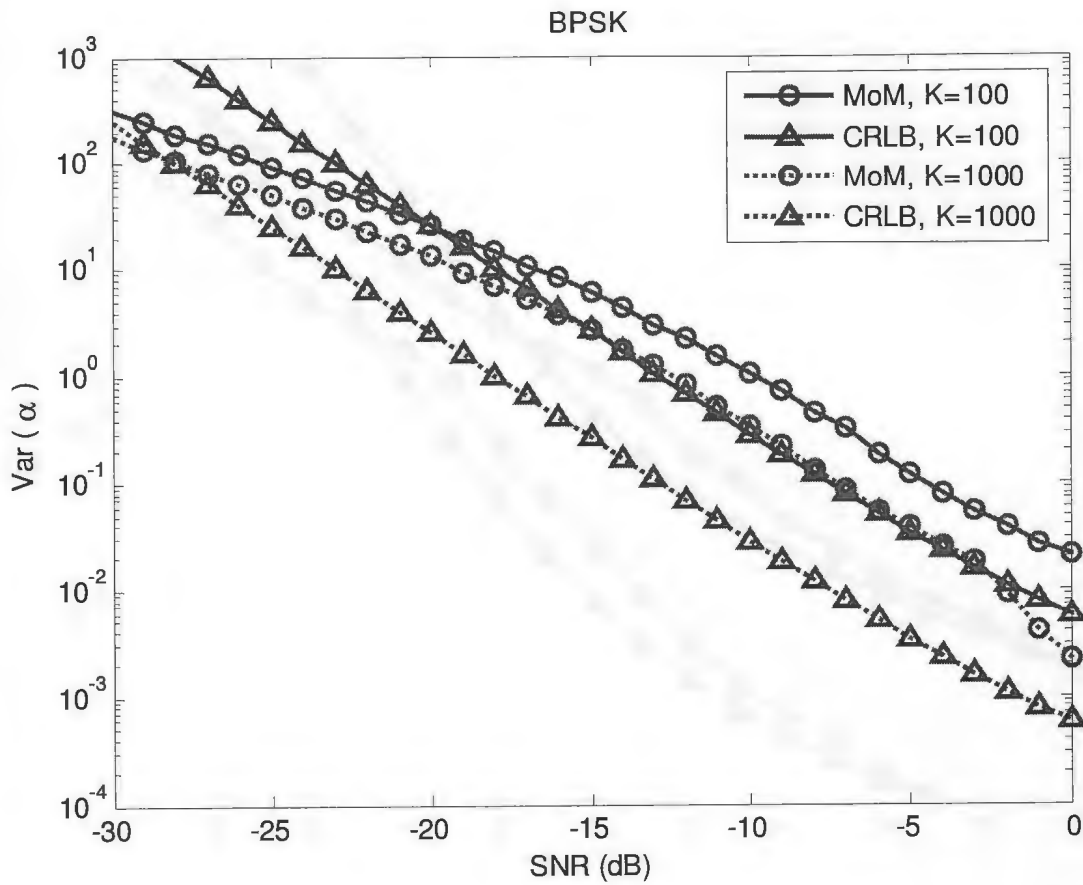


Fig. 8. Comparison of the variance of channel amplitude MoM estimators and corresponding CRLB for BPSK signals.

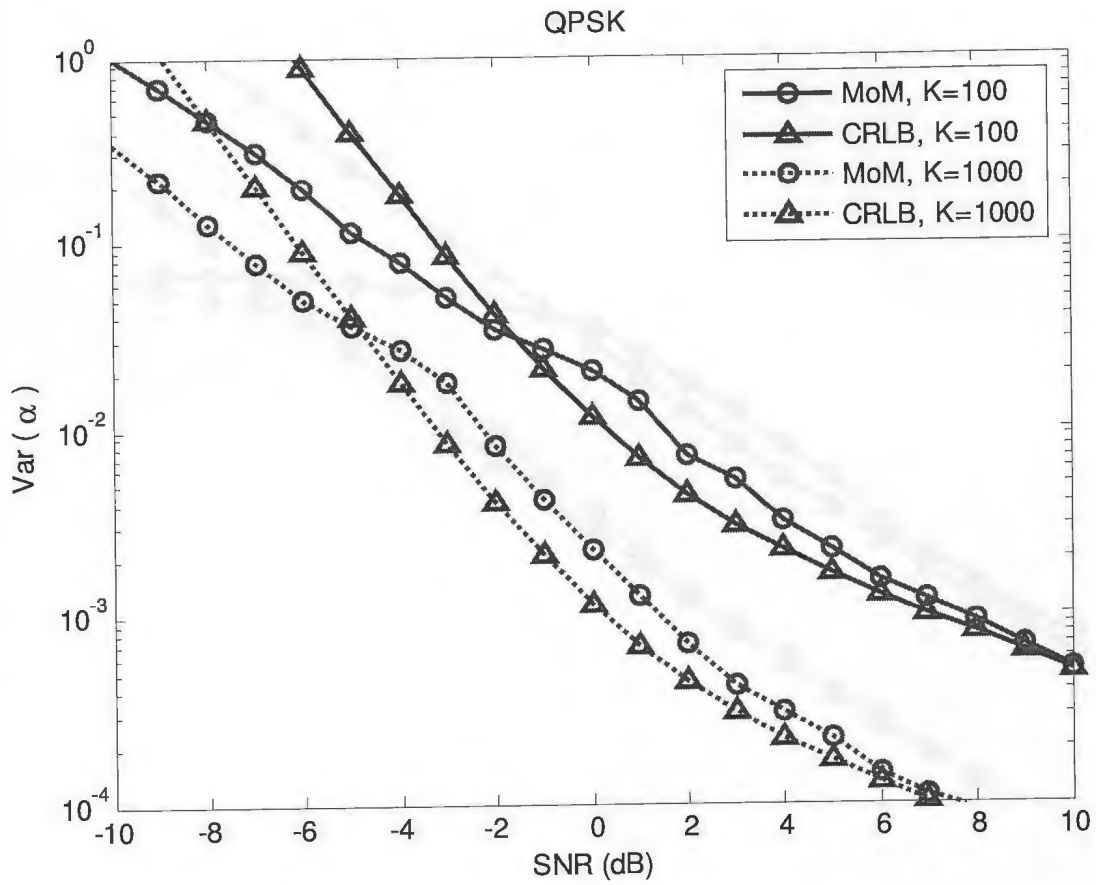


Fig. 9. Comparison of the variance of channel amplitude MoM estimators and corresponding CRLB for QPSK signals.

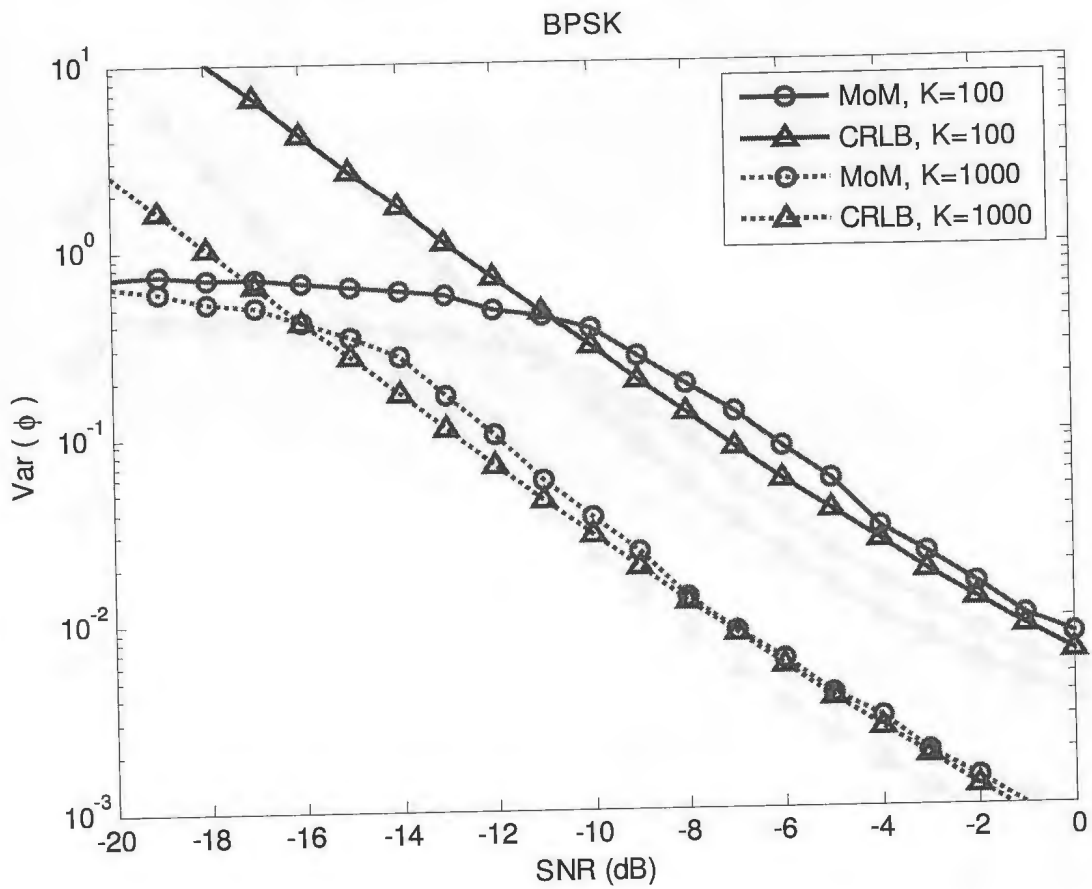


Fig. 10. Comparison of the variance of channel phase MoM estimators and corresponding CRLB for BPSK signals.

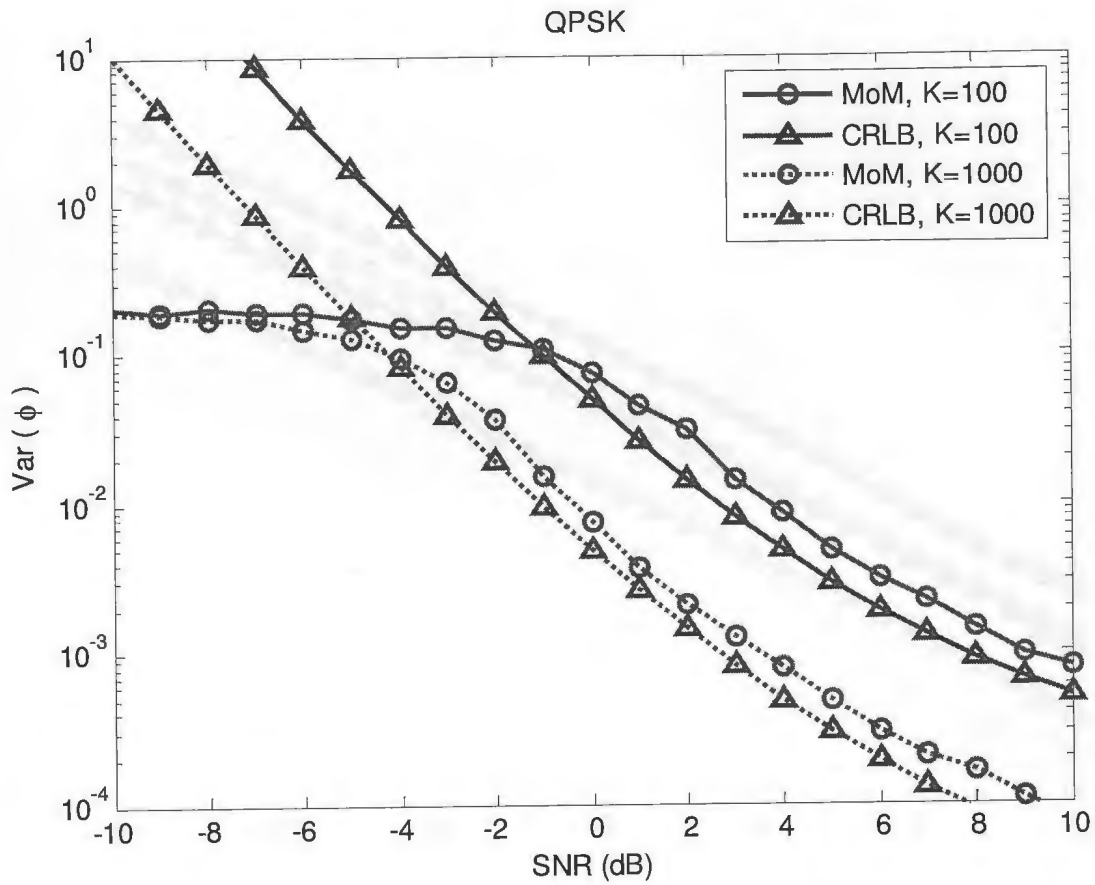


Fig. 11. Comparison of the variance of channel phase MoM estimators and corresponding CRLB for QPSK signals.

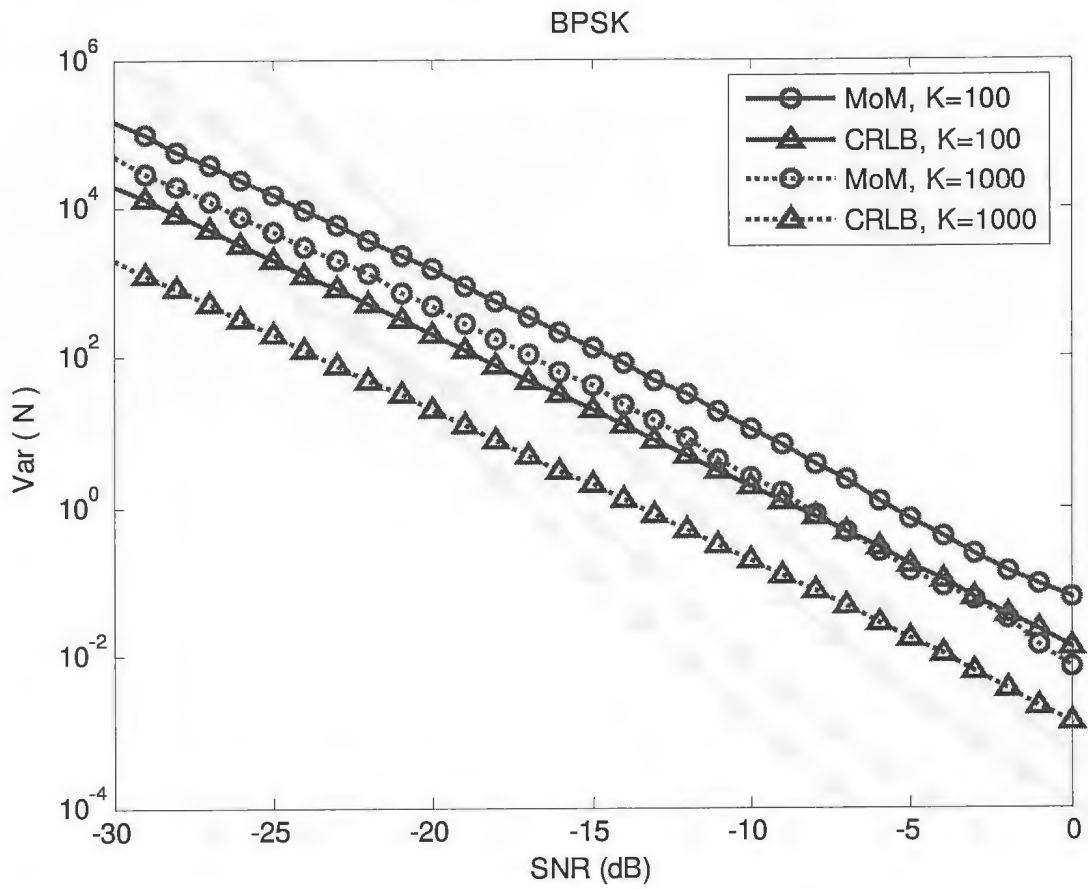


Fig. 12. Comparison of the variance of noise power MoM estimators and corresponding CRLB for BPSK signals.

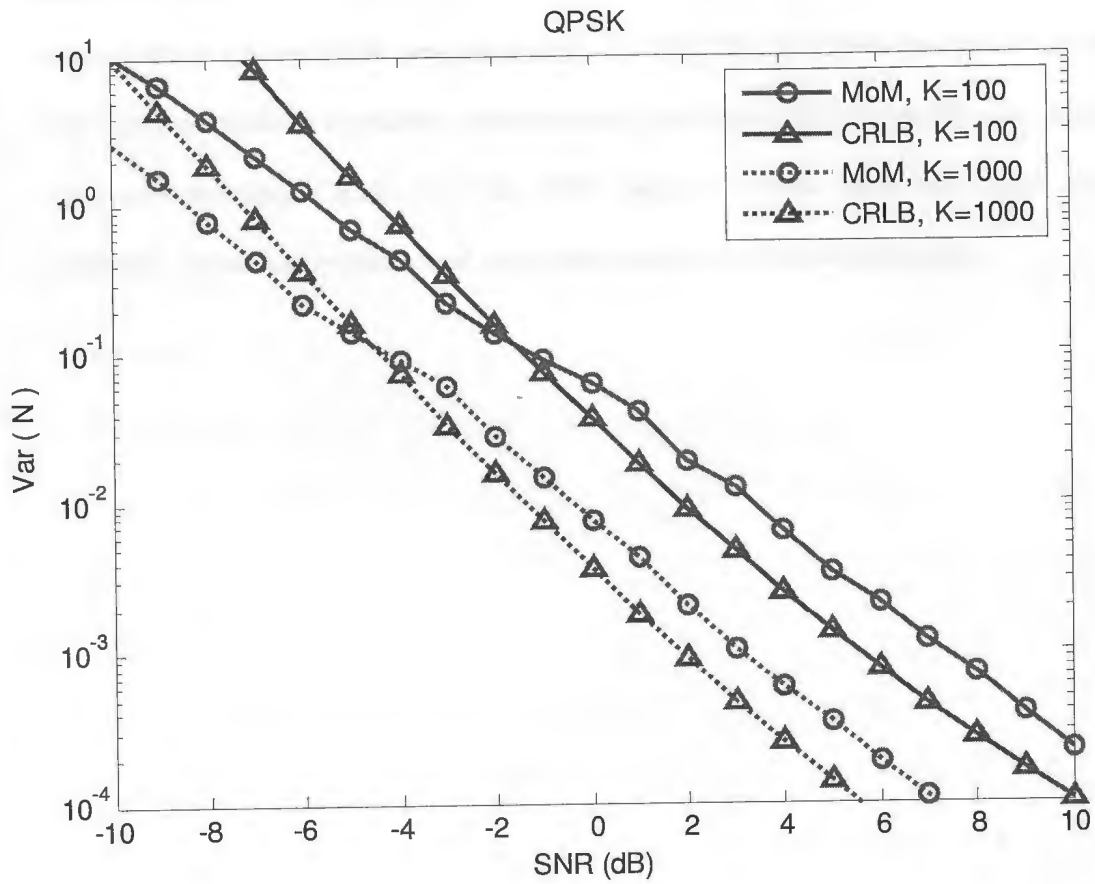


Fig. 13. Comparison of the variance of noise power MoM estimators and corresponding CRLB for QPSK signals.

3.5. Chapter Summary

In this Chapter, we presented the expressions of CRLBs of channel amplitude, phase and noise power estimators, for BPSK and QPSK signals. These expressions are evaluated for a broad SNR range and with $K = 100$ and $K = 1000$ processed symbols. The variance of MoM estimators, which are used with the QHLRT classifier, is compared with corresponding CRLB. For the SNR range in which these estimators remain unbiased¹, numerical results reveal reasonable accuracy of MoM estimators.

CHAPTER 4

4. APPLICATION OF CRAMER-RAO LOWER BOUND (CRLB) TO MODULATION CLASSIFICATION

In this work, we have considered the modulation classification of linearly digitally modulated signals, and investigated the performance of the HLRT- and QHLRT-based classifiers. The QHLRT algorithm, which employs MoM estimators of the unknown parameters, has been shown to be a better solution in terms of computational complexity, yet with reasonable classification performance. The ALRT-based classifier with perfect knowledge of the unknown parameters was used as an idealized reference against which performance of the HLRT- and QHLRT-based classifiers was evaluated. This approach is too optimistic, because error free estimation is not possible in real systems, and estimates deviate from the true parameter values.

In this Chapter, we propose an alternative idealized reference for blind QHLRT-based classifiers which employ unbiased and normally-distributed estimators of the unknown parameters. This is referred to as the QHLRT-idealized reference (QHLRT-IR) classifier.

For the QHLRT-based classifiers which employ asymptotically unbiased and normally-distributed estimators of unknown parameters, this idealized reference classifier applies only in a certain SNR range¹.

4.1. Proposed QHLRT-idealized reference (QHLRT-IR) Classifier

With the QHLRT-IR classifier, the likelihood function under the i th hypothesis, i.e., H_i : the i th modulation was transmitted, is computed by averaging over unknown

constellation points and using unbiased and normally-distributed estimators of the unknown parameters², with mean as the true value of the parameter and variance given by the CRLB of the parameter estimator. Hence, the likelihood function under the i th hypothesis, $\text{LF}_{\text{QHLRT-B}}^{(i)}(\mathbf{r})$, can be written as

$$\text{LF}_{\text{QHLRT-B}}^{(i)}(\mathbf{r}) = \prod_{k=1}^K \frac{1}{M_i} \sum_{m=1}^{M_i} \frac{1}{\pi \hat{N}^{(i)}} \exp\left\{-\frac{1}{\hat{N}^{(i)}} |r_k - \hat{\alpha}^{(i)} e^{j\hat{\phi}^{(i)}} s_{k,m}^{(i)}|^2\right\}, \quad i=1, \dots, N_{\text{mod}}, \quad (3.22)$$

where $\hat{\alpha}^{(i)}$, $\hat{\phi}^{(i)}$ and $\hat{N}^{(i)}$ are normally-distributed unbiased estimates of the channel amplitude, α , phase, ϕ , and noise power, N , under hypothesis H_i , respectively, i.e., $\mathcal{N}(\theta^{(i)}, \text{CRLB}_{\theta^{(i)}})$, with $\theta^{(i)}$ as any of these parameters under H_i and \mathcal{N} stands for normal distribution. Then, with the LFs calculated under all N_{mod} hypotheses, the criterion in (2.14) is applied for decision-making.

In general, the QHLRT-IR classifier provides an upper bound on the classification performance of blind QHLRT-based classifiers, which employ unbiased and normally-distributed estimators of the unknown parameters. For the QHLRT-based classifiers which employ asymptotically unbiased and normally-distributed estimators of unknown parameters¹, this provides the upper bound on classification performance in a certain SNR range¹. With a certain estimation technique and for a specific modulation format, the SNR range in which the asymptotic results apply, depends on the number of processed symbols, K . In such cases, the asymptotic SNR range can be found beforehand from simulations for a given value of K .

Simulation results achieved with the QHLRT-IR and QHLRT (which employs MoM estimators of the unknown parameters) classifiers² are presented in the sequel. Note that the MoM estimators of these unknown parameters are asymptotically unbiased [9], [12] and normally-distributed¹ (according to our simulation results).

4.2. Simulation Results

Classification results achieved with the ALRT, QHLRT-IR and QHLRT classifiers to discriminate between BPSK and QPSK signals in additive white Gaussian noise (AWGN) channel are presented, with $\theta = [\alpha N \phi]^\dagger$ as unknown parameters. Note that these classifiers can also be extended for block fading channels³. The average probability of correct classification, P_{cc} , defined in (2.47) is used as performance measure.

The number of Monte Carlo trials used to calculate $P_c^{(ii)}$ in (2.47) is 1000.

In Fig. 14, the average probability of correct classification, P_{cc} , is plotted against SNR. These results are obtained with $K = 100$ processed symbols. Apparently, ALRT performs the best. For example, a P_{cc} of 0.9 is achieved with the ALRT, QHLRT-IR and QHLRT algorithms at an SNR of -5 dB, -2.8 dB and -1.6 dB, respectively. The classification performance of the QHLRT-IR classifier is better than the QHLRT classifier above a certain SNR value (-4.5 dB in Fig. 14), whereas below this SNR, the performance of the QHLRT-IR classifier is lower than the performance of the QHLRT classifier. With $K = 100$ processed symbols, the QHLRT-IR classifier provides the upper bound on the classification performance of the QHLRT classifier at SNR greater than -4.5 dB. This is because the MoM estimators of channel amplitude, phase and noise

power (employed by the QHLRT classifier) are asymptotically unbiased [9], [12] and normally-distributed¹ (according to our simulation results).

Note that with the average probability of correct classification as performance measure, these classification results reflect the performance of all parameter estimators for both BPSK and QPSK. Thus, at low SNR, we see the combined effect of parameter estimators, for both BPSK and QPSK. The -4.5 dB SNR value is in between the SNR values at which MoM parameter estimators for BPSK and QPSK become biased¹ (see Fig. 8-Fig. 13, Section 3.4, for the SNR values at which MoM parameter estimators become biased).

In Fig. 15, the average probability of correct classification, P_{cc} , achieved with $K=1000$ processed symbols is plotted against SNR. A better estimation accuracy is achieved when a longer observation interval is available at the receive-side, and thus, the SNR at which the curves for the QHLRT-IR and QHLRT classifiers cross-over, is lower than with $K=100$, i.e., -8.7 dB compared to -4.5 dB. Note that this is in agreement with the results presented for the variance of the MoM parameter estimators and corresponding CRLBs (see Fig. 8-Fig. 13, Section 3.4).

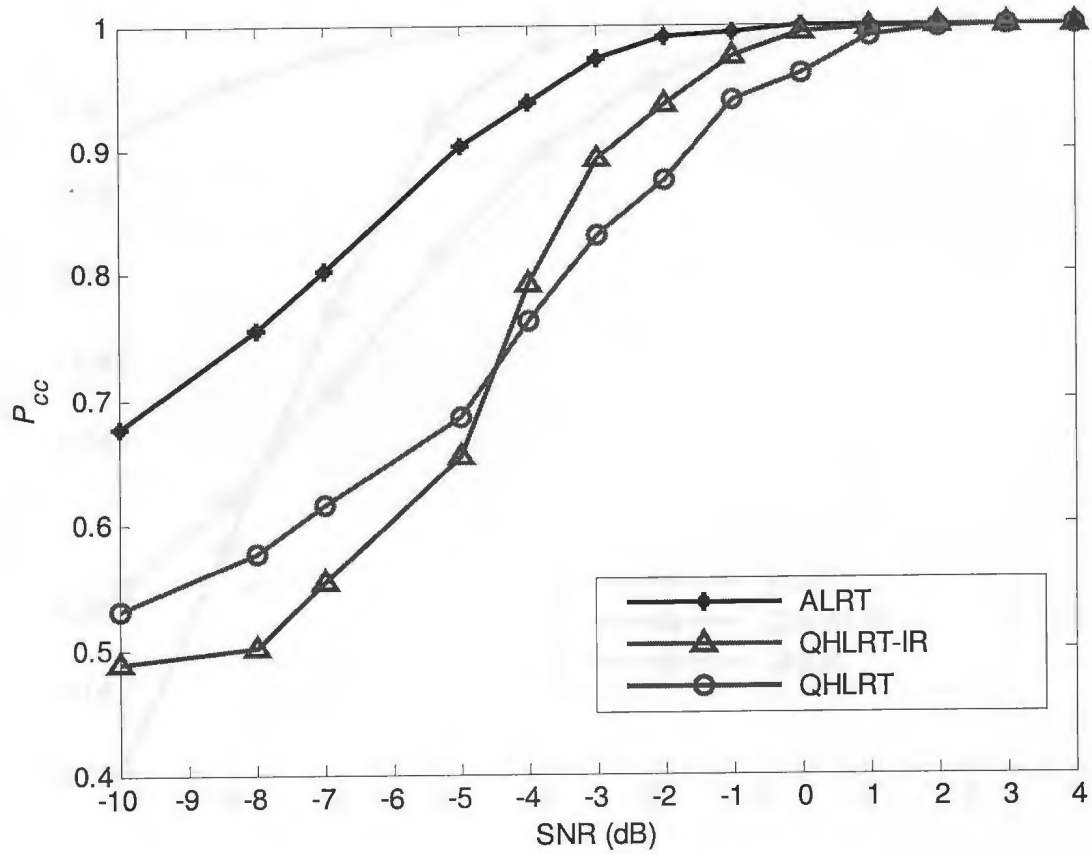


Fig. 14. Performance comparison of ALRT, QHLRT-IR and QHLRT classifiers in AWGN, when discriminating BPSK and QPSK, with $K = 100$ symbols.

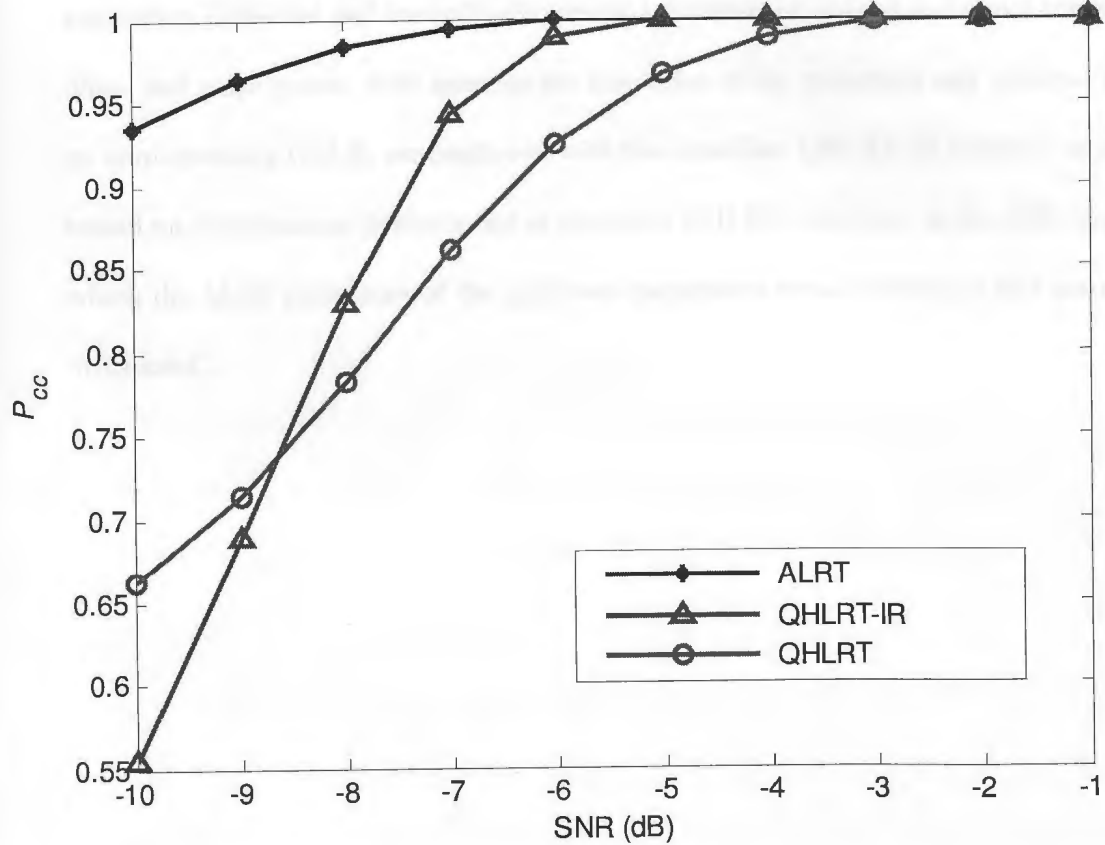


Fig. 15. Performance comparison of ALRT, QHLRT-IR and QHLRT classifiers in AWGN, when discriminating BPSK and QPSK, with $K = 1000$ symbols.

4.3. Chapter Summary

In this Chapter, we apply the CRLB in modulation classification, by developing a QHLRT-idealized reference (QHLRT-IR) classifier based on the CRLB of the parameter estimators. Unbiased and normally-distributed estimators of unknown channel amplitude, phase and noise power, with mean as the true value of the parameter and variance given by corresponding CRLB, are employed with this classifier. QHLRT-IR provides an upper bound on classification performance of proposed QHLRT classifier, in the SNR range in which the MoM estimators of the unknown parameters remain unbiased and normally-distributed¹.

CHAPTER 5

5. SUMMARY AND FUTURE WORK

In this thesis, likelihood-based blind modulation classification (MC) algorithms for linearly digitally modulated signals are investigated, with unknown channel amplitude, phase and noise power. A low complexity algorithm, yet providing reasonable classification performance, is sought. In addition, idealized reference classification algorithms are investigated, against which performance of proposed classifiers are compared.

The major contributions of this thesis include the following:

- Performance and complexity of Hybrid Likelihood Ratio Test (HLRT)- and Quasi HLRT (QHLRT)-based algorithms are studied for linear digital modulation classification in slowly-varying flat fading channels³, with unknown channel amplitude, phase and noise power. It is shown that the HLRT-based algorithm suffers from high computational complexity, whereas the QHLRT is less complex, yet providing a similar classification performance. However, the QHLRT algorithm can fail due to the inadequacy of method-of-moment (MoM) to estimate the channel amplitude⁷ and noise power, especially at low signal-to-noise ratio (SNR). Note that the HLRT is only simulated for BPSK and QPSK signals due to its high complexity.
- The performance of MoM estimators is further studied in terms of their variance. Cramer-Rao Lower Bounds (CRLBs) of the estimators of the unknown channel amplitude, phase and noise power are derived for BPSK and QPSK signals. It is

shown that the variance of MoM estimators is close to corresponding CRLBs, as long as the MoM estimators remain unbiased¹ (high enough SNR). When these estimators become biased (at low SNR), the Cramer-Rao bound ceases to provide the lower bound for the variance of the MoM estimators. An increase in the number of processed symbols, K , leads to a reduction in the SNR at which the MoM estimators become biased. This is due to improved estimation accuracy with a longer observation interval.

- An idealized reference classification algorithm (QHLRT-IR) which employs unbiased and normally-distributed estimators of channel amplitude, phase and noise power, with mean as the true value of the parameter, and variance given by the CRLB of the parameter estimator, is developed. This is only a theoretical algorithm, and cannot be realized in practice. This classifier provides an upper bound on classification performance of blind QHLRT-based classifiers², which employ unbiased and normally-distributed estimators of the unknown parameters. For the QHLRT-based classifiers, which employ asymptotically unbiased and normally-distributed estimators of unknown parameters¹, this classifier provides the upper bound on classification only in certain SNR range¹.
- Performance of Average Likelihood Ratio Test (ALRT), QHLRT-IR and QHLRT classifiers are studied for BPSK and QPSK signals in additive white Gaussian noise (AWGN) channel, with unknown channel amplitude, phase and noise power. As expected, ALRT outperforms the other two classifiers. On the other hand, the performance of the QHLRT-IR classifier is better than QHLRT, as long as the MoM

estimators of the unknown parameters for BPSK and QPSK remain unbiased and normally-distributed¹. In this SNR range, QHLRT performance is close to the QHLRT-IR classifier. These results are useful to analyze the performance of QHLRT for different SNRs and a specific value of processed symbols, K .

Suggested future work is as follows:

- CRLBs for higher constellations, such as M -PSK and M -QAM ($M \geq 8$) can be derived and compared with the variance of corresponding MoM estimators.
- The QHLRT-IR classifier can be extended for constellations other than BPSK and QPSK.
- We have observed that the QHLRT-based classifier may fail due to the inadequacy of the MoM estimators of channel amplitude⁷ and noise power (especially at low SNR). Therefore, accurate and low complexity techniques for parameter estimation in a large SNR range need to be sought.
- The classifiers studied here need to be further extended to more unknown parameters, such as carrier frequency offset, timing offset, pulse shape, etc.
- CRLBs of estimators of unknown parameters, other than those studied here, can be similarly derived and studied.

Following the above steps, one can move closer to the development of a more general kind of modulation classifier, which is simple, and works for all linear digital modulations and a larger number of unknown parameters.

REFERENCES

- [1]. A. Polydoros and K. Kim, "On the detection and classification of quadrature digital modulations in broad-band noise," *IEEE Trans. Commun.*, vol. 38, pp. 1199-1211, 1990.
- [2]. W. Wei and J. M. Mendel, "Maximum-likelihood classification for digital amplitude-phase modulations," *IEEE Trans. Commun.*, vol. 48, pp. 189-193, 2000.
- [3]. P. Panagiotou, A. Anastasopoulos, and A. Polydoros, "Likelihood ratio tests for modulation classification," in *Proc. IEEE MILCOM 2000*, pp. 670-674.
- [4]. O. A. Dobre et al., "On the classification of linearly modulated signals in fading channels", in *Proc. Conference on Information Sciences and Systems (CISS)*, 2004, Princeton University (in CD).
- [5]. A. Abdi, O. A. Dobre, R. Chauchy, Y. Bar-Ness, and W. Su, "Modulation classification in fading channels using antenna arrays," in *Proc. IEEE MILCOM 2004*, pp. 211-217.
- [6]. O. A. Dobre, F. Hameed, "Likelihood-based algorithms for linear digital modulation classification in fading channels", in *Proc. IEEE CCECE 2006*, Ottawa, Canada.
- [7]. O. A. Dobre, A. Abdi, Y. Bar-Ness, and W. Su, "Blind modulation classification: a concept whose time has come," in *Proc. IEEE Sarnoff Symposium 2005*, pp. 223-228.

- [8]. W. Dai, Y. Wang, and J. Wang, "Joint power estimation and modulation classification using second- and higher statistics," in *Proc. IEEE WCNC 2002*, pp. 155-158.
- [9]. A. Swami and B. M. Sadler, "Hierarchical digital modulation classification using cumulants," *IEEE Trans. Commun.*, vol. 48, pp. 416-429, 2000.
- [10]. C. M. Spooner, "On the utility of sixth-order cyclic cumulants for RF signal classification", in *Proc. IEEE ASILOMAR 2001*, pp. 890-897.
- [11]. O. A. Dobre, Y. Bar-Ness, and W. Su, "Robust QAM modulation classification algorithm using cyclic cumulants", in *Proc. IEEE WCNC 2004*, pp. 745-748.
- [12]. G. N. Tavares, L. M. Tavares, and M. S. Piedade, "On the Miller-Chang Lower Bound for NDA Carrier Phase Estimation," *IEEE Trans. on Commun.*, vol. 52, pp. 1867-1871, Nov. 2004.
- [13]. Y. V. Zakharov, V. M. Baronkin, and D. A. J. Pearce, "Asymptotic and Modified Cramer-Rao Bounds for Frequency Estimation in Parallel Fading Channels," *IEEE Trans. on Signal Processing*, vol. 54, pp. 1554-1557, Apr. 2006.
- [14]. J. G. Proakis, *Digital Communications*, 4th ed. New York: McGraw Hill, 2000.
- [15]. U. Mengali and A. N. D'Andrea, *Synchronization Techniques for Digital Receivers*. New York: Plenum, 1997.
- [16]. G. L. Stuber, *Principles of Mobile Communication*, 2nd ed. Boston, MA: Kluwer, 2001.
- [17]. S. M. Kay, *Fundamentals of Statistical Signal Processing, Estimation Theory*. Englewood Cliffs, NJ: Prentice Hall, 1993, vol. 1.

- [18]. N. S. Alagha, "Cramer-Rao bounds of SNR estimates for BPSK and QPSK modulated signals," *IEEE Commun. Lett.*, vol. 5, pp. 10-12, 2001.
- [19]. W. G. Cowley, "Phase and frequency estimation for PSK packets: bounds and algorithms," *IEEE Trans. Commun.*, vol. 44, pp. 26-28, 1996.
- [20]. I. S. Gradshteyn, I. M. Ryzhik, A. Jeffrey, *Table of Integrals, Series and Products*, 5th ed. Academic Press, 1994.

APPENDIX A

Signal at the output of receive matched filter

Substituting (2.1) and (2.4) in (2.5), one obtains the output of the receive matched filter, sampled at $t = kT$, as follows.

$$r_k = \sqrt{2} \int_{(k-1)T}^{kT} [\operatorname{Re}\{\sqrt{2}\alpha e^{j\varphi} s_k^{(i)} u_T(t - (k-1)T) e^{j2\pi f_c t}\} + n(t)] e^{-j2\pi f_c t} dt, \quad (A.1)$$

$$k = 1, \dots, K, \quad 0 \leq t \leq KT, \quad i = 1, \dots, N_{\text{mod}},$$

$$r_k = \frac{\sqrt{2}}{2} \int_{(k-1)T}^{kT} \sqrt{2}\alpha e^{j\varphi} s_k^{(i)} u_T(t - (k-1)T) dt$$

$$+ \frac{\sqrt{2}}{2} \int_{(k-1)T}^{kT} \sqrt{2}\alpha e^{-j\varphi} s_k^{(i)*} u_T(t - (k-1)T) e^{-j4\pi f_c t} dt + \sqrt{2} \int_{(k-1)T}^{kT} n(t) e^{-j2\pi f_c t} dt \quad (A.2)$$

$$, \quad k = 1, \dots, K, \quad 0 \leq t \leq KT,$$

As $\int_{(k-1)T}^{kT} \alpha e^{-j\varphi} s_k^{(i)*} u_T(t - (k-1)T) e^{-j4\pi f_c t} dt = 0$, (A.2) becomes,

$$r_k = \alpha e^{j\varphi} s_k^{(i)} T + \sqrt{2} \int_{(k-1)T}^{kT} n(t) e^{-j2\pi f_c t} dt, \quad (A.3)$$

or, equivalently,

$$r_k = \alpha e^{j\varphi} s_k^{(i)} T + n_k, \quad k = 1, \dots, K, \quad (A.4)$$

with $n_k = \sqrt{2} \int_{(k-1)T}^{kT} n(t) e^{-j2\pi f_c t} dt$, $k = 1, \dots, K$.

The result in (A.4) is used in (2.6), Section 2.1.

APPENDIX B

Derivation of (2.16), (2.21), (2.27) and (2.32), from Section 2.2.1.1

Subsequently, derivation of (2.16), (2.21), (2.27) and (2.32), given in Section 2.2.1.1, is performed.

Derivation of (2.16)

Substituting the expression of the LF given in (2.11) into (2.15), it becomes

$$\frac{\partial}{\partial \varphi} \left[\frac{1}{(\pi N)^K} \exp \left\{ -\frac{1}{N} \|\mathbf{r} - \alpha e^{j\varphi} \mathbf{s}^{(i)}\|^2 \right\} \right] = 0, \quad (\text{B.1})$$

$$\frac{1}{(\pi N)^K} \exp \left\{ -\frac{1}{N} \|\mathbf{r} - \alpha e^{j\varphi} \mathbf{s}^{(i)}\|^2 \right\} \frac{\partial}{\partial \varphi} \left[-\frac{1}{N} \|\mathbf{r} - \alpha e^{j\varphi} \mathbf{s}^{(i)}\|^2 \right] = 0, \quad (\text{B.2})$$

$$\text{with } \frac{1}{(\pi N)^K} \neq 0, \exp \left\{ -\frac{1}{N} \|\mathbf{r} - \alpha e^{j\varphi} \mathbf{s}^{(i)}\|^2 \right\} \neq 0, \text{ and } \frac{1}{N} \neq 0.$$

This leads to

$$\frac{\partial}{\partial \varphi} \|\mathbf{r} - \alpha e^{j\varphi} \mathbf{s}^{(i)}\|^2 = 0, \quad (\text{B.3})$$

$$\frac{\partial}{\partial \varphi} [|r_1 - \alpha e^{j\varphi} s_1^{(i)}|^2 + \dots + |r_K - \alpha e^{j\varphi} s_K^{(i)}|^2] = 0, \quad (\text{B.4})$$

$$\frac{\partial}{\partial \varphi} [(r_1 - \alpha e^{j\varphi} s_1^{(i)})(r_1 - \alpha e^{j\varphi} s_1^{(i)})^* + \dots + (r_K - \alpha e^{j\varphi} s_K^{(i)})(r_K - \alpha e^{j\varphi} s_K^{(i)})^*] = 0, \quad (\text{B.5})$$

$$[(r_1 - \alpha e^{j\varphi} s_1^{(i)})(j\alpha e^{-j\varphi} s_1^{(i)*}) + (r_1^* - \alpha e^{-j\varphi} s_1^{(i)*})(-j\alpha e^{j\varphi} s_1^{(i)})] + \dots \quad (\text{B.6})$$

$$\dots + [(r_K - \alpha e^{j\varphi} s_K^{(i)})(j\alpha e^{-j\varphi} s_K^{(i)*}) + (r_K^* - \alpha e^{-j\varphi} s_K^{(i)*})(-j\alpha e^{j\varphi} s_K^{(i)})] = 0,$$

$$e^{-j\varphi} [r_1 s_1^{(i)*} + \dots + r_K s_K^{(i)*}] - \alpha [s_1^{(i)} s_1^{(i)*} + \dots + s_K^{(i)} s_K^{(i)*}] - e^{j\varphi} [r_1^* s_1^{(i)} + \dots + r_K^* s_K^{(i)}] \quad (\text{B.7})$$

$$+ \alpha [s_1^{(i)} s_1^{(i)*} + \dots + s_K^{(i)} s_K^{(i)*}] = 0,$$

$$e^{-j\varphi} \mathbf{s}^{(i)H} \mathbf{r} = e^{j\varphi} \mathbf{r}^H \mathbf{s}^{(i)}. \quad (\text{B.8})$$

The result in (B.8) is given in (2.16), Section 2.2.1.1.

Derivation of (2.21)

Substituting the expression of the LF given in (2.11) into (2.20), one gets

$$\frac{\partial}{\partial \alpha} \left[\frac{1}{(\pi N)^K} \exp \left\{ -\frac{1}{N} \|\mathbf{r} - \alpha e^{j\varphi} \mathbf{s}^{(i)}\|^2 \right\} \right] = 0, \quad (\text{B.9})$$

$$\frac{1}{(\pi N)^K} \exp \left\{ -\frac{1}{N} \|\mathbf{r} - \alpha e^{j\varphi} \mathbf{s}^{(i)}\|^2 \right\} \frac{\partial}{\partial \alpha} \left[-\frac{1}{N} \|\mathbf{r} - \alpha e^{j\varphi} \mathbf{s}^{(i)}\|^2 \right] = 0, \quad (\text{B.10})$$

with $\frac{1}{(\pi N)^K} \neq 0$, $\exp \left\{ -\frac{1}{N} \|\mathbf{r} - \alpha e^{j\varphi} \mathbf{s}^{(i)}\|^2 \right\} \neq 0$, and $\frac{1}{N} \neq 0$.

This leads to

$$\frac{\partial}{\partial \alpha} \|\mathbf{r} - \alpha e^{j\varphi} \mathbf{s}^{(i)}\|^2 = 0, \quad (\text{B.11})$$

$$\frac{\partial}{\partial \alpha} [|r_1 - \alpha e^{j\varphi} s_1^{(i)}|^2 + \dots + |r_K - \alpha e^{j\varphi} s_K^{(i)}|^2] = 0, \quad (\text{B.12})$$

$$\frac{\partial}{\partial \alpha} [(r_1 - \alpha e^{j\varphi} s_1^{(i)})(r_1 - \alpha e^{j\varphi} s_1^{(i)})^* + \dots + (r_K - \alpha e^{j\varphi} s_K^{(i)})(r_K - \alpha e^{j\varphi} s_K^{(i)})^*] = 0, \quad (\text{B.13})$$

$$[(r_1 - \alpha e^{j\varphi} s_1^{(i)})(-s_1^{(i)*} e^{-j\varphi}) + (r_1^* - \alpha e^{-j\varphi} s_1^{(i)*})(-s_1^{(i)} e^{j\varphi})] + \dots \quad (\text{B.14})$$

$$\dots + [(r_K - \alpha e^{j\varphi} s_K^{(i)})(-s_K^{(i)*} e^{-j\varphi}) + (r_K^* - \alpha e^{-j\varphi} s_K^{(i)*})(-s_K^{(i)} e^{j\varphi})] = 0,$$

$$e^{-j\varphi} [r_1 s_1^{(i)*} + \dots + r_K s_K^{(i)*}] - \alpha [s_1^{(i)} s_1^{(i)*} + \dots + s_K^{(i)} s_K^{(i)*}] + e^{j\varphi} [r_1^* s_1^{(i)} + \dots + r_K^* s_K^{(i)}] - \alpha [s_1^{(i)*} s_1^{(i)} + \dots + s_K^{(i)*} s_K^{(i)}] = 0, \quad (\text{B.15})$$

and finally,

$$2\alpha \|\mathbf{s}^{(i)}\|^2 = e^{-j\varphi} \mathbf{s}^{(i)H} \mathbf{r} + e^{j\varphi} \mathbf{r}^H \mathbf{s}^{(i)}. \quad (\text{B.16})$$

The result in (B.16) is given in (2.21), Section 2.2.1.1.

Derivation of (2.27)

Substituting the expression of the LF given in (2.11) into (2.26), one gets

$$\frac{\partial}{\partial N} \left[\frac{1}{(\pi N)^K} \exp \left\{ -\frac{1}{N} \|\mathbf{r} - \alpha e^{j\varphi} \mathbf{s}^{(i)}\|^2 \right\} \right] = 0, \quad (\text{B.17})$$

$$\frac{1}{(\pi N)^K} \frac{\partial}{\partial N} \left[\exp \left\{ -\frac{1}{N} \|\mathbf{r} - \alpha e^{j\varphi} \mathbf{s}^{(i)}\|^2 \right\} \right] + \frac{\partial}{\partial N} \left[\frac{1}{(\pi N)^K} \right] \exp \left\{ -\frac{1}{N} \|\mathbf{r} - \alpha e^{j\varphi} \mathbf{s}^{(i)}\|^2 \right\} = 0, \quad (\text{B.18})$$

$$\left[\frac{1}{\pi^K N^{K+2}} (\|\mathbf{r} - \alpha e^{j\varphi} \mathbf{s}^{(i)}\|^2) - \frac{K}{\pi^K N^{K+1}} \right] \exp \left\{ -\frac{1}{N} \|\mathbf{r} - \alpha e^{j\varphi} \mathbf{s}^{(i)}\|^2 \right\} = 0, \quad (\text{B.19})$$

with $\exp \left\{ -\frac{1}{N} \|\mathbf{r} - \alpha e^{j\varphi} \mathbf{s}^{(i)}\|^2 \right\} \neq 0$,

and finally under the hypothesis H_i , (B.19) becomes

$$\hat{N}^{(i)} = \frac{1}{K} \|\mathbf{r} - \alpha e^{j\varphi} \mathbf{s}^{(i)}\|^2, \quad i = 1, \dots, N_{\text{mod}}. \quad (\text{B.20})$$

The result derived in (B.20) is given in (2.27), Section 2.2.1.1.

Derivation of (2.32)

The norm in the LF given in (2.12) can be expanded as

$$\begin{aligned} \|\mathbf{r} - \hat{\alpha}^{(i)} e^{j\hat{\varphi}^{(i)}} \mathbf{s}^{(i)}\|^2 &= |r_1 - \hat{\alpha}^{(i)} e^{j\hat{\varphi}^{(i)}} s_1^{(i)}|^2 + \dots + |r_K - \hat{\alpha}^{(i)} e^{j\hat{\varphi}^{(i)}} s_K^{(i)}|^2 \\ &= [r_1 r_1^* + \dots + r_K r_K^*] - \hat{\alpha}^{(i)} e^{j\hat{\varphi}^{(i)}} [r_1^* s_1^{(i)} + \dots + r_K^* s_K^{(i)}] \\ &\quad - \hat{\alpha}^{(i)} e^{-j\hat{\varphi}^{(i)}} [r_1 s_1^{(i)*} + \dots + r_K s_K^{(i)*}] + \hat{\alpha}^{(i)2} [s_1^{(i)} s_1^{(i)*} + \dots + s_K^{(i)} s_K^{(i)*}] \\ \|\mathbf{r} - \hat{\alpha}^{(i)} e^{j\hat{\varphi}^{(i)}} \mathbf{s}^{(i)}\|^2 &= \|\mathbf{r}\|^2 - \hat{\alpha}^{(i)} e^{j\hat{\varphi}^{(i)}} \mathbf{r}^H \mathbf{s}^{(i)} - \hat{\alpha}^{(i)} e^{-j\hat{\varphi}^{(i)}} \mathbf{s}^{(i)H} \mathbf{r} + \hat{\alpha}^{(i)2} \|\mathbf{s}^{(i)}\|^2. \end{aligned} \quad (\text{B.21})$$

By substituting (2.30), (2.31) and (2.23) into (B.21), one can easily show that,

$$\|\mathbf{r} - \hat{\alpha}^{(i)} e^{j\hat{\varphi}^{(i)}} \mathbf{s}^{(i)}\|^2 = \|\mathbf{r}\|^2 - |\mathbf{r}^H \mathbf{s}^{(i)}|^2 / \|\mathbf{s}^{(i)}\|^2, \quad i = 1, \dots, N_{\text{mod}}. \quad (\text{B.22})$$

The result derived in (B.22) is given in (2.32), Section 2.2.1.1.

APPENDIX C

First-, Second-, Third- and Fourth-Order Moments of Noise

The channel noise can be expressed in terms of in-phase and quadrature-phase components as $n_k = I_{n,k} + jQ_{n,k}$, with $I_{n,k}$ and $Q_{n,k}$ independent zero-mean Gaussian random variables. We also have that

$$\text{var}\{I_{n,k}\} = \text{E}[I_{n,k}^2] = N/2, \text{ and,} \quad (\text{C.1})$$

$$\text{var}\{Q_{n,k}\} = \text{E}[Q_{n,k}^2] = N/2. \quad (\text{C.2})$$

Using these results, the first-, second-, third- and fourth-order moments of the noise are as follows.

$$\text{I. } \text{E}[n_k] = \text{E}[(I_{n,k} + jQ_{n,k})] = \text{E}[I_{n,k}] + j\text{E}[Q_{n,k}] = 0. \quad (\text{C.3})$$

$$\text{II. } \text{E}[n_k^*] = \text{E}[(I_{n,k} - jQ_{n,k})] = \text{E}[I_{n,k}] - j\text{E}[Q_{n,k}] = 0. \quad (\text{C.4})$$

$$\begin{aligned} \text{III. } \text{E}[(n_k^*)^2] &= \text{E}[(I_{n,k} - jQ_{n,k})^2] = \text{E}[I_{n,k}^2 - j2I_{n,k}Q_{n,k} + (jQ_{n,k})^2] \\ &= \text{E}[I_{n,k}^2] - \text{E}[Q_{n,k}^2] - j2\text{E}[I_{n,k}] \text{E}[Q_{n,k}] \\ &= \frac{N}{2} - \frac{N}{2} = 0. \end{aligned} \quad (\text{C.5})$$

$$\begin{aligned} \text{IV. } \text{E}[n_k^2] &= \text{E}[(I_{n,k} + jQ_{n,k})^2] = \text{E}[I_{n,k}^2 + j2I_{n,k}Q_{n,k} + (jQ_{n,k})^2] \\ &= \text{E}[I_{n,k}^2] - \text{E}[Q_{n,k}^2] + j2\text{E}[I_{n,k}] \text{E}[Q_{n,k}] \\ &= \frac{N}{2} - \frac{N}{2} = 0. \end{aligned} \quad (\text{C.6})$$

$$\text{V. } \text{E}[|n_k|^4] = \text{E}[(I_{n,k}^2 + Q_{n,k}^2)^2] = \text{E}[I_{n,k}^4 + 2I_{n,k}^2Q_{n,k}^2 + Q_{n,k}^4]$$

$$= E[I_{n,k}^4] + 2E[I_{n,k}^2]E[Q_{n,k}^2] + E[Q_{n,k}^4].$$

For a Gaussian random variable, the fourth cumulant is zero, i.e.,

$$E[I_{n,k}^4] - 3(E[I_{n,k}^2])^2 = 0 \Rightarrow E[I_{n,k}^4] = \frac{3}{4}N^2.$$

Similarly,

$$E[Q_{n,k}^4] = \frac{3}{4}N^2.$$

Therefore,

$$E[|n_k|^4] = \frac{3}{4}N^2 + 2\left(\frac{N}{2}\right)\left(\frac{N}{2}\right) + \frac{3}{4}N^2 = 2N^2. \quad (\text{C.7})$$

The results obtained from (C.3) to (C.7) are used in Section 2.2.2.1.

APPENDIX D

Second- and Fourth-Order Moments of the Received Signal

The second-order moment (one conjugation) of the received signal in (2.8) is given as,

$$M_{21} = E[|r_k|^2] = E[(x_k^{(i)} + n_k)(x_k^{(i)} + n_k)^*], \quad k = 1, \dots, K, \quad (D.1)$$

$$= E[|x_k^{(i)}|^2] + E[|n_k|^2] + E[x_k^{(i)}]E[n_k^*] + E[x_k^{(i)*}]E[n_k]. \quad (D.2)$$

By using (2.38), (2.39), (C.3) and (C.4) this becomes,

$$M_{21} = S^{(i)} + N. \quad (D.3)$$

Similarly, the fourth-order moment (two conjugations) of the received signal is given as,

$$M_{42} = E[|r_k|^4] = E[(x_k^{(i)} + n_k)^2 (x_k^{(i)*} + n_k^*)^2], \quad k = 1, \dots, K, \quad (D.4)$$

$$= E[(x_k^{(i)2} + n_k^2 + 2x_k^{(i)}n_k)(x_k^{(i)*2} + n_k^{*2} + 2x_k^{(i)*}n_k^*)], \quad (D.5)$$

$$\begin{aligned} &= E[|x_k^{(i)}|^4] + E[x_k^{(i)2}]E[(n_k^*)^2] + 2E[x_k^{(i)}|x_k^{(i)}|^2]E[n_k^*] + E[n_k^2]E[(x_k^{(i)*})^2] \\ &\quad + E[|n_k|^4] + 2E[x_k^{(i)*}]E[n_k]E[|n_k|^2] + 2E[x_k^{(i)}|x_k^{(i)}|^2]E[n_k] \\ &\quad + 2E[x_k^{(i)}]E[n_k^*]E[|n_k|^2] + 4E[|x_k^{(i)}|^2]E[|n_k|^2] \end{aligned} \quad (D.6)$$

By using (2.38), (2.39), (C.3), (C.4), (C.5), (C.6) and (C.7), this becomes,

$$M_{42} = E[|x_k^{(i)}|^4] + 2N^2 + 4S^{(i)}N, \text{ or}$$

$$M_{42} = b^{(i)}S^{(i)2} + 4S^{(i)}N + 2N^2, \quad (D.7)$$

where $b^{(i)} = E[|x_k^{(i)}|^4] / (E[|x_k^{(i)}|^2])^2 = E[|s_k^{(i)}|^4] / (E[|s_k^{(i)}|^2])^2$, $i = 1, \dots, N_{\text{mod}}$.

Eq. (D.3) and (D.7) are given as (2.40) and (2.41), respectively in Section 2.2.2.1

APPENDIX E

Derivation of (3.9)

From (2.10), with $\boldsymbol{\theta} = [\alpha N \varphi]^\dagger$ as unknown parameters we have

$$f(\mathbf{r} | \{s_k^{(i)}\}, \boldsymbol{\theta}) = \prod_{k=1}^K \frac{1}{\pi N} \exp\left\{-\frac{1}{N} |r_k - \alpha e^{j\varphi} s_k^{(i)}|^2\right\}. \quad (\text{E.1})$$

It can be written as

$$f(\mathbf{r} | \{s_k^{(i)}\}, \boldsymbol{\theta}) = \prod_{k=1}^K \frac{1}{\pi N} \exp\left\{-\frac{1}{N} (|r_k|^2 - \alpha e^{j\varphi} r_k^* s_k^{(i)} - \alpha e^{-j\varphi} r_k (s_k^{(i)})^* + \alpha^2 (s_k^{(i)})^2)\right\}. \quad (\text{E.2})$$

Averaging (E.2) over BPSK symbols, i.e., $s^{(i)} \in \{-1, 1\}$, this becomes

$$f_B(\mathbf{r} | \boldsymbol{\theta}) = \frac{1}{2} \prod_{k=1}^K \frac{1}{\pi N} \left[\exp\left\{-\frac{1}{N} (|r_k|^2 - \alpha e^{j\varphi} r_k^* - \alpha e^{-j\varphi} r_k + \alpha^2)\right\} \right. \\ \left. + \exp\left\{-\frac{1}{N} (|r_k|^2 + \alpha e^{j\varphi} r_k^* + \alpha e^{-j\varphi} r_k + \alpha^2)\right\} \right], \quad (\text{E.3})$$

and with $2 \operatorname{Re}\{r_k e^{-j\varphi}\} = r_k^* e^{j\varphi} + r_k e^{-j\varphi}$, (E.3) reduces to

$$f_B(\mathbf{r} | \boldsymbol{\theta}) = \prod_{k=1}^K \frac{1}{\pi N} \exp\left\{-\frac{1}{N} (|r_k|^2 + \alpha^2)\right\} \cosh\left(\frac{2\alpha}{N} \operatorname{Re}\{r_k e^{-j\varphi}\}\right). \quad (\text{E.4})$$

The result in (E.4) is used in (3.9), Section 3.2.

APPENDIX F

Derivation of Fisher Information Matrix (FIM) for BPSK and QPSK Signals

In this Appendix, we present the derivations of the FIM for BPSK and QPSK signals with the channel amplitude, α , phase, φ , and noise power, N , as unknowns. Results derived here are presented in Sections 3.2 and 3.3.

From (2.8), we have

$$r_k e^{-j\varphi} = \alpha s_k + n_k e^{-j\varphi}, \quad k = 1, \dots, K. \quad (\text{F.1})$$

It is well known that multiplication of a complex Gaussian process by a random phase produces another complex Gaussian process with the same statistics [19]. Thus,

$$n_k e^{-j\varphi} = w_k^I + jw_k^Q, \quad (\text{F.2})$$

is a complex Gaussian process, and (F.1) becomes

$$(I(k) + jQ(k))(\cos \varphi - j \sin \varphi) = \alpha s_k + w_k^I + jw_k^Q,$$

or, equivalently,

$$(I(k) \cos \varphi + Q(k) \sin \varphi) + j(-I(k) \sin \varphi + Q(k) \cos \varphi) = (\alpha s_k + w_k^I) + jw_k^Q, \quad (\text{F.3})$$

where $r_k = I(k) + jQ(k)$ with $I(k)$ and $Q(k)$, the in-phase and quadrature-phase components, respectively.

Derivations of FIM, with $\boldsymbol{\theta} = [\alpha \ N \ \varphi]^T$ as unknown parameters and for the BPSK signals, is presented in the sequel. Derivations for the QPSK can be similarly carried out. The FIM for BPSK signals is given as

$$\mathbf{I}_B(\boldsymbol{\theta}) = \begin{bmatrix} -E\left(\frac{\partial^2 \ln f_B(\mathbf{r}|\boldsymbol{\theta})}{\partial \alpha^2}\right) & -E\left(\frac{\partial^2 \ln f_B(\mathbf{r}|\boldsymbol{\theta})}{\partial \alpha \partial N}\right) & -E\left(\frac{\partial^2 \ln f_B(\mathbf{r}|\boldsymbol{\theta})}{\partial \alpha \partial \varphi}\right) \\ -E\left(\frac{\partial^2 \ln f_B(\mathbf{r}|\boldsymbol{\theta})}{\partial N \partial \alpha}\right) & -E\left(\frac{\partial^2 \ln f_B(\mathbf{r}|\boldsymbol{\theta})}{\partial N^2}\right) & -E\left(\frac{\partial^2 \ln f_B(\mathbf{r}|\boldsymbol{\theta})}{\partial N \partial \varphi}\right) \\ -E\left(\frac{\partial^2 \ln f_B(\mathbf{r}|\boldsymbol{\theta})}{\partial \varphi \partial \alpha}\right) & -E\left(\frac{\partial^2 \ln f_B(\mathbf{r}|\boldsymbol{\theta})}{\partial \varphi \partial N}\right) & -E\left(\frac{\partial^2 \ln f_B(\mathbf{r}|\boldsymbol{\theta})}{\partial \varphi^2}\right) \end{bmatrix}. \quad (\text{F.4})$$

Henceforth, we use the following notations to represent the elements of the FIM in (F.4),

$$\mathbf{I}_B(\boldsymbol{\theta}) = \begin{bmatrix} [\mathbf{I}_B(\boldsymbol{\theta})]_{11} & [\mathbf{I}_B(\boldsymbol{\theta})]_{12} & [\mathbf{I}_B(\boldsymbol{\theta})]_{13} \\ [\mathbf{I}_B(\boldsymbol{\theta})]_{21} & [\mathbf{I}_B(\boldsymbol{\theta})]_{22} & [\mathbf{I}_B(\boldsymbol{\theta})]_{23} \\ [\mathbf{I}_B(\boldsymbol{\theta})]_{31} & [\mathbf{I}_B(\boldsymbol{\theta})]_{32} & [\mathbf{I}_B(\boldsymbol{\theta})]_{33} \end{bmatrix}. \quad (\text{F.5})$$

Each element of the FIM in (F.4) is solved separately, as follows.

a) Calculation of $[\mathbf{I}_B(\boldsymbol{\theta})]_{12}$

By differentiating the log-likelihood function given in (3.10) w.r.t. α^9 , one gets

$$\begin{aligned} \frac{\partial \ln f_B(\mathbf{r}|\boldsymbol{\theta})}{\partial \alpha} &= -\frac{2K\alpha}{N} \\ &+ \frac{2}{N} \sum_{k=1}^K (I(k) \cos \varphi + Q(k) \sin \varphi) \tanh\left(\frac{2\alpha}{N} (I(k) \cos \varphi + Q(k) \sin \varphi)\right). \end{aligned} \quad (\text{F.6})$$

Differentiating (F.6) w.r.t. N^9 , this becomes

$$\begin{aligned} \frac{\partial^2 \ln f_B(\mathbf{r}|\boldsymbol{\theta})}{\partial \alpha \partial N} &= \frac{2K\alpha}{N^2} \\ &- \frac{2}{N^2} \sum_{k=1}^K (I(k) \cos \varphi + Q(k) \sin \varphi) \tanh\left(\frac{2\alpha}{N} (I(k) \cos \varphi + Q(k) \sin \varphi)\right) \\ &- \frac{4\alpha}{N^3} \sum_{k=1}^K (I(k) \cos \varphi + Q(k) \sin \varphi)^2 \text{sech}^2\left(\frac{2\alpha}{N} (I(k) \cos \varphi + Q(k) \sin \varphi)\right). \end{aligned} \quad (\text{F.7})$$

By applying expectation w.r.t. \mathbf{r} , as in (3.4), this can be written as

⁹ $I(k)$ and $Q(k)$ are the real and imaginary parts of observed signal samples r_k , respectively, which are thus known at the receive-side.

$$E \left[\frac{\partial^2 \ln f_B(\mathbf{r} | \boldsymbol{\theta})}{\partial \alpha \partial N} \right] = E_1^a + E_2^a + E_3^a, \quad (\text{F.8})$$

where $E_1^a = E \left[\frac{2K\alpha}{N^2} \right]$,

$$E_2^a = E \left[\sum_{k=1}^K -\frac{2}{N^2} (I(k) \cos \varphi + Q(k) \sin \varphi) \tanh \left(\frac{2\alpha}{N} (I(k) \cos \varphi + Q(k) \sin \varphi) \right) \right], \text{ and}$$

$$E_3^a = E \left[\sum_{k=1}^K -\frac{4\alpha}{N^3} (I(k) \cos \varphi + Q(k) \sin \varphi)^2 \operatorname{sech}^2 \left(\frac{2\alpha}{N} (I(k) \cos \varphi + Q(k) \sin \varphi) \right) \right].$$

As $2K\alpha/N^2$ is independent of \mathbf{r} , it is straightforward that

$$E_1^a = \frac{2K\alpha}{N^2}. \quad (\text{F.9})$$

The second expectation, given in (F.8), can be written as

$$E_2^a = E \left[\sum_{k=1}^K \Lambda(r_k) \right], \quad (\text{F.10})$$

$$\text{where } \Lambda(r_k) = -\frac{2}{N^2} \operatorname{Re} \{ r_k e^{-j\varphi} \} \tanh \left(\frac{2\alpha}{N} \operatorname{Re} \{ r_k e^{-j\varphi} \} \right),$$

with $\operatorname{Re} \{ r_k e^{-j\varphi} \} = I(k) \cos \varphi + Q(k) \sin \varphi$. By using (3.4) and (3.9) in (F.10), this becomes

$$E_2^a = \underbrace{\int_{-\infty}^{\infty} \cdots \int_{-\infty}^{\infty}}_K \sum_k \Lambda(r_k) f_B(r_1 \cdots r_K | \boldsymbol{\theta}) dr_1 \cdots dr_K. \quad (\text{F.11})$$

As $\{r_k\}_{k=1}^K$ are independent of each other, thus, (F.11) becomes

$$E_2^a = \sum_{k=1}^K \underbrace{\int_{-\infty}^{\infty} \cdots \int_{-\infty}^{\infty}}_K \Lambda(r_k) [f_B(r_1 | \boldsymbol{\theta}) \cdots f_B(r_K | \boldsymbol{\theta})] dr_1 \cdots dr_K. \quad (\text{F.12})$$

Combining the fact that $\Lambda(r_1)$ depends on r_1 and not on the remaining r_k 's, and that

$$\underbrace{\int_{-\infty}^{\infty} \cdots \int_{-\infty}^{\infty}}_{K-1} [f_B(r_2 | \boldsymbol{\theta}) \cdots f_B(r_K | \boldsymbol{\theta})] dr_2 \cdots dr_K = 1, \quad (\text{F.13})$$

the expectation of $\Lambda(r_1)$ is just an integral over the variable r_1 . The same applies for all k 's and so we can drop the subscript k in (F.12), and this becomes

$$\begin{aligned} E_2^a &= K \int_{-\infty}^{\infty} \Lambda(r) f_B(r | \boldsymbol{\theta}) dr \\ &= KE[\Lambda(r)]. \end{aligned} \quad (\text{F.14})$$

By dropping the dependency on k , this can be further written as

$$E_2^a = KE \left[-\frac{2}{N^2} (I \cos \varphi + Q \sin \varphi) \tanh\left(\frac{2\alpha}{N} (I \cos \varphi + Q \sin \varphi)\right) \right]. \quad (\text{F.15})$$

By using (F.3) with the dependency on k dropped and changing the variables, (F.15) becomes

$$E_2^a = K \int_{-\infty}^{\infty} \int_{-\infty}^{\infty} \left[\left(-\frac{2}{N^2} (\alpha s + w^I) \tanh\left(\frac{2\alpha}{N} (\alpha s + w^I)\right) \right) \times \left(\frac{1}{\pi N} \exp\left\{-\frac{1}{N} ((\alpha s + w^I)^2 + (w^Q)^2 + \alpha^2)\right\} \cosh\left(\frac{2\alpha}{N} (\alpha s + w^I)\right) \right) \right] dw^I dw^Q. \quad (\text{F.16})$$

As the above expectation is equal for each BPSK symbol [19], therefore, averaging over BPSK symbols ($s \in \{-1, 1\}$) makes no difference. Thus, (F.16) can be written as

$$E_2^a = \frac{K}{2} \int_{-\infty}^{\infty} \int_{-\infty}^{\infty} \sum_{s \in \{-1, 1\}} \left[\left(-\frac{2}{N^2} (\alpha s + w^I) \tanh\left(\frac{2\alpha}{N} (\alpha s + w^I)\right) \right) \times \left(\frac{1}{\pi N} \exp\left\{-\frac{1}{N} ((\alpha s + w^I)^2 + (w^Q)^2 + \alpha^2)\right\} \cosh\left(\frac{2\alpha}{N} (\alpha s + w^I)\right) \right) \right] dw^I dw^Q. \quad (\text{F.17})$$

By applying the summation over the BPSK signal constellation ($s \in \{-1, 1\}$), (F.17) becomes

$$\begin{aligned}
E_2^a &= -\frac{K \exp\{-\frac{\alpha^2}{N}\}}{\pi N^3} \int_{-\infty}^{\infty} \int_{-\infty}^{\infty} (\alpha + w') \exp\{-\frac{1}{N}((\alpha + w')^2 + (w^e)^2)\} \sinh(\frac{2\alpha}{N}(\alpha + w')) dw' dw^e \\
&\quad - \frac{K \exp\{-\frac{\alpha^2}{N}\}}{\pi N^3} \int_{-\infty}^{\infty} \int_{-\infty}^{\infty} (-\alpha + w') \exp\{-\frac{1}{N}((-\alpha + w')^2 + (w^e)^2)\} \sinh(\frac{2\alpha}{N}(-\alpha + w')) dw' dw^e.
\end{aligned} \tag{F.18}$$

With the change in variables, $u = \alpha + w'$ and $v = -\alpha + w'$ in the first and second term on right hand side of (F.18), respectively, this becomes

$$E_2^a = -\frac{2K \exp\{-\frac{\alpha^2}{N}\}}{\pi N^3} \int_{-\infty}^{\infty} \exp\{-\frac{(w^e)^2}{N}\} dw^e \int_{-\infty}^{\infty} u \exp\{-\frac{u^2}{N}\} \sinh(\frac{2\alpha u}{N}) du. \tag{F.19}$$

By using 3.562-3 in [20], i.e., $\int_{-\infty}^{\infty} u \exp\{-\frac{u^2}{N}\} \sinh(\frac{2\alpha u}{N}) du = \frac{\alpha}{2} \sqrt{\pi N} \exp\{\frac{\alpha^2}{N}\}$, (F.19)

reduces to

$$E_2^a = -\frac{2K\alpha}{N^2}. \tag{F.20}$$

The third expectation, given in (F.8), can be written as

$$E_3^a = E[\sum_{k=1}^K \Lambda(r_k)], \tag{F.21}$$

where $\Lambda(r_k) = -\frac{4\alpha}{N^3} (\text{Re}\{r_k e^{-j\varphi}\})^2 \text{sech}^2(\frac{2\alpha}{N} \text{Re}\{r_k e^{-j\varphi}\})$,

with $\text{Re}\{r_k e^{-j\varphi}\} = I(k) \cos \varphi + Q(k) \sin \varphi$. By using (3.4) and (3.9) in (F.21), this becomes

$$E_3^a = \underbrace{\int_{-\infty}^{\infty} \cdots \int_{-\infty}^{\infty}}_K \sum_k \Lambda(r_k) f_B(r_1 \cdots r_K | \theta) dr_1 \cdots dr_K. \tag{F.22}$$

As $\{r_k\}_{k=1}^K$ are independent of each other, thus, (F.22) becomes

$$E_3^a = \sum_{k=1}^K \underbrace{\int_{-\infty}^{\infty} \cdots \int_{-\infty}^{\infty}}_K \Lambda(r_k) [f_B(r_1 | \theta) \cdots f_B(r_k | \theta)] dr_1 \cdots dr_k \quad (\text{F.23})$$

Combining the fact that $\Lambda(r_1)$ depends on r_1 and not on the remaining r_k 's, and that

$$\underbrace{\int_{-\infty}^{\infty} \cdots \int_{-\infty}^{\infty}}_{K-1} [f_B(r_2 | \theta) \cdots f_B(r_k | \theta)] dr_2 \cdots dr_k = 1, \quad (\text{F.24})$$

the expectation of $\Lambda(r_1)$ is just an integral over the variable r_1 . The same applies for all k 's and so we can drop the subscript k in (F.23), and this becomes

$$\begin{aligned} E_3^a &= K \int_{-\infty}^{\infty} \Lambda(r) f_B(r | \theta) dr \\ &= KE[\Lambda(r)]. \end{aligned} \quad (\text{F.25})$$

By dropping the dependency on k , this can be further written as

$$E_3^a = KE \left[-\frac{4\alpha}{N^3} (I \cos \varphi + Q \sin \varphi)^2 \operatorname{sech}^2 \left(\frac{2\alpha}{N} (I \cos \varphi + Q \sin \varphi) \right) \right]. \quad (\text{F.26})$$

By using (F.3) with the dependency on k dropped and changing the variables, (F.26) becomes

$$E_3^a = K \int_{-\infty}^{\infty} \int_{-\infty}^{\infty} \left[\left(-\frac{4\alpha}{N^3} (\alpha s + w')^2 \operatorname{sech}^2 \left(\frac{2\alpha}{N} (\alpha s + w') \right) \right) \times \left(\frac{1}{\pi N} \exp \left\{ -\frac{1}{N} ((\alpha s + w')^2 + (w'')^2 + \alpha^2) \right\} \cosh \left(\frac{2\alpha}{N} (\alpha s + w') \right) \right) \right] dw' dw''. \quad (\text{F.27})$$

As the above expectation is equal for each BPSK symbol [19], therefore, averaging over BPSK symbols ($s \in \{-1, 1\}$) makes no difference. Thus, (F.27) can be written as

$$E_3^a = \frac{K}{2} \int_{-\infty}^{\infty} \int_{-\infty}^{\infty} \sum_{s \in \{-1,1\}} \left[\begin{aligned} & \left(-\frac{4\alpha}{N^3} (\alpha s + w')^2 \operatorname{sech}^2 \left(\frac{2\alpha}{N} (\alpha s + w') \right) \right) \\ & \times \left(\frac{1}{\pi N} \exp \left\{ -\frac{1}{N} ((\alpha s + w')^2 + (w^e)^2 + \alpha^2) \right\} \cosh \left(\frac{2\alpha}{N} (\alpha s + w') \right) \right) \end{aligned} \right] dw' dw^e. \quad (\text{F.28})$$

By applying the summation over the BPSK signal constellation ($s \in \{-1,1\}$), (F.28)

becomes

$$E_3^a = -\frac{2K\alpha \exp\{-\frac{\alpha^2}{N}\}}{\pi N^4} \int_{-\infty}^{\infty} \exp\{-\frac{(w^e)^2}{N}\} dw^e \left[\begin{aligned} & \int_{-\infty}^{\infty} \frac{(\alpha + w')^2 \exp\{-\frac{1}{N}(\alpha + w')^2\}}{\cosh(\frac{2\alpha}{N}(\alpha + w'))} dw' \\ & + \int_{-\infty}^{\infty} \frac{(-\alpha + w')^2 \exp\{-\frac{1}{N}(-\alpha + w')^2\}}{\cosh(\frac{2\alpha}{N}(-\alpha + w'))} dw' \end{aligned} \right]. \quad (\text{F.29})$$

With the change in variables, $u = \frac{\alpha + w'}{\sqrt{N/2}}$ and $v = \frac{-\alpha + w'}{\sqrt{N/2}}$ in the first and second term

on right hand side of (F.29), respectively, this reduces to

$$E_3^a = -\frac{2K\alpha \exp\{-\gamma\}}{N^2 \sqrt{2\pi}} \int_{-\infty}^{\infty} \frac{u^2 \exp(-u^2/2)}{\cosh(u\sqrt{2\gamma})} du. \quad (\text{F.30})$$

By substituting (F.9), (F.20), (F.30) and (3.12) in (F.8), this becomes

$$E \left[\frac{\partial^2 \ln f_B(\mathbf{r} | \boldsymbol{\theta})}{\partial \alpha \partial N} \right] = \frac{2K\alpha}{N^2} f_1(\gamma). \quad (\text{F.31})$$

b) Calculation of $[I_B(\boldsymbol{\theta})]_{11}$

By differentiating the log-likelihood function given in (3.10) twice w.r.t. α , one gets

$$\frac{\partial \ln f_B(\mathbf{r}|\boldsymbol{\theta})}{\partial \alpha} = -\frac{2K\alpha}{N} + \frac{2}{N} \sum_{k=1}^K (I(k) \cos \varphi + Q(k) \sin \varphi) \tanh\left(\frac{2\alpha}{N} (I(k) \cos \varphi + Q(k) \sin \varphi)\right),$$

and

$$\frac{\partial^2 \ln f_B(\mathbf{r}|\boldsymbol{\theta})}{\partial \alpha^2} = -\frac{2K}{N} + \frac{4}{N^2} \sum_{k=1}^K (I(k) \cos \varphi + Q(k) \sin \varphi)^2 \operatorname{sech}^2\left(\frac{2\alpha}{N} (I(k) \cos \varphi + Q(k) \sin \varphi)\right) \quad (\text{F.32})$$

By applying expectation w.r.t. \mathbf{r} , as in (3.4), this can be written as

$$\mathbb{E} \left[\frac{\partial^2 \ln f_B(\mathbf{r}|\boldsymbol{\theta})}{\partial \alpha^2} \right] = \mathbb{E}_1^b + \mathbb{E}_2^b, \quad (\text{F.33})$$

where $\mathbb{E}_1^b = \mathbb{E} \left[-\frac{2K}{N} \right]$ and

$$\mathbb{E}_2^b = \mathbb{E} \left[\sum_{k=1}^K \frac{4}{N^2} (I(k) \cos \varphi + Q(k) \sin \varphi)^2 \operatorname{sech}^2\left(\frac{2\alpha}{N} (I(k) \cos \varphi + Q(k) \sin \varphi)\right) \right].$$

As $-2K/N$ is independent of \mathbf{r} , it is straightforward that

$$\mathbb{E}_1^b = -\frac{2K}{N}. \quad (\text{F.34})$$

The second expectation given in (F.33) can be derived by following same steps as for \mathbb{E}_3^a

and is given as

$$\mathbb{E}_2^b = \frac{2K}{N} \frac{\exp\{-\gamma\}}{\sqrt{2\pi}} \int_{-\infty}^{\infty} \frac{u^2 \exp(-u^2/2)}{\cosh(u\sqrt{2\gamma})} du. \quad (\text{F.35})$$

By substituting (F.34), (F.35) and (3.12) in (F.33), this becomes

$$\mathbb{E} \left[\frac{\partial^2 \ln f_B(\mathbf{r}|\boldsymbol{\theta})}{\partial \alpha^2} \right] = -\frac{2K}{N} + \frac{2K}{N} f_1(\gamma). \quad (\text{F.36})$$

c) Calculation of $[I_B(\theta)]_{22}$

By differentiating the log-likelihood function given in (3.10) twice w.r.t. N , one gets

$$\begin{aligned} \frac{\partial \ln f_B(\mathbf{r}|\theta)}{\partial N} &= -\frac{K}{N} + \frac{1}{N^2} \sum_{k=1}^K (I^2(k) + Q^2(k) + \alpha^2) \\ &\quad - \frac{2\alpha}{N^2} \sum_{k=1}^K (I(k) \cos \varphi + Q(k) \sin \varphi) \tanh\left(\frac{2\alpha}{N} (I(k) \cos \varphi + Q(k) \sin \varphi)\right), \end{aligned}$$

and

$$\begin{aligned} \frac{\partial^2 \ln f_B(\mathbf{r}|\theta)}{\partial N^2} &= \left(\frac{K}{N^2} - \frac{2K\alpha^2}{N^3}\right) - \frac{2}{N^3} \sum_{k=1}^K (I^2(k) + Q^2(k)) \\ &\quad + \frac{4\alpha^2}{N^4} \sum_{k=1}^K (I(k) \cos \varphi + Q(k) \sin \varphi)^2 \operatorname{sech}^2\left(\frac{2\alpha}{N} (I(k) \cos \varphi + Q(k) \sin \varphi)\right) \quad (\text{F.37}) \\ &\quad + \frac{4\alpha}{N^3} \sum_{k=1}^K (I(k) \cos \varphi + Q(k) \sin \varphi) \tanh\left(\frac{2\alpha}{N} (I(k) \cos \varphi + Q(k) \sin \varphi)\right). \end{aligned}$$

By applying expectation w.r.t. \mathbf{r} , as in (3.4), this can be written as

$$E\left[\frac{\partial^2 \ln f_B(\mathbf{r}|\theta)}{\partial N^2}\right] = E_1^c + E_2^c + E_3^c + E_4^c, \quad (\text{F.38})$$

$$\text{where } E_1^c = E\left[\frac{K}{N^2} - \frac{2K\alpha^2}{N^3}\right], \quad E_2^c = E\left[\sum_{k=1}^K -\frac{2}{N^3} (I^2(k) + Q^2(k))\right],$$

$$E_3^c = E\left[\sum_{k=1}^K \frac{4\alpha^2}{N^4} (I(k) \cos \varphi + Q(k) \sin \varphi)^2 \operatorname{sech}^2\left(\frac{2\alpha}{N} (I(k) \cos \varphi + Q(k) \sin \varphi)\right)\right] \text{ and}$$

$$E_4^c = E\left[\sum_{k=1}^K \frac{4\alpha}{N^3} (I(k) \cos \varphi + Q(k) \sin \varphi) \tanh\left(\frac{2\alpha}{N} (I(k) \cos \varphi + Q(k) \sin \varphi)\right)\right].$$

As $(K/N^2) - (2K\alpha^2/N^3)$ is independent of \mathbf{r} , it is straightforward that

$$E_1^c = \frac{K}{N^2} - \frac{2K\alpha^2}{N^3}. \quad (\text{F.39})$$

The second expectation, given in (F.38), can be written as

$$E_2^c = E\left[\sum_{k=1}^K \Lambda(r_k)\right], \quad (\text{F.40})$$

where $\Lambda(r_k) = -\frac{2}{N^3} |r_k|^2$, with $|r_k|^2 = I^2(k) + Q^2(k)$. By using (3.4) and (3.9) in (F.40),

this becomes

$$E_2^c = \underbrace{\int_{-\infty}^{\infty} \cdots \int_{-\infty}^{\infty}}_K \sum_k \Lambda(r_k) f_B(r_1 \cdots r_K | \theta) dr_1 \cdots dr_K. \quad (\text{F.41})$$

As $\{r_k\}_{k=1}^K$ are independent of each other, thus, (F.41) becomes

$$E_2^c = \sum_{k=1}^K \underbrace{\int_{-\infty}^{\infty} \cdots \int_{-\infty}^{\infty}}_K \Lambda(r_k) [f_B(r_1 | \theta) \cdots f_B(r_K | \theta)] dr_1 \cdots dr_K. \quad (\text{F.42})$$

Combining the fact that $\Lambda(r_1)$ depends on r_1 and not on the remaining r_k 's, and that

$$\underbrace{\int_{-\infty}^{\infty} \cdots \int_{-\infty}^{\infty}}_{K-1} [f_B(r_2 | \theta) \cdots f_B(r_K | \theta)] dr_2 \cdots dr_K = 1, \quad (\text{F.43})$$

the expectation of $\Lambda(r_1)$ is just an integral over the variable r_1 . The same applies for all

k 's and so we can drop the subscript k in (F.42), and this becomes

$$\begin{aligned} E_2^c &= K \int_{-\infty}^{\infty} \Lambda(r) f_B(r | \theta) dr \\ &= KE[\Lambda(r)]. \end{aligned} \quad (\text{F.44})$$

By dropping the dependency on k , this can be further written as

$$E_2^c = KE \left[-\frac{2}{N^3} (I^2 + Q^2) \right]. \quad (\text{F.45})$$

By using (F.3) with the dependency on k dropped and changing the variables, (F.45)

becomes

$$E_2^c = K \int_{-\infty}^{\infty} \int_{-\infty}^{\infty} \left[\left(-\frac{2}{N^3} ((\alpha s + w')^2 + (w^{\varrho})^2) \right) \times \left(\frac{1}{\pi N} \exp\left\{-\frac{1}{N} ((\alpha s + w')^2 + (w^{\varrho})^2 + \alpha^2)\right\} \cosh\left(\frac{2\alpha}{N} (\alpha s + w')\right) \right) \right] dw' dw^{\varrho}. \quad (\text{F.46})$$

As the above expectation is equal for each BPSK symbol [19], therefore, averaging over BPSK symbols ($s \in \{-1, 1\}$) makes no difference. Thus, (F.46) can be written as

$$E_2^c = \frac{K}{2} \int_{-\infty}^{\infty} \int_{-\infty}^{\infty} \sum_{s \in \{-1, 1\}} \left[\left(-\frac{2}{N^3} ((\alpha s + w')^2 + (w^{\varrho})^2) \right) \times \left(\frac{1}{\pi N} \exp\left\{-\frac{1}{N} ((\alpha s + w')^2 + (w^{\varrho})^2 + \alpha^2)\right\} \cosh\left(\frac{2\alpha}{N} (\alpha s + w')\right) \right) \right] dw' dw^{\varrho}. \quad (\text{F.47})$$

By applying the summation over the BPSK signal constellation ($s \in \{-1, 1\}$) and simplifying, (F.47) becomes

$$\begin{aligned} E_2^c &= -\frac{K \exp\left\{-\frac{\alpha^2}{N}\right\}}{\pi N^4} \int_{-\infty}^{\infty} \exp\left\{-\frac{(w^{\varrho})^2}{N}\right\} dw^{\varrho} \int_{-\infty}^{\infty} (\alpha s + w')^2 \exp\left\{-\frac{1}{N} (\alpha + w')^2\right\} \cosh\left(\frac{2\alpha}{N} (\alpha + w')\right) dw' \\ &\quad - \frac{K \exp\left\{-\frac{\alpha^2}{N}\right\}}{\pi N^4} \int_{-\infty}^{\infty} \exp\left\{-\frac{(w^{\varrho})^2}{N}\right\} dw^{\varrho} \int_{-\infty}^{\infty} (-\alpha s + w')^2 \exp\left\{-\frac{1}{N} (-\alpha + w')^2\right\} \cosh\left(\frac{2\alpha}{N} (-\alpha + w')\right) dw' \\ &\quad - \frac{K \exp\left\{-\frac{\alpha^2}{N}\right\}}{\pi N^4} \int_{-\infty}^{\infty} (w^{\varrho})^2 \exp\left\{-\frac{(w^{\varrho})^2}{N}\right\} dw^{\varrho} \int_{-\infty}^{\infty} \exp\left\{-\frac{1}{N} (\alpha + w')^2\right\} \cosh\left(\frac{2\alpha}{N} (\alpha + w')\right) dw' \\ &\quad - \frac{K \exp\left\{-\frac{\alpha^2}{N}\right\}}{\pi N^4} \int_{-\infty}^{\infty} (w^{\varrho})^2 \exp\left\{-\frac{(w^{\varrho})^2}{N}\right\} dw^{\varrho} \int_{-\infty}^{\infty} \exp\left\{-\frac{1}{N} (-\alpha + w')^2\right\} \cosh\left(\frac{2\alpha}{N} (-\alpha + w')\right) dw'. \end{aligned} \quad (\text{F.48})$$

With the change in variables, $u = \alpha + w'$ and $v = -\alpha + w'$, (F.48) becomes

$$E_2^c = -\frac{8K \exp\{-\frac{\alpha^2}{N}\}}{\pi N^4} \int_{-\infty}^{\infty} \exp\{-\frac{(w^\varrho)^2}{N}\} dw^\varrho \int_{-\infty}^{\infty} u^2 \exp\{-\frac{u^2}{N}\} \cosh(\frac{2\alpha u}{N}) du$$

$$-\frac{8K \exp\{-\frac{\alpha^2}{N}\}}{\pi N^4} \int_{-\infty}^{\infty} (w^\varrho)^2 \exp\{-\frac{(w^\varrho)^2}{N}\} dw^\varrho \int_{-\infty}^{\infty} \exp\{-\frac{u^2}{N}\} \cosh(\frac{2\alpha u}{N}) du. \quad (F.49)$$

Using 3.562-6, 3.461-2 and 3.546-2 in [20], i.e.,

$$\int_0^{\infty} u^2 \exp\{-\frac{u^2}{N}\} \cosh(\frac{2\alpha u}{N}) du = \frac{\sqrt{\pi N}}{4} (N + 2\alpha^2) \exp\{\frac{\alpha^2}{N}\},$$

$$\int_0^{\infty} (w^\varrho)^2 \exp\{-\frac{(w^\varrho)^2}{N}\} dw^\varrho = \frac{N\sqrt{\pi N}}{2} \quad \text{and} \quad \int_0^{\infty} \exp\{-\frac{u^2}{N}\} \cosh(\frac{2\alpha u}{N}) du = \frac{\sqrt{\pi N}}{2} \exp\{\frac{\alpha^2}{N}\},$$

(F.49) reduces to

$$E_3^c = -\frac{2K}{N^2} - \frac{2K\alpha^2}{N^3}. \quad (F.50)$$

By following similar derivations as for E_3^a and E_2^a , the third and fourth expectation in (F.38) are derived, respectively, and are given by

$$E_3^c = \frac{2\alpha^2 \exp\{-\gamma\}}{N^3 \sqrt{2\pi}} \int_{-\infty}^{\infty} \frac{u^2 \exp(-u^2/2)}{\cosh(u\sqrt{2\gamma})} du, \quad (F.51)$$

and

$$E_4^c = \frac{4K\alpha^2}{N^3}. \quad (F.52)$$

By substituting (F.39), (F.50), (F.51), (F.52) and (3.12) in (F.38), this becomes

$$E \left[\frac{\partial^2 \ln f_B(\mathbf{r}|\boldsymbol{\theta})}{\partial N^2} \right] = -\frac{K}{N^2} + \frac{2\alpha^2}{N^3} f_1(\gamma). \quad (F.53)$$

d) Calculation of $[I_B(\theta)]_{33}$

By differentiating the log-likelihood function given in (3.10) twice w.r.t. φ , one gets

$$\frac{\partial \ln f_B(\mathbf{r}|\theta)}{\partial \varphi} = \frac{2\alpha}{N} \sum_{k=1}^K (-I(k) \sin \varphi + Q(k) \cos \varphi) \tanh\left(\frac{2\alpha}{N}(I(k) \cos \varphi + Q(k) \sin \varphi)\right), \quad (\text{F.54})$$

and

$$\begin{aligned} \frac{\partial^2 \ln f_B(\mathbf{r}|\theta)}{\partial \varphi^2} = & -\frac{2\alpha}{N} \sum_{k=1}^K (I(k) \cos \varphi + Q(k) \sin \varphi) \tanh\left(\frac{2\alpha}{N}(I(k) \cos \varphi + Q(k) \sin \varphi)\right) \\ & + \frac{4\alpha^2}{N^2} \sum_{k=1}^K (-I(k) \sin \varphi + Q(k) \cos \varphi)^2 \text{sech}^2\left(\frac{2\alpha}{N}(I(k) \cos \varphi + Q(k) \sin \varphi)\right). \end{aligned} \quad (\text{F.55})$$

By applying expectation w.r.t. \mathbf{r} , as in (3.4), this can be written as

$$E\left[\frac{\partial^2 \ln f_B(\mathbf{r}|\theta)}{\partial \varphi^2}\right] = E_1^d + E_2^d, \quad (\text{F.56})$$

where $E_1^d = E\left[\sum_{k=1}^K -\frac{2\alpha}{N}(I(k) \cos \varphi + Q(k) \sin \varphi) \tanh\left(\frac{2\alpha}{N}(I(k) \cos \varphi + Q(k) \sin \varphi)\right)\right]$ and

$$E_2^d = E\left[\sum_{k=1}^K \frac{4\alpha^2}{N^2} (-I(k) \sin \varphi + Q(k) \cos \varphi)^2 \text{sech}^2\left(\frac{2\alpha}{N}(I(k) \cos \varphi + Q(k) \sin \varphi)\right)\right].$$

By following a similar derivation as for E_2^a , the first expectation in (F.56) can be derived

and is given as

$$E_1^d = -\frac{2K\alpha^2}{N}. \quad (\text{F.57})$$

The second expectation, given in (F.56), can be written as

$$E_2^d = E\left[\sum_{k=1}^K \Lambda(r_k)\right], \quad (\text{F.58})$$

where $\Lambda(r_k) = \frac{4\alpha^2}{N^2} (\text{Im}\{r_k e^{-j\varphi}\})^2 \text{sech}^2\left(\frac{2\alpha}{N} \text{Re}\{r_k e^{-j\varphi}\}\right)$,

with $\text{Im}\{r_k e^{-j\varphi}\} = -I(k) \sin \varphi + Q(k) \cos \varphi$ and $\text{Re}\{r_k e^{-j\varphi}\} = I(k) \cos \varphi + Q(k) \sin \varphi$. By

using (3.4) and (3.9) in (F.58), this becomes

$$E_2^d = \underbrace{\int_{-\infty}^{\infty} \cdots \int_{-\infty}^{\infty}}_K \sum_k \Lambda(r_k) f_B(r_1 \cdots r_K | \boldsymbol{\theta}) dr_1 \cdots dr_K. \quad (\text{F.59})$$

As $\{r_k\}_{k=1}^K$ are independent of each other, thus, (F.59) becomes

$$E_2^d = \sum_{k=1}^K \underbrace{\int_{-\infty}^{\infty} \cdots \int_{-\infty}^{\infty}}_K \Lambda(r_k) [f_B(r_1 | \boldsymbol{\theta}) \cdots f_B(r_K | \boldsymbol{\theta})] dr_1 \cdots dr_K. \quad (\text{F.60})$$

Combining the fact that $\Lambda(r_1)$ depends on r_1 and not on the remaining r_k 's, and that

$$\underbrace{\int_{-\infty}^{\infty} \cdots \int_{-\infty}^{\infty}}_{K-1} [f_B(r_2 | \boldsymbol{\theta}) \cdots f_B(r_K | \boldsymbol{\theta})] dr_2 \cdots dr_K = 1. \quad (\text{F.61})$$

the expectation of $\Lambda(r_1)$ is just an integral over the variable r_1 . The same applies for all

k 's and so we can drop the subscript k in (F.60), and this becomes

$$\begin{aligned} E_2^d &= K \int_{-\infty}^{\infty} \Lambda(r) f_B(r | \boldsymbol{\theta}) dr \\ &= KE[\Lambda(r)]. \end{aligned} \quad (\text{F.62})$$

By dropping the dependency on k , this can be further written as

$$E_2^d = KE \left[\frac{4\alpha^2}{N^2} (-I \sin \varphi + Q \cos \varphi)^2 \text{sech}^2 \left(\frac{2\alpha}{N} (I \cos \varphi + Q \sin \varphi) \right) \right]. \quad (\text{F.63})$$

By using (F.3) with the dependency on k dropped and changing the variables, (F.63)

becomes

$$E_2^d = K \int_{-\infty}^{\infty} \int_{-\infty}^{\infty} \left[\left(\frac{4\alpha^2}{N^2} (w^\varrho)^2 \text{sech}^2 \left(\frac{2\alpha}{N} (\alpha s + w^I) \right) \right) \times \left(\frac{1}{\pi N} \exp \left\{ -\frac{1}{N} ((\alpha s + w^I)^2 + (w^\varrho)^2 + \alpha^2) \right\} \cosh \left(\frac{2\alpha}{N} (\alpha s + w^I) \right) \right) \right] dw^I dw^\varrho. \quad (\text{F.64})$$

As the above expectation is equal for each BPSK symbol [19], therefore, averaging over BPSK symbols ($s \in \{-1, 1\}$) makes no difference. Thus, (F.64) can be written as

$$E_2^d = \frac{K}{2} \int_{-\infty}^{\infty} \int_{-\infty}^{\infty} \sum_{s \in \{-1, 1\}} \left[\left(\frac{4\alpha^2}{N^2} (w^\varrho)^2 \operatorname{sech}^2 \left(\frac{2\alpha}{N} (\alpha s + w') \right) \right) \times \left(\frac{1}{\pi N} \exp \left\{ -\frac{1}{N} ((\alpha s + w')^2 + (w^\varrho)^2 + \alpha^2) \right\} \cosh \left(\frac{2\alpha}{N} (\alpha s + w') \right) \right) \right] dw' dw^\varrho. \quad (\text{F.65})$$

By applying the summation over the BPSK signal constellation ($s \in \{-1, 1\}$) and simplifying, (F.65) becomes

$$E_2^d = \frac{2K\alpha^2 \exp\{-\frac{\alpha^2}{N}\}}{\pi N^3} \int_{-\infty}^{\infty} (w^\varrho)^2 \exp\{-\frac{(w^\varrho)^2}{N}\} dw^\varrho \left[\int_{-\infty}^{\infty} \frac{\exp\{-\frac{1}{N}(\alpha + w')^2\}}{\cosh(\frac{2\alpha}{N}(\alpha + w'))} dw' + \int_{-\infty}^{\infty} \frac{\exp\{-\frac{1}{N}(-\alpha + w')^2\}}{\cosh(\frac{2\alpha}{N}(-\alpha + w'))} dw' \right]. \quad (\text{F.66})$$

By using 3.461-2 in [20], i.e., $\int_0^{\infty} (w^\varrho)^2 \exp\{-\frac{(w^\varrho)^2}{N}\} dw^\varrho = \frac{N\sqrt{\pi N}}{2}$, (F.66) becomes

$$E_2^d = \frac{K\alpha^2 \exp\{-\frac{\alpha^2}{N}\}}{N\sqrt{\pi N}} \left[\int_{-\infty}^{\infty} \frac{\exp\{-\frac{1}{N}(\alpha + w')^2\}}{\cosh(\frac{2\alpha}{N}(\alpha + w'))} dw' + \int_{-\infty}^{\infty} \frac{\exp\{-\frac{1}{N}(-\alpha + w')^2\}}{\cosh(\frac{2\alpha}{N}(-\alpha + w'))} dw' \right]. \quad (\text{F.67})$$

With the change in variables, $u = \frac{\alpha + w'}{\sqrt{N/2}}$ and $v = \frac{-\alpha + w'}{\sqrt{N/2}}$, in the first and second term

on right hand side of (F.67), respectively, this reduces to

$$E_2^d = \frac{2K\alpha^2 \exp\{-\gamma\}}{N \sqrt{2\pi}} \int_{-\infty}^{\infty} \frac{\exp(-u^2/2)}{\cosh(u\sqrt{2\gamma})} du. \quad (\text{F.68})$$

By substituting (F.57), (F.68) and (3.13) in (F.56), this becomes

$$E\left[\frac{\partial^2 \ln f_B(\mathbf{r}|\boldsymbol{\theta})}{\partial \varphi^2}\right] = -\frac{2K\alpha^2}{N} + \frac{2K\alpha^2}{N} f_2(\gamma). \quad (\text{F.69})$$

e) Calculation of $[\mathbf{I}_B(\boldsymbol{\theta})]_{31}$

By differentiating the log-likelihood function given in (3.10) w.r.t. φ and α^9 , one gets

$$\frac{\partial \ln f_B(\mathbf{r}|\boldsymbol{\theta})}{\partial \varphi} = \frac{2\alpha}{N} \sum_{k=1}^K (-I(k) \sin \varphi + Q(k) \cos \varphi) \tanh\left(\frac{2\alpha}{N} (I(k) \cos \varphi + Q(k) \sin \varphi)\right),$$

and

$$\begin{aligned} \frac{\partial^2 \ln f_B(\mathbf{r}|\boldsymbol{\theta})}{\partial \varphi \partial \alpha} &= \frac{2}{N} \sum_{k=1}^K (-I(k) \sin \varphi + Q(k) \cos \varphi) \tanh\left(\frac{2\alpha}{N} (I(k) \cos \varphi + Q(k) \sin \varphi)\right) \\ &+ \frac{4\alpha}{N^2} \sum_{k=1}^K (-I(k) \sin \varphi + Q(k) \cos \varphi) (I(k) \cos \varphi + Q(k) \sin \varphi) \\ &\times \text{sech}^2\left(\frac{2\alpha}{N} (I(k) \cos \varphi + Q(k) \sin \varphi)\right). \end{aligned} \quad (\text{F.70})$$

By applying expectation w.r.t. \mathbf{r} , as in (3.4), this can be written as

$$E\left[\frac{\partial^2 \ln f_B(\mathbf{r}|\boldsymbol{\theta})}{\partial \varphi \partial \alpha}\right] = E_1^e + E_2^e, \quad (\text{F.71})$$

where $E_1^e = E\left[\sum_{k=1}^K \frac{2}{N} (-I(k) \sin \varphi + Q(k) \cos \varphi) \tanh\left(\frac{2\alpha}{N} (I(k) \cos \varphi + Q(k) \sin \varphi)\right)\right]$ and

$$\begin{aligned} E_2^e &= E\left[\sum_{k=1}^K \frac{4\alpha}{N^2} (-I(k) \sin \varphi + Q(k) \cos \varphi) (I(k) \cos \varphi + Q(k) \sin \varphi) \right. \\ &\quad \left. \times \text{sech}^2\left(\frac{2\alpha}{N} (I(k) \cos \varphi + Q(k) \sin \varphi)\right)\right]. \end{aligned}$$

The first expectation, given in (F.71), can be written as

$$E_1^e = E\left[\sum_{k=1}^K \Lambda(r_k)\right], \quad (\text{F.72})$$

where $\Lambda(r_k) = \frac{2}{N} \text{Im}\{r_k e^{-j\varphi}\} \tanh\left(\frac{2\alpha}{N} \text{Re}\{r_k e^{-j\varphi}\}\right)$,

with $\text{Im}\{r_k e^{-j\varphi}\} = -I(k) \sin \varphi + Q(k) \cos \varphi$ and $\text{Re}\{r_k e^{-j\varphi}\} = I(k) \cos \varphi + Q(k) \sin \varphi$. By using (3.4) and (3.9) in (F.72), this becomes

$$E_1^e = \underbrace{\int_{-\infty}^{\infty} \cdots \int_{-\infty}^{\infty}}_K \sum_k \Lambda(r_k) f_B(r_1 \cdots r_K | \theta) dr_1 \cdots dr_K. \quad (\text{F.73})$$

As $\{r_k\}_{k=1}^K$ are independent of each other, thus, (F.73) becomes

$$E_1^e = \sum_{k=1}^K \underbrace{\int_{-\infty}^{\infty} \cdots \int_{-\infty}^{\infty}}_K \Lambda(r_k) [f_B(r_1 | \theta) \cdots f_B(r_K | \theta)] dr_1 \cdots dr_K. \quad (\text{F.74})$$

Combining the fact that $\Lambda(r_1)$ depends on r_1 and not on the remaining r_k 's, and that

$$\underbrace{\int_{-\infty}^{\infty} \cdots \int_{-\infty}^{\infty}}_{K-1} [f_B(r_2 | \theta) \cdots f_B(r_K | \theta)] dr_2 \cdots dr_K = 1, \quad (\text{F.75})$$

the expectation of $\Lambda(r_1)$ is just an integral over the variable r_1 . The same applies for all k 's and so we can drop the subscript k in (F.74), and this becomes

$$\begin{aligned} E_1^e &= K \int_{-\infty}^{\infty} \Lambda(r) f_B(r | \theta) dr \\ &= KE[\Lambda(r)]. \end{aligned} \quad (\text{F.76})$$

By dropping the dependency on k , this can be further written as

$$E_1^e = KE \left[\frac{2}{N} (-I \sin \varphi + Q \cos \varphi) \tanh\left(\frac{2\alpha}{N} (I \cos \varphi + Q \sin \varphi)\right) \right]. \quad (\text{F.77})$$

By using (F.3) with the dependency on k dropped and changing the variables, (F.77) becomes

$$E_1^e = K \int_{-\infty}^{\infty} \int_{-\infty}^{\infty} \left[\left(\frac{2w^\varrho}{N} \tanh\left(\frac{2\alpha}{N} (\alpha s + w')\right) \right) \times \left(\frac{1}{\pi N} \exp\left\{-\frac{1}{N} ((\alpha s + w')^2 + (w^\varrho)^2 + \alpha^2)\right\} \cosh\left(\frac{2\alpha}{N} (\alpha s + w')\right) \right) \right] dw' dw^\varrho. \quad (\text{F.78})$$

As the above expectation is equal for each BPSK symbol [19], therefore, averaging over BPSK symbols ($s \in \{-1, 1\}$) makes no difference. Thus, (F.78) can be written as

$$E_1^e = \frac{K}{2} \int_{-\infty}^{\infty} \int_{-\infty}^{\infty} \sum_{s \in \{-1, 1\}} \left[\left(\frac{2w^\varrho}{N} \tanh\left(\frac{2\alpha}{N}(\alpha s + w')\right) \right) \times \left(\frac{1}{\pi N} \exp\left\{-\frac{1}{N}((\alpha s + w')^2 + (w^\varrho)^2 + \alpha^2)\right\} \cosh\left(\frac{2\alpha}{N}(\alpha s + w')\right) \right) \right] dw' dw^\varrho. \quad (\text{F.79})$$

By separating the integrals in (F.79), this becomes

$$E_1^e = \frac{K \exp\left\{-\frac{\alpha^2}{N}\right\}}{\pi N^2} \int_{-\infty}^{\infty} w^\varrho \exp\left\{-\frac{(w^\varrho)^2}{N}\right\} dw^\varrho \int_{-\infty}^{\infty} \sum_{s \in \{-1, 1\}} \left[\exp\left\{-\frac{1}{N}(\alpha + w')^2\right\} \sinh\left(\frac{2\alpha}{N}(\alpha + w')\right) \right] dw'. \quad (\text{F.80})$$

As $\int_{-\infty}^{\infty} w^\varrho \exp\left\{-\frac{(w^\varrho)^2}{N}\right\} dw^\varrho = 0$, therefore, (F.80) reduces to

$$E_1^e = 0. \quad (\text{F.81})$$

The second expectation, given in (F.71), can be written as

$$E_2^e = \text{E}\left[\sum_{k=1}^K \Lambda(r_k)\right], \quad (\text{F.82})$$

$$\text{where } \Lambda(r_k) = \frac{4\alpha}{N^2} \text{Im}\{r_k e^{-j\varphi}\} \text{Re}\{r_k e^{-j\varphi}\} \text{sech}^2\left(\frac{2\alpha}{N} \text{Re}\{r_k e^{-j\varphi}\}\right),$$

$$\text{with } \text{Im}\{r_k e^{-j\varphi}\} = -I(k) \sin \varphi + Q(k) \cos \varphi \quad \text{and} \quad \text{Re}\{r_k e^{-j\varphi}\} = I(k) \cos \varphi + Q(k) \sin \varphi.$$

By using (3.4) and (3.9) in (F.82), this becomes

$$E_2^e = \underbrace{\int_{-\infty}^{\infty} \cdots \int_{-\infty}^{\infty}}_K \sum_k \Lambda(r_k) f_B(r_1 \cdots r_K | \boldsymbol{\theta}) dr_1 \cdots dr_K. \quad (\text{F.83})$$

As $\{r_k\}_{k=1}^K$ are independent of each other, thus, (F.83) becomes

$$E_2^e = \sum_{k=1}^K \underbrace{\int_{-\infty}^{\infty} \cdots \int_{-\infty}^{\infty}}_K \Lambda(r_k) [f_B(r_1 | \theta) \cdots f_B(r_K | \theta)] dr_1 \cdots dr_K. \quad (\text{F.84})$$

Combining the fact that $\Lambda(r_1)$ depends on r_1 and not on the remaining r_k 's, and that

$$\underbrace{\int_{-\infty}^{\infty} \cdots \int_{-\infty}^{\infty}}_{K-1} [f_B(r_2 | \theta) \cdots f_B(r_K | \theta)] dr_2 \cdots dr_K = 1, \quad (\text{F.85})$$

the expectation of $\Lambda(r_1)$ is just an integral over the variable r_1 . The same applies for all

k 's and so we can drop the subscript k in (F.84), and this becomes

$$\begin{aligned} E_2^e &= K \int_{-\infty}^{\infty} \Lambda(r) f_B(r | \theta) dr \\ &= KE[\Lambda(r)]. \end{aligned} \quad (\text{F.86})$$

By dropping the dependency on k , this can be further written as

$$E_2^e = KE \left[\frac{4\alpha}{N^2} (-I \sin \varphi + Q \cos \varphi)(I \cos \varphi + Q \sin \varphi) \operatorname{sech}^2 \left(\frac{2\alpha}{N} (I \cos \varphi + Q \sin \varphi) \right) \right]. \quad (\text{F.87})$$

By using (F.3) with the dependency on k dropped and changing the variables, (F.87) becomes

$$E_2^e = K \int_{-\infty}^{\infty} \int_{-\infty}^{\infty} \left[\left(\frac{4\alpha w^{\varrho}}{N^2} (\alpha s + w') \operatorname{sech}^2 \left(\frac{2\alpha}{N} (\alpha s + w') \right) \right) \times \left(\frac{1}{\pi N} \exp \left\{ -\frac{1}{N} ((\alpha s + w')^2 + (w^{\varrho})^2 + \alpha^2) \right\} \cosh \left(\frac{2\alpha}{N} (\alpha s + w') \right) \right) \right] dw' dw^{\varrho}. \quad (\text{F.88})$$

As the above expectation is equal for each BPSK symbol [19], therefore, averaging over BPSK symbols ($s \in \{-1, 1\}$) makes no difference. Thus, (F.88) can be written as

$$E_2^e = \frac{K}{2} \int_{-\infty}^{\infty} \int_{-\infty}^{\infty} \sum_{s \in \{-1,1\}} \left[\left(\frac{4\alpha w^{\varrho}}{N^2} (\alpha s + w') \operatorname{sech}^2 \left(\frac{2\alpha}{N} (\alpha s + w') \right) \right) \times \left(\frac{1}{\pi N} \exp \left\{ -\frac{1}{N} ((\alpha s + w')^2 + (w^{\varrho})^2 + \alpha^2) \right\} \cosh \left(\frac{2\alpha}{N} (\alpha s + w') \right) \right) \right] dw' dw^{\varrho}. \quad (\text{F.89})$$

By separating the integrals in (F.89), this becomes

$$E_2^e = \frac{2K\alpha \exp\{-\frac{\alpha^2}{N}\}}{\pi N^3} \int_{-\infty}^{\infty} w^{\varrho} \exp\{-\frac{(w^{\varrho})^2}{N}\} dw^{\varrho} \int_{-\infty}^{\infty} \sum_{s \in \{-1,1\}} \left[\frac{(\alpha s + w') \exp\{-\frac{1}{N} (\alpha s + w')^2\}}{\cosh(\frac{2\alpha}{N} (\alpha s + w'))} \right] dw'. \quad (\text{F.90})$$

As $\int_{-\infty}^{\infty} w^{\varrho} \exp\{-\frac{(w^{\varrho})^2}{N}\} dw^{\varrho} = 0$, therefore, (F.90) reduces to

$$E_2^e = 0. \quad (\text{F.91})$$

By substituting (F.81) and (F.91) in (F.71), this becomes

$$E \left[\frac{\partial^2 \ln f_B(\mathbf{r} | \boldsymbol{\theta})}{\partial \varphi \partial \alpha} \right] = 0. \quad (\text{F.92})$$

f) Calculation of $[I_B(\boldsymbol{\theta})]_{32}$

By differentiating the log-likelihood function given in (3.10) w.r.t. φ and N^9 , one gets

$$\frac{\partial \ln f_B(\mathbf{r} | \boldsymbol{\theta})}{\partial \varphi} = \frac{2\alpha}{N} \sum_{k=1}^K (-I(k) \sin \varphi + Q(k) \cos \varphi) \tanh \left(\frac{2\alpha}{N} (I(k) \cos \varphi + Q(k) \sin \varphi) \right),$$

and

$$\begin{aligned} \frac{\partial^2 \ln f_B(\mathbf{r}|\boldsymbol{\theta})}{\partial\phi\partial N} &= -\frac{2\alpha}{N^2} \sum_{k=1}^K (-I(k) \sin \phi + Q(k) \cos \phi) \tanh\left(\frac{2\alpha}{N} (I(k) \cos \phi + Q(k) \sin \phi)\right) \\ &\quad - \frac{4\alpha^2}{N^3} \sum_{k=1}^K (-I(k) \sin \phi + Q(k) \cos \phi) (I(k) \cos \phi + Q(k) \sin \phi) \operatorname{sech}^2\left(\frac{2\alpha}{N} (I(k) \cos \phi + Q(k) \sin \phi)\right). \end{aligned} \quad (\text{F.93})$$

By applying expectation w.r.t. \mathbf{r} , as in (3.4), this can be written as

$$\mathbb{E} \left[\frac{\partial^2 \ln f_B(\mathbf{r}|\boldsymbol{\theta})}{\partial\phi\partial N} \right] = E_1^f + E_2^f, \quad (\text{F.94})$$

where $E_1^f = \mathbb{E} \left[\sum_{k=1}^K -\frac{2\alpha}{N^2} (-I(k) \sin \phi + Q(k) \cos \phi) \tanh\left(\frac{2\alpha}{N} (I(k) \cos \phi + Q(k) \sin \phi)\right) \right]$ and

$$\begin{aligned} E_2^f &= \mathbb{E} \left[\sum_{k=1}^K -\frac{4\alpha^2}{N^3} (-I(k) \sin \phi + Q(k) \cos \phi) (I(k) \cos \phi + Q(k) \sin \phi) \right. \\ &\quad \left. \times \operatorname{sech}^2\left(\frac{2\alpha}{N} (I(k) \cos \phi + Q(k) \sin \phi)\right) \right]. \end{aligned}$$

By following same steps as to derive E_1^e and E_2^e , the first and second expectation in (F.94) are derived, respectively, and are given as

$$E_1^f = 0, \quad (\text{F.95})$$

and

$$E_2^f = 0. \quad (\text{F.96})$$

By substituting (F.95) and (F.96) in (F.94), this becomes

$$\mathbb{E} \left[\frac{\partial^2 \ln f_B(\mathbf{r}|\boldsymbol{\theta})}{\partial\phi\partial N} \right] = 0. \quad (\text{F.97})$$

The FIM for QPSK signals, with $\boldsymbol{\theta} = [\alpha N \phi]^T$ as unknown parameters, can be similarly derived. Tedious computations are involved. Final results are presented in Section 3.3.

The undersigned hereby recommended to the School of Graduate Studies acceptance of the thesis

**BLIND MODULATION CLASSIFICATION OF
LINEARLY DIGITALLY MODULATED SIGNALS**

Submitted by Fahed Hameed
In partial fulfillment of the requirements for the
Degree of Master of Engineering

**Thesis Supervisor
Dr. Octavia A. Dobre**

**Associate Dean, Graduate Studies & Research
Dr. R. Venkatesan**

